TRANSPORTATION RESEARCH RECORD

488

Formerly issued as Highway Research Record

Safety Appurtenances

11 reports prepared for the 53rd Annual Meeting of the Highway Research Board

subject areas
22 highway design
27 bridge design
51 highway safety

TRB

TRANSPORTATION RESEARCH BOARD

NATIONAL RESEARCH COUNCIL

Washington, D. C., 1974

NOTICE

These papers report research work of the authors that was done at institutions named by the authors. The papers were offered to the Transportation Research Board of the National Research Council for publication and are published here in the interest of the dissemination of information from research, one of the major functions of the Transportation Research Board.

Before publication, each paper was reviewed by members of the TRB committee named as its sponsor and accepted as objective, useful, and suitable for publication by the National Research Council. The members of the review committee were chosen for recognized scholarly competence and with due consideration for the balance of disciplines appropriate to the subject concerned.

Responsibility for the publication of these reports rests with the sponsoring committee. However, the opinions and conclusions expressed in the reports are those of the individual authors and not necessarily those of the sponsoring committee, the Transportation Research Board, or the National Research Council.

Each report is reviewed and processed according to the procedures established and monitored by the Report Review Committee of the National Academy of Sciences. Distribution of the report is approved by the President of the Academy upon satisfactory completion of the review process.

The National Research Council is the principal operating agency of the National Academy of Sciences and the National Academy of Engineering, serving government and other organizations. The Transportation Research Board evolved from the 54-year-old Highway Research Board. The TRB incorporates all former HRB activities but also performs additional functions under a broader scope involving all modes of transportation and the interactions of transportation with society.

TRR 488
ISBN 0-309-02274-6
LC Cat. Card No. 74-7835
Price: $3.00

CONTENTS

FOREWORD

The 11 papers in this RECORD address several topics relating to improving safety aspects of the roadside environment. Included are papers dealing with the interaction of the vehicle with impact attenuation devices, guardrails, bridge rails, median barriers, utility poles, signposts, and embankment slopes. Included also is a paper dealing with wind-induced vibrations of overhead sign supports. These papers will be of interest to those highway engineers responsible for the design, construction, and maintenance of highway safety appurtenances.

Walker, Warner, and Young report the results of a series of vehicle tests on a crash attenuator using lightweight concrete energy-absorbing cartridges. Favorable results were obtained with both head-on impacts using subcompact vehicles and angle impacts using standard-sized vehicles.

Marquis, Hayes, and Hirsch describe the development of a chain-link-fence vehicle-arresting system capable of safely entrapping an errant vehicle entering the median area between twin bridges. The net system is mounted on steel delineator posts and attached at each end to coils of metal tape designed to absorb energy through bending. Safety aspects of the system are enhanced by using breakaway supporting posts throughout.

The abridgment by Warner and Friedman discusses the future requirements for highway crash attenuators in view of scheduled improvements in vehicle crashworthiness performance and the trend toward smaller vehicles. They conclude that resulting savings due to the cost of smaller, stiffer attenuators should allow protection at two to three times as many sites.

The paper by Bronstad and Michie reports on the application of the breakaway cable terminal concept to the development of a new median barrier terminal. The terminal design was tested with both standard and subcompact vehicles and provided a significant improvement in performance over other currently specified terminals.

The criticality of mounting height of the standard W-beam traffic barrier led to the investigation of different barrier configurations. Bronstad, Michie, Viner, and Behm report on the testing of a triple corrugated beam known as the Thrie beam, which is $1\frac{1}{2}$ times the width of the W-beam. Findings of the test program indicate that the beam can be mounted to posts of existing systems needing upgrading. Further, the rub rail of median barriers can be eliminated, thus effecting a cost reduction.

The abridgment by Brewer provides an analytical solution for optimizing the design of box barrier beams by providing asymmetric sections with added thickness to the roadside flange of the beam.

Michie, Bronstad, and Alison describe the development of an approach rail-bridge rail transition using the Aluminum Association balanced rail system. Based on the results of the final test, the overall performance of the transition section was judged satisfactory considering the accepted performance criteria and present traffic barrier technology.

Criteria for installing guardrail protection at embankments are based on the relative severity of a vehicle leaving the road and going down an embankment as compared to striking the guardrail. The severity of leaving the roadway was determined by use of a dynamic vehicle simulation model. Ross and Post report on full-scale vehicle embankment tests that were used to validate the Texas Transportation Institute's version of the highway-vehicle-object simulation model and to substantiate the criteria on guardrail need.

The feasibility of modifying existing timber utility poles so that they will break away under vehicle impact was investigated by Wolfe, Bronstad, Michie, and Wong. Pendulum tests were used to demonstrate the ease with which the poles could be modified into

breakaway structures. Utility company perspectives are pointed out in discussions by Peacock and Onishi.

Strizki, Powers, Jagannath, and Reilly describe the results of 26 full-scale crash tests on steel and aluminum U-posts. Tests were conducted using both subcompact and standard vehicle impacts of sign installations containing from one to four posts. The authors found, among other things, that simultaneously impacting more than one steel post or more than three aluminum posts produced conditions that do not satisfy present Federal Highway Administration criteria. They also found that the aluminum signposts produced less severe speed changes than the steel posts when only a partial number of posts were impacted.

The final abridged paper by Kumar, Tung, Mirza, and Smith presents the results of an analytical investigation of the safety of tri-chord overhead sign support structures against wind. The study included investigation of the adequacy of the gust factor recommended by the AASHO Specifications governing the design of sign support structures and the effectiveness of stockbridge dampers in reducing vortex excitation vibration.

ANGLE AND SMALL-CAR IMPACT TESTS OF AN ARTICULATED GORE BARRIER EMPLOYING LIGHTWEIGHT CONCRETE ENERGY-ABSORBING CARTRIDGES

Grant W. Walker, Dynamics Research and Manufacturing, Inc., Sacramento;
Charles Y. Warner, Brigham Young University; and
Bruce O. Young, Energy Absorption Systems, Inc., Sacramento

A crash attenuator for errant vehicles, employing lightweight concrete energy-absorbing cartridges, has been further tested to demonstrate its capabilities to decelerate lightweight cars without excessive loads and to deflect standard-sized automobiles in side impact at high speeds and angles. Favorable test results were experienced in all phases of the testing. A Volkswagen sedan that impacted the attenuator at 58 mph (93 km/h) was driven away with 9½ in. (241 mm) of maximum front-end crush. Fendering tests involving standard-sized cars traveling at speeds up to 68 mph (109 km/h) were successfully performed, without seriously deteriorating the residual head-on capability of the attenuator. Analyses of the results of these and previous tests show that the attenuator stroke is very nearly independent of vehicle mass, causing about the same average deceleration in 60-mph head-on impacts of the 1,800-lbm (817-kg) Volkswagen and a 3,700-lbm (1678-kg) Rambler. For impacts of the same weight vehicle at different velocities, the average deceleration is roughly proportional to the 1.6 power of impact velocity.

•HIGHWAY CRASH ATTENUATORS are proving themselves as effective lifesaving systems in installations across the nation. This paper reports tests of an improved attenuator system that evolved from concepts originally applied in the water cell attenuator, coupled with sophisticated use of vermiculite concrete as an energy absorber. Prototype tests reported earlier (1) compared the system with its water cell predecessor for head-on impacts and showed improvements in deceleration profile, as compared to the water cell performance, which had been documented earlier (3, 4). This paper reports tests of an improved system involving a low-speed, lightweight car and angle impact performance and results of field trials on maintenance and refurbishment. The system demonstrated very good performance in all tests, matching or exceeding the performance of all competitive systems known to the authors and improving on the constant-stroke characteristics of the water cushion attenuator. Notable improvements in both fendering and light-car head-on performance are possible because of large attenuator weight reductions, as compared to the water cushion system.

A significant part of the total cost of crash attenuation systems results from corrective maintenance following impact. A recent California study, comparing real-world performance of three different prototype crash attenuator systems, is cited to give preliminary quantification to this problem (5).

DESCRIPTION OF ATTENUATOR SYSTEM

The basic features of the attenuator are shown in Figure 1. The construction of the device has been discussed in previous papers and will only be briefly treated here (1,2). The energy-absorbing mechanism employed involves the controlled fracture of a concrete matrix and controlled crushing of vermiculite aggregate particles. Control is provided by geometric and structural constraints: Cells are designed to resist axial

forces. The center void produces a gradual force buildup over the initial part of the stroke of each cell, allowing accommodation of inertial loads in high-speed impacts.

After the void fills by crushing, the concrete matrix is thrust through the orifice between the wires. Debris is contained within the pleated aluminum sheath and is further crushed when a sufficiently broad area is reached. The cells are glued to light, stiff plates to form cartridges and are sealed inside waterproof plastic or fiber packages. These packages are inserted into the "sandwich" hardware developed for the Hi-Dro Cell attenuator (3).

The vermiculite aggregate and wire-helix orifice built into the basic cells provide a velocity-sensitive system that is similar to, but superior in performance to, the water system originally used (4). The concrete cartridges are much lighter than the water system, so that initial deceleration in high-speed tests may be more readily controlled. The overall system exhibits constant-stroke behavior over the range of speeds and vehicle weights normally encountered, as is seen below.

Figure 2 shows details of attenuator construction.

DESCRIPTION OF TESTS

The tests reported in this paper were performed on leased facilities at the Lincoln, California, airport. Cars were either cable-guided and towed or driven by live drivers using special safety equipment.

Photographic data were obtained by two high-speed (~1000 pps) movie cameras and two standard-speed movie cameras. Documentary still photographs were also taken. Electronic acceleration data were recorded by a biaxial accelerometer pack mounted in the passenger compartment behind the driver's seat. A 500-ft (152-m) hard line connected the accelerometer pack with stationary readout equipment. Longitudinal and lateral accelerations were recorded. Figures 3, 4, and 5 show acceleration histories for the various tests.

Lightweight-Car Head-On Impacts

Two tests were performed on the Hi-Dri attenuator to evaluate lightweight car performance. A preliminary test with a Karmann Ghia VW was conducted to evaluate test conditions. The vehicle impacted at slightly more than 50 mph (80 km/h) with minimal damage. Acceleration loads were light, and the total stopping distance was approximately 10 ft (3.05 m).

A standard 1962 Volkswagen sedan impacted at 58 mph (93 km/h). Total stopping distance was 13 ft (3.96 m). The front-end crush was only 9½ in. (241 mm). (The spare tire was in place in the front truck compartment.) Following the test, the engine was started, and the VW was backed from the Hi-Dri attenuator on its own power and driven from the site, with the front fenders rubbing the wheels. Had the impact occurred on the freeway, the car could have been driven a few miles to get help. After the fenders were pulled away from the tires, the test vehicle was driven a distance of 40 miles (64 km) at freeway speeds. The front wheels were still in alignment. Figure 6 shows photographs of these tests.

Occupants of the VW could easily have survived the impact. Occupants wearing lap and shoulder belts could have escaped without injury (7).

Angle Impacts Into the Side of the Attenuator

Two high-speed angle impacts were performed with a standard-sized car on a nominal 20-ft (6.1-m) long standard eight-bay unit protecting a rigid 3.5-ft (1.07-m) wide barrier. The vehicles weighed approximately 4,000 lbm (1800 kg) and impacted at 60 mph (97 km/h) or greater. The impact angle relative to the axis of the unit was 15 deg. This, added to the 5-deg half-wedge divergence of the attenuator, resulted in a 20-deg impact angle with the face.

The impact point on the unit was nominally 6 ft (1.83 m) ahead of the rigid corner. It was selected to provide a severe test for the attenuator. The highest impact loading

Figure 1. Hi-Dri cartridge vehicle attenuator.

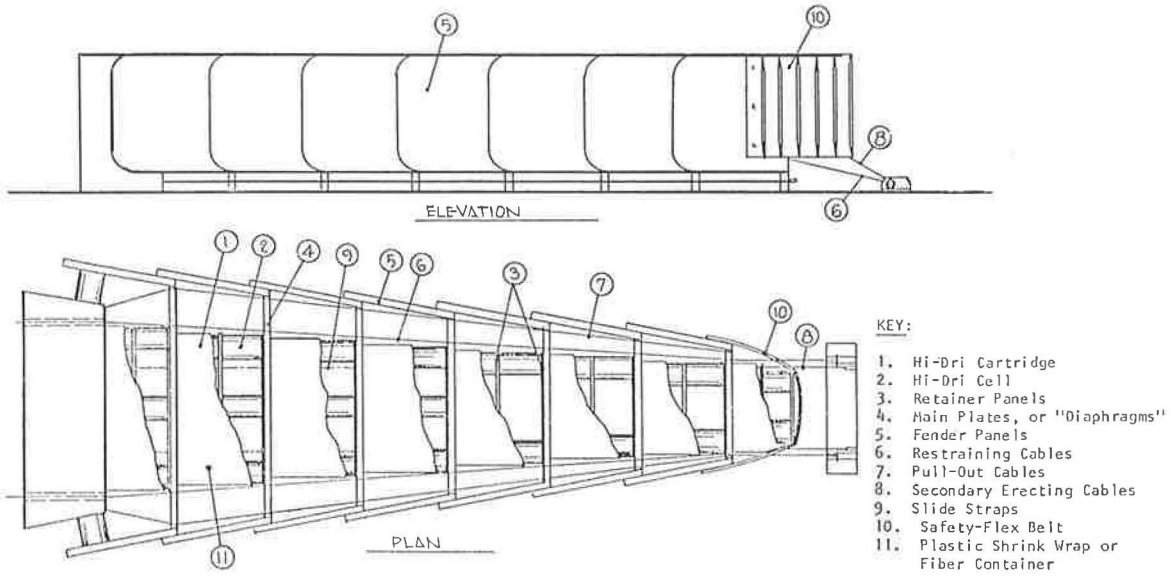

Figure 2. Hi-Dri cartridge.

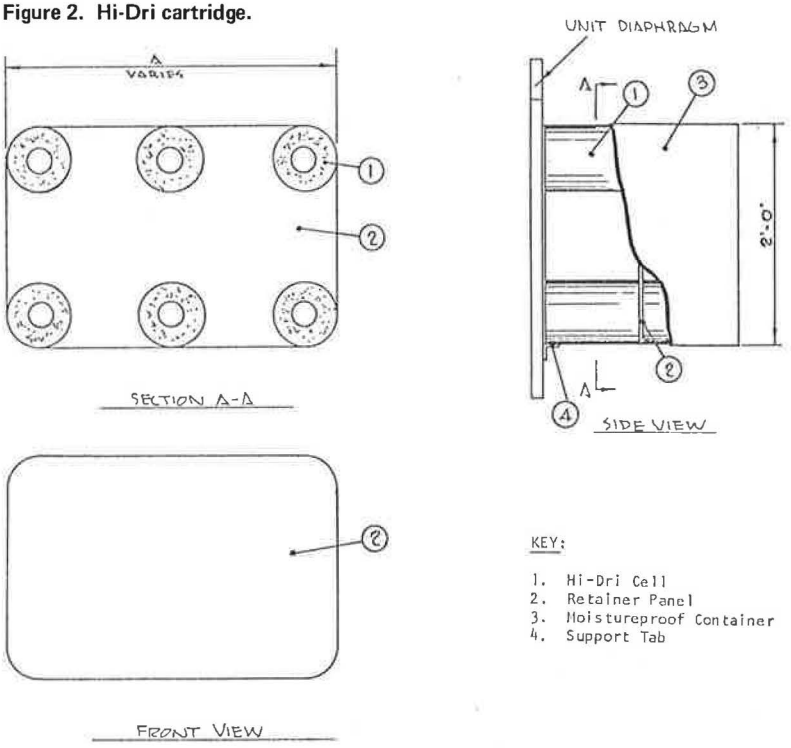

Figure 3. Acceleration trace of head-on impact following high-speed angle impact.

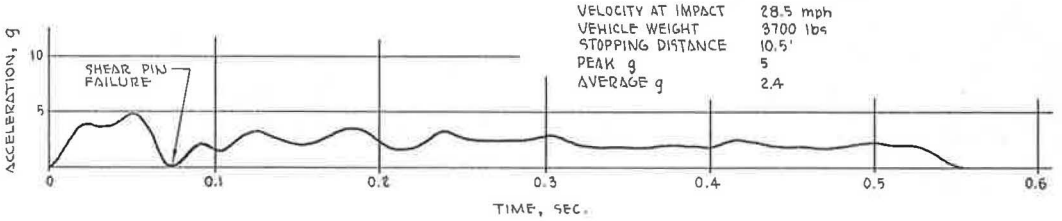

Figure 4. Longitudinal acceleration of head-on impact with Volkswagen sedan.

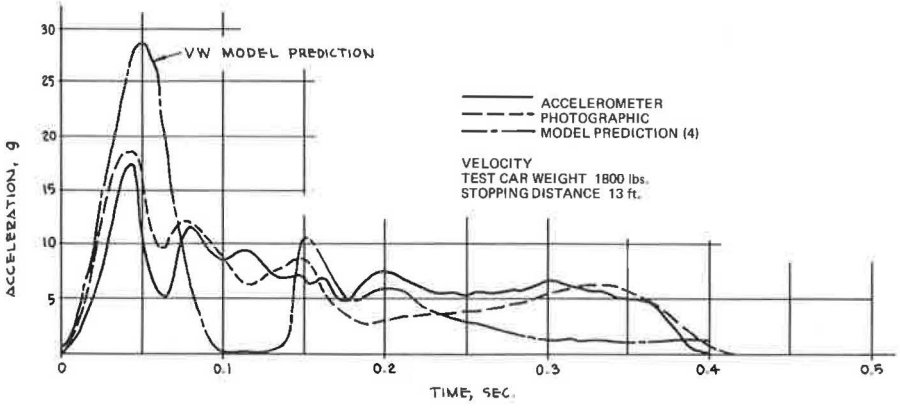

Figure 5. 20-deg angle impacts with standard-sized cars: (a) lateral and (b) longitudinal accelerations of 4,000-lbm vehicle traveling at 60 mph and (c) longitudinal acceleration of 3,700-lbm vehicle traveling at 68 mph.

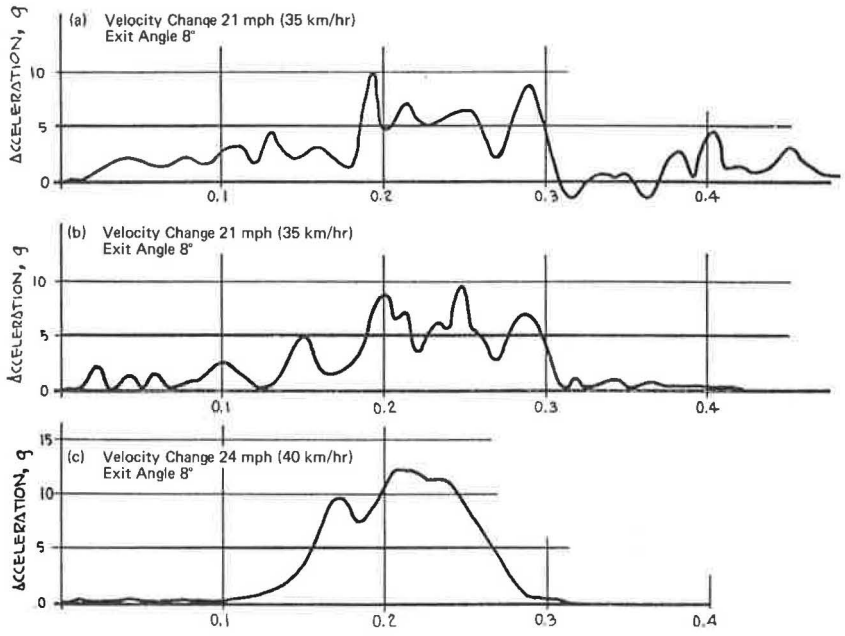

Figure 6. Subcompact cars after (a) 58-mph impact and (b) 50-mph impact.

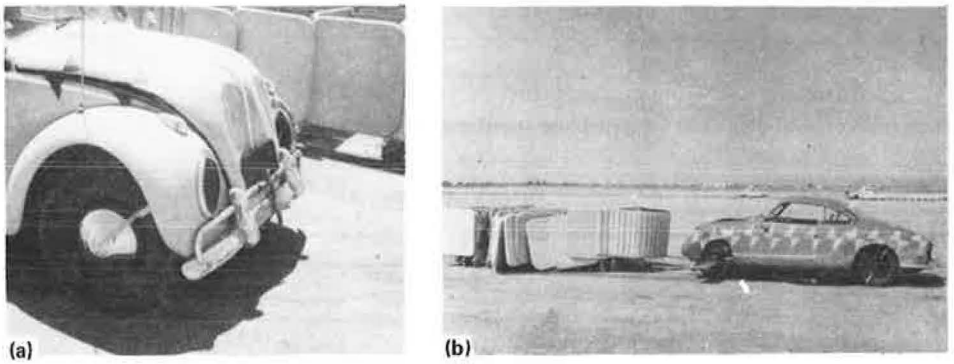

occurred in the two to three bays just ahead of the rigid barrier (commonly referred to as the coffin corner area). Impacts at this point ensure high loads on the vehicle and attenuator.

In the first test, a 1960 Chevrolet Bel Air four-door sedan impacted at 68 mph (109 km/h) and 20 deg. The exit angle was 8 deg with the face of the unit, resulting in a 28-deg total change of direction. After impact the test vehicle followed a curving path back to the side of the road and came to rest 165 ft (50 m) from the point of impact. The left front quarter panel of the vehicle was severely damaged. The left front wheel was torn loose from the lower control arm. The change of velocity during impact was 24 mph (38 km/h). Unfortunately, electronic acceleration data were lost during this test.

Photographic data indicated a smooth redirection of the vehicle with a roll about the longitudinal axis of only 15 deg away from the barrier. The left side of the car rose approximately 1 ft (0.3 m) from the ground, but the right wheels remained on the ground throughout the test. Three side panels on the attenuator were moderately damaged, but they remained in place and were judged capable to resist further side impacts until replaced. Approximately 10 percent of the head-on energy-absorbing capability of the unit was destroyed during this angle impact, but the shear pins remained intact and kept the unit erect, thus preserving its capability to sustain another head-on or angle impact without maintenance.

A second test was run at 60 mph (97 km/h) to further demonstrate fendering capability. A 1962 Dodge four-door sedan weighing approximately 4,000 lbm (1800 kg) impacted the side of the unit at the same point and angle as before. The results were almost identical except that there was less damage to the attenuator and car. The exit angle of the second test car was 9 deg, compared with 8 deg for the first car. There was no roll about the longitudinal axis of the second test vehicle. The change of velocity during impact was 21 mph (34 km/h). The peak longitudinal acceleration was 10 g, with an average of less than 4 g during the 150-msec duration of highest deceleration. The peak recorded lateral acceleration was 10 g with 4.5 g average during the highest 150 msec.

Low-Speed Impact of Standard-Weight Vehicle

Immediately following the 60-mph angle impact, a low-speed head-on test was run to demonstrate the capability of the attenuator to sustain repeated impacts without maintenance. A test truck weighing 3,700 lbm (1678 kg) with driver impacted the attenuator at 28.5 mph (46 km/h), without exhausting unit capacity.

The acceleration trace shown in Figure 3 demonstrates the velocity-sensitive characteristic of the cells compared with much higher g loads when impacted at higher speeds. Following the peak loading of 5 g, which parted the shear pins, the acceleration was 2.4 g for 400 msec. The driver reported no discomfort. Total stopping distance was 10.5 ft (3.2 m). Figure 7 shows photographs taken during and after this test.

REDIRECTION IN ANGLE IMPACTS

The lightweight concrete system offers improved performance in angle impacts as compared to the water cell attenuator. The vermiculite cells provide an initial compression resistance to the "diaphragms" as impact load is transferred from the side panels to the diaphragms. This keeps them vertical, which in turn maintains a vertical face for each of the side panels. The initial low-force yield of the energy-absorbing cartridges reduces loads on the attenuator structure. After initial yield, the firm resistance of the cells prevents tipping of the side panels, to the degree seen in the water tube attenuator. Concrete cells are positioned near the top of the 40-in. (1.02-m) high diaphragms at the back of the unit. This is done primarily to prevent head-on impacting vehicles from leaving the ground. The high position of the cells also helps to maintain a firm vertical face to resist the force of a vehicle impacting at an angle.

The fendering performance of the Hi-Dri sandwich is somewhat better than that of the same system using water cells, primarily because the decreased weight of the attenuator allows the use of more tension in the erecting cables without excessive light-car loads in head-on impacts. The energy-absorption capability of the unit at the rear corner was enhanced by positioning two small cartridges facing the side of the rear side panel.

Side panel damage was moderate during the fendering impacts. The units could probably have sustained repeated fendering impacts without service.

CONSTANT-STROKE CHARACTERISTICS

A constant-stroke attenuator offers performance and cost advantages over a constant-force system. Performance advantages accrue because vehicle decelerations are essentially the same for a given impact velocity, regardless of vehicle weight and because vehicle deceleration decreases as velocity decreases. Cost advantages accrue in situations where space is limited, inasmuch as large and small cars are decelerated in about the same distance.

A precisely constant-stroke device would provide a resisting force given by

$$\overline{F} = W\overline{G} = kWV_o^2 \tag{1}$$

where $\overline{F}$ = average attenuator force, W = vehicle weight, $\overline{G}$ = average deceleration of the vehicle, V_o = impact velocity, and k = a proportionality constant.

The actual characteristics of the Hi-Dri attenuator are shown in Figure 8 for three head-on test conditions, representing standard car near design speed and two other impacts at roughly half weight and half speed. A reasonable fit to this data is provided by the equation

$$\overline{F} = W\overline{G} = 0.0231W^{0.92}\ V_o 1.6 \tag{2}$$

Figure 9 shows a comparison of the ideal constant-stroke performance of Eq. 1, referenced to the standard-car high-speed impact, and the actual performace with an approximation of Eq. 2. As can be seen, the attenuator approaches constant-stroke behavior very closely for vehicles of different weights, at least over the range tested.

It should be noted that these equations reflect the average forces and decelerations. Peak forces will be higher in every case and will be accentuated in the case of the small car because even small inertias will cause large forces on initial impact. One of the most significant advantages of the lightweight concrete attenuator system is demonstrated in Figure 5. Because of its low mass, the small car is particularly sensitive to momentum exchange with heavy barrier components. This is shown by comparison of the predicted vehicle deceleration for the Hi-Dro Cell attenuator with those measured on the lightweight concrete system. The difference is even more dramatic when comparison is made with the 40-mph Hi-Dro cushion Volkswagen test performed by TTI (4). The TTI test indicated a peak vehicle deceleration of about 15 g at 40 mph—roughly the same as that seen in the Hi-Dri system at 60 mph. The reason for this dramatic reduction is made quite clear by momentum analysis. The energy-absorbing materials in the Hi-Dri cushion weigh slightly more than one-tenth of those in the Hi-Dro cushion—about 500 lbm versus about 5,000 lbm (152 kg versus 1520 kg). This weight reduction has produced the excellent light-car response demonstrated here while allowing increase in the secondary erecting cable shear-pin strength and corresponding improvement in fendering impact modes. But even peak forces on the light car with this attenuator will not exceed the average force on the same car when it impacts a constant-force attenuator designed for the heavy car.

The attenuator does not approach constant-stroke behavior as nearly for different velocities as for different vehicle weights, but it does offer significant force reductions for lower speed impacts, as compared to fixed-force systems.

MAINTENANCE CONSIDERATIONS

The problem of placing an attenuator back into service as quickly as possible following a high-speed head-on impact is significant. It deserves, and has received, intensive design attention. The costs of materials, manpower, and equipment expended in maintenance efforts constitute a very significant part of the overall attenuator cost.

Several attempts have been made to gather appropriate crash information for evaluation of actual attenuator performance. The California Division of Highways has a study

Figure 7. Three views of attenuator during and following 29-mph head-on impact immediately after 60-mph angle impact.

Figure 8. Constant-stroke characteristics of attenuator.

SYMBOL	VEHICLE	WEIGHT (lb.)	IMPACT SPEED (mph)	AVERAGE DECELERATION (g)	ATTENUATOR STROKE (ft)	CAR CRUSH (ft)
———	VOLKSWAGEN	1800	58	8.62	12.25	.79
—·—·—	RAMBLER	3700	56	7.22	13.67	.83
— — —	TEST TRUCK	3700	28.5	2.50	10.50	0

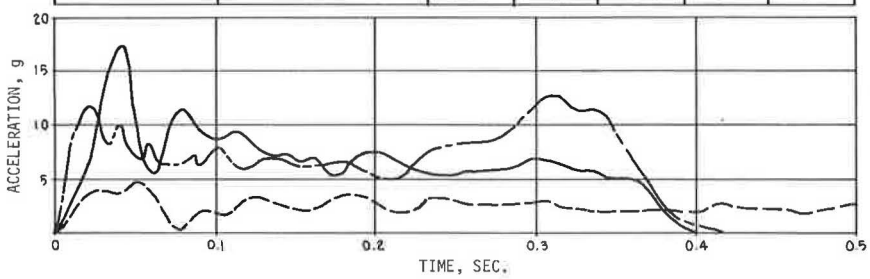

in progress (5) in which three different attenuator designs at nine freeway sites are monitored. Extensive records have been maintained on systems at a total of nine installations, giving a complete economic history. Also, at three of the sites, a closed-circuit television record is made of each impact, from which vehicle speed, mass, and trajectory can be estimated. Reported accidental property losses and injuries are also being tabulated.

Table 1 gives a summary of the data recorded through July 1973. (Each row gives data for one impact.) It illustrates one important feature of attenuator economics that must be addressed in the near future. Maintenance costs can far outstrip initial costs in relatively short periods of use. This has been a significant problem in many areas already. Money earmarked to assist states in the purchase and installation of attenuator hardware has not always found counterpart funds for maintenance. Hence many good attenuator installations have gone wanting for repairs; other sites are not protected at all because maintenance budgets are inadequate to sustain installations.

In the California study of impacts on steel drum attenuator systems in actual service during a 2-year period, repair costs averaged about $1,000 per impact in reported accidents and more than $200 per unreported accident. But a more important consideration than repair cost is the risk of bodily injury to maintenance personnel, due to accidents during the repair process, measured in terms of man-hours of exposure to traffic. For the steel drum barriers, in reported accidents, this averaged over 40 man-hours per accident, whereas for the water tube attenuator and the Fibco sand barrier exposure averaged about 20 man-hours per reported accident (5).

The Hi-Dri attenuator system is known to have still further maintenance man-hour advantages over the water cell attenuator. Although the same basic hardware is employed, the concrete cartridges are designed to allow quick replacement. Individual cartridges are light enough to be handled easily by two men. They are set into the eight to 10 bays between the major plates or diaphragms. Each cartridge consists of eight to 12 individual cells glued into a structural unit between thin plates and covered by waterproof material to form a cartridge. The total weight of the nine cartridges needed for the average attenuator is less than 500 lbm (227 kg), easily carried in a half-ton pickup truck.

The cartridges are inserted in the top of the unit. They rest on small metal brackets bolted to the main diaphragms. This makes it possible to place the cartridge into the attenuator without field adjustment. A complete set of recharge cartridges has been placed into the unit by two men in as little as 75 s, under ideal conditions. Under actual field conditions, with a trained two-man crew the time should be significantly less than the average values reported in the California study.

This was demonstrated recently in the test environment. Following several head-on impacts reported in this test series, the attenuator was pulled to its original position by a half-ton pickup truck. After the shear pins were replaced in the erection cable clevises, the spent cartridges were removed and replaced. A two-man crew completely refurbished the attenuator in less than 12 min. Under most conditions, the total time of reservicing should be no more than 20 to 25 min, or less than 1 man-hour per accident, with no more equipment than can be carried to the site in a half-ton pickup.

The relatively sophisticated design of the support hardware for this system makes it capable of sustaining repeated fendering impacts without much loss of head-on capability. This feature can offer a significant extra margin of protection between visits of the maintenance crew.

WEATHERABILITY

Users of attenuator systems are understandably concerned with weather resistance capability. This was recognized at the early stages of development of the Hi-Dri system. The vermiculite concrete is kept moisture-free and protected from the erosive effects of the elements by casing the light in a pleated aluminum foil wrap and sealing with a roofing tar-and-chip coating. Further protection is provided by a sealed, weather-resistant fiber cartridge package, which also provides for quick and easy reburbishment. In the unlikely event that moisture should penetrate these three barriers, it is improb-

Figure 9. Fixed-stroke comparisons.

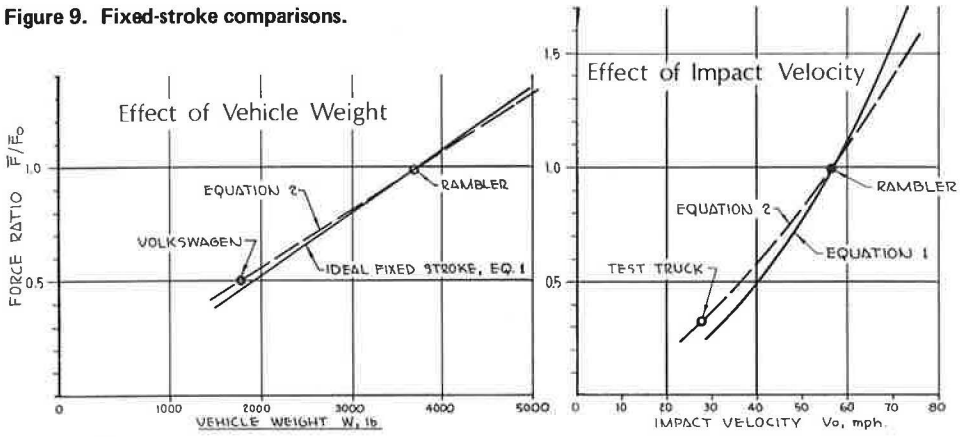

Table 1. Attenuator comparison.

Barrier	Year	Total Cost of Repair (dollars)	Injury	Disabled Vehicle	Estimated Speed (mph)	Man-Hours of Exposure to Traffic
Sand inertial (Fibco)	1971	1,334	yes	yes	65	36
	1972	646	no	no	60	10
Total		1,980				46
Average		940			62.5	23
Steel (Texas)	1971	2,806	yes	yes	55	38
		2,200	yes	yes	65	50
	1972	529	yes	yes	65	53
		686	no	yes	65	46
		675	yes	yes	50	58
		1,180	no	yes	60	42
		196	no	yes	55	8
	1973	558	yes	yes	65	35
		654	yes	yes	55	52
Total		9,484			470	382
Average		1,053.77			59	42.4
Water tube	1971	99	yes	yes	65	11
		88	no	yes	65	10
	1972	329	yes	yes	55	23
		117	no	yes	40	14
		152	yes	yes	55	18
		358	yes	yes	65	24
		246	yes	yes	65	18
	1973	2,058	yes	yes	60	—[a]
		283	no	yes	60	25
		96	yes	yes		13
Total		3,826			530	156
Average		382.60			59	19.5

Note: 1 mph = 1.6 km/h.

[a]Not stated.

able that attenuator performance will be substantially deterioriated. The asphaltic cement used in the preparation of the concrete cells is, in itself, moisture resistant. Cells used in an early test program were removed from the site, left in the open, and exposed to the rain, sun, frost, and wind for more than a year without measurable decrement of strength characteristics.

CONCLUSIONS

The following conclusions are warranted by the results of tests covered in this and previous reports (1, 2, 3, 4).

1. The performance of the Hi-Dri attenuator is significantly better than that of the Hi-Dro cushion attenuator, especially for lightweight vehicle impacts;
2. Multiple-hit capability without service following a severe side angle hit has been demonstrated;
3. The velocity-sensitive characteristics of the Hi-Dri cartridges make it possible to design the shortest possible unit for a range of car weights and impact velocities, while providing a margin of safety for high-velocity impacts that exceed design specifications;
4. The Hi-Dri attenuator may be refurbished after 60-mph (97-km/h) frontal impact by two men in a light pickup truck in less than 30 min or less than 1 man-hour of exposure to traffic per accident;
5. Traffic interference from flying debris during impact with the attenuator is eliminated (there is no debris discharge from a Hi-Dri unit when struck within design conditions); and
6. Design provision for three levels of moistureproofing has eliminated concerns regarding weatherability.

REFERENCES

1. Walker, G. W., Young, B. O., and Warner, C. Y. Crash Tests of an Articulated Energy-Absorption Gore Barrier Employing Lightweight Concrete Cartridges. Highway Research Record 386, 1972, pp. 19-27.
2. Warner, C. Y., and Walker, G. W. Crash Test Performance of a Prototype Lightweight Concrete Energy-Absorbing Guardrail System. Highway Research Record 343, 1971, pp. 13-18.
3. Warner, C. Y. Hydraulic-Plastic Cushions for Attenuation of Roadside Barrier Impacts. Highway Research Record 259, 1969, pp. 24-34.
4. Warner, C. Y., and Free, J. C. Water-Plastic Crash Attenuation System: Test Performance and Model Prediction. Highway Research Record 343, 1971, pp. 83-92.
5. Preliminary Results of a Maintenance and Performance Study of Three Attenuator Types at Nine Los Angeles Freeway Sites. Los Angeles Regional Office, California Division of Highways, Aug. 20, 1973 (final report due in early 1974).
6. Patrick, L. M., and Trosien, K. R. Volunteer, Anthropometric Dummy, and Cadaver Responses With Three and Four Point Restraints. Automotive Engineering Congress, Society of Automotive Engineers, SAE Paper 710079, Jan. 1971.

VEHICLE-ARRESTING SYSTEM USING CHAIN-LINK FENCE

E. L. Marquis, G. G. Hayes, and T. J. Hirsch, Texas Transportation Institute, Texas A&M University

Several areas along highways can be dangerous to errant high-speed vehicles that run off the roadway. Among these are medians between twin bridge approaches, dead ends, and barriers that close off entrance and exit ramps. A chain-link vehicle-arresting system was designed to prevent motorists from entering the median area between twin bridges and was tested. When the system proved a failure, it was modified by the manufacturer and retested under head-on and angle impacts. Retesting verified that dangerous median configurations could be successfully protected by a net system. It was also found that breakaway support posts would improve vehicle entrapment in the net.

•SEVERAL FEATURES or areas along highways can be hazardous to vehicles leaving the travel way at high speeds. In many cases, conventional guardrails or crash cushions are not an effective or economical means of preventing vehicles from entering these hazardous areas. Some obvious areas of this type are

1. Median areas or holes between twin bridges on divided highways,
2. Dead ends or termination of roads or highways, and
3. Barriers to close off entrance and exit ramps on freeways.

The chain-link-fence vehicle-arresting system reported on here was designed specifically to prevent motorists from entering the median area or hole between twin bridges on divided highways. At the present time, either guardrails or no protective device is used in these areas. Guardrails, if used, will generally be inadequate to prevent a high-speed vehicle from entering this hazardous area because the vehicle will be impacting it almost head-on. The device reported on here is composed of a chain-link fence mounted on standard 2-lbm/ft (3-kg/m) steel delineator posts. Each end of the fence is attached to a Van Zelm metal bender energy absorber mounted on a standard wooden guardrail post (Fig. 1). Devices similar to this metal bender have been used at automobile drag race tracks under the trade name of Dragnet. The Texas Highway Department has a barrier at the Bolivar Ferry Landing near Galveston that uses the metal benders as an energy absorber.

Several tests have been conducted on similar installations (1, 3) in which the net between the metal benders was straight and level. District 11 of the Texas Highway Department had a potential installation in which the net connecting the two metal benders would traverse a median ditch with 12:1 side slopes (Fig. 1). Officials of this district were concerned about the interaction of an errant vehicle and a dragnet system spanning a ditch section of this configuration.

A test site with 12:1 side slopes was developed at the TTI proving grounds to simulate field conditions. Then the dragnet system was installed. A head-on test was conducted, and the metal bender tapes failed to perform as intended. The manufacturer had modified the design of the system to simplify and improve the installation of the metal bender units. A hole of sufficient size to fit over the top of a standard 7-in. (180-mm) guardrail post was placed in the center of the metal bender. The closure of the case provided an axle for the coil of tape to spin around. No bushing or bearing had been provided between this axle and the coil of metal tape. Consequently, during the test, the tape tightened around the axle and locked up, resulting in tape breakage. The manufacturer, who provided brass bushings for all metal benders in stock, new

tapes, and some financial support for retesting, was contacted. The retesting with brass bushings verified that the median configuration could be successfully protected by a dragnet system. As a result of the first retest, it was found that the fence support post could be made to break away to improve the fence-vehicle entrapment performance. For the final test, the fence posts were cut 4 in. (100 mm) above ground line, and a simple bolted lap splice was used as a breakaway feature.

DESCRIPTION OF ARRESTING SYSTEM

The basic arresting system consists of a chain-link fence attached through cables at each end of energy-absorbing devices. These devices, called metal benders, are cases containing a coil of metal tape that emerges from the case after bending back and forth around a series of stainless steel pins. The ends of the tapes are attached with cables to the net. When a vehicle engages the fence (or net), the end tapes are pulled out through the series of pins and exert a stopping force that is dependent on the size of the tape.

Figure 1 shows the system tested here. In this test series, the design resistance of each metal bender was 4,000 lbm (1800 kg). Previous tests of a similar system indicated that reasonably accurate predictions can be made of the amount of tape required and the stopping distance for a vehicle of known weight and impact speed (1).

The net itself consisted of 11-gauge chain-link fence, 48 in. (1.2 m) high, with $\frac{3}{8}$-in. (9.5 mm) galvanized restraining cables threaded through the top and bottom. The net was supported in an upright position by five 2-lbm/ft (3-kg/m) Texas Highway Department standard delineator posts driven 2 ft (0.6 m) into the ground. The posts were cut and lap-spliced with brass screws to provide the breakaway feature. The net was attached to the back side of the posts with aluminum wire ties.

The metal benders themselves were mounted on 7-in. (180-mm) diameter wooden guardrail posts embedded 48 in. (1.2 m) in 12-in. (0.3-m) diameter concrete footings. The metal bender case with its contained coil of tape fits around the post and rests on a collar that allows the case to turn in the direction of the applied force. Other metal benders, tape tensions, and net arrangements can be designed to fit the intended site. Figure 2 shows the layout of an installation on US-59 in Texas.

VEHICLE AND INSTRUMENTATION

The vehicle used in all three full-scale tests was a 1965 Pontiac sedan that weighed 4,400 lbm (1995 kg) including an anthropometric dummy secured in the driver's seat with a lap belt anchored through a load cell that indicated lap-belt force.

Longitudinal and lateral accelerometers were mounted on each longitudinal frame member to sense vehicle accelerations. A flash bulb and an event mark on the electronic data were actuated by a tape switch on the front bumper. This allowed the electronic data with high-speed film to be synchronized. All electronic data were transmitted by telemetry to a ground station where the data were recorded on magnetic tape and displayed in analog form on a strip chart.

In addition to documentary motion pictures, the tests were recorded on high-speed film, which includes timing marks. This film was analyzed to give time-displacement data for the vehicle. Two data cameras were oriented perpendicular to the vehicle's path and had overlapping fields of view. The sequential photographs (Figs. 3, 6, and 8) were made from these high-speed motion pictures.

DESCRIPTION OF TESTS

Test 2146-D1

Test 2146-D1 was a head-on impact in the center of the net at 62.9 mph (101.2 km/h). The tapes coiled inside the metal bender cases tightened on the inner case wall (or core) and locked up with the result that the net broke free. The tape on the left parted at the connection to the cables after 6 ft (1.8 m) of tape was pulled from the metal bender, whereas the tape on the right played out about 6 ft and then parted near the metal bender. At this time the vehicle had traveled 21.1 ft (6.43 m) and had slowed to

55 mph (88.5 km/h). The average deceleration to this point was 1.4 g. The test data for all tests are given in Table 1, and Figure 3 shows sequential photographs of the first test. Figure 4 shows the vehicle after the test.

Static Tests

It was evident from the results of test D1 that the metal bender tapes must be coiled around a core that is free to turn. Consequently, a brass bushing (Fig. 5) was added, and static tests of the metal bender were conducted. These static tests were conducted by using a small crane to pull the tape at very slow speeds (about 1 fps or 0.3 m/s). A load cell was placed in line with the tape and crane to measure the pull-out force during the tests. About 50 ft (15 m) of tape was pulled during each test. The loads on the tape were relatively constant at 3,950 lbf (17 570 N) (rated capacity of MPB-5 metal bender was 4,000 lbf or 17 800 N).

Dynamic Test of Metal Bender With Bushing

After the static tests, a new tape was installed in one metal bender that was attached to an iron pipe, and the running end of the tape was attached through 200 ft of 1-in. (60 m of 250-mm) cable to a 5-ton (4.5-Mg) truck. The truck was driven at about 25 mph (40 km/h) past the metal bender and reached the end of the cable. The truck's momentum pulled out 67 ft (20 m) of tape, and no tendency to bind was observed. At this stage, it was felt that the dragnet was ready for further full-scale testing.

Test 2146-D2

Test D2 was intended as a rerun of test D1. The center, head-on impact speed was 57.1 mph (91.5 km/h). The vehicle stopped 60 ft (18 m) after impact, and again the center support post was bent over and allowed the vehicle to pass over it, whereas the net broke away from the other posts. Sequential photographs are shown in Figure 6. The net entrapped the front of the vehicle quite low as shown in Figure 7. The center post bending away from the vehicle may have caused this.

The left-hand tape pulled out 37 ft (11.3 m), whereas the right-hand tape pulled out 39 ft (11.9 m). This represents about 300 kip/ft (5.25 MN/m) of work, assuming 4,000 lbf (17 800 N) on each tape, as compared to 480 kip/ft (7.0 MN/m) of kinetic energy in the vehicle at impact. The predicted stopping distance (1) was 85 ft (26 m), which is 25 ft (7.6 m) more than observed. However, the theory does not include friction with the ground or other sources of energy loss. The predicted peak deceleration was 1.7 g, as compared to 2.0 g measured by the accelerometers. The decelerations are near to the accelerometer's lower limits, and thus the accelerometer data are only approximate.

The vehicle, which stopped while traveling in a straight line, did not exhibit any unstable behavior and was not damaged. The deceleration forces were well below the accepted tolerance levels for properly restrained or unrestrained humans (2).

Test 2146-D3

In test D3, the vehicle was directed into the center of the net at 30 deg to the perpendicular to the net. The wire mesh was reused. The deformation due to the previous test can be seen in Figure 8. The impact speed was 60.1 mph (96.7 km/h) giving an initial kinetic energy of 530 kip/ft (7.7 MN/m). The vehicle swerved slightly to the left as it went into the simulated median, and the left front bumper struck the guidance cable anchor just prior to impact with the net. This put a large peak on the accelerometer data from the left frame member (and a lesser one on the data from the other side), which masked the initial reaction with the net. The vehicle was stopped in a relatively straight line in 65 ft (20 m) with 34 ft (10 m) of tape expended on the left and 52 ft (16 m) on the right. Again, the predicted stopping distance of 92 ft (28 m) was higher than observed, but the effects of striking the anchor post, friction with the ground, and going uphill after impact were not included in the estimate. Sequential photographs are shown in Figure 8.

In the test, the center net-support post was made breakaway by cutting it in two

Figure 1. Chain-link vehicle-arresting system.

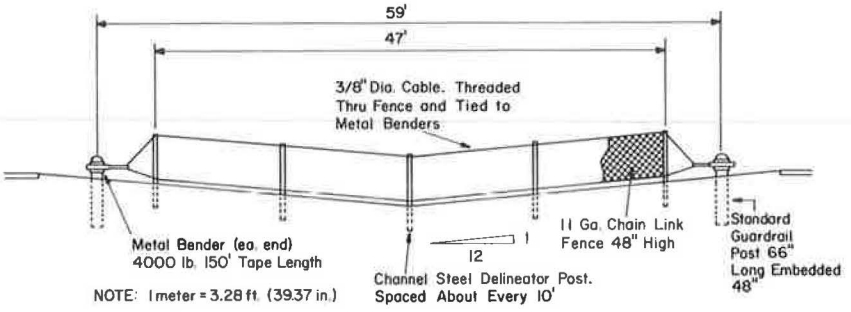

Figure 2. Layout of installation on US-59.

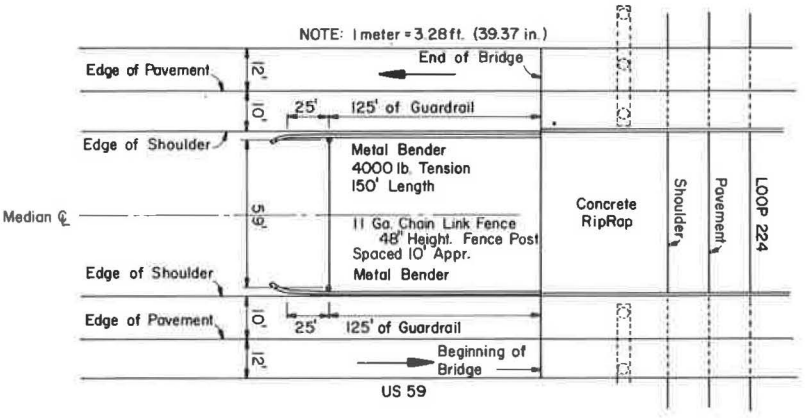

Table 1. Test data.

Specification	Test D1	D2	D3
Angle (deg)	0	0	30
Film data			
Initial speed (fps)	92.2	83.8	88.1
Final speed (fps)	80.8[a]	0	0
Maximum forward travel (ft)	21.1	59.8	69.4
Time to maximum forward travel (s)	0.26[a]	1.31	1.49
Average deceleration (g)[b]	1.4[a]	2.0	1.8
Electronic data			
Peak longitudinal deceleration (g)	3.1	2.0	—[c]
Peak lateral deceleration (g)	2.8	6.3	—[c]
Peak seat-belt force (lbf)	148	220	150
Physical measurements			
Tape runout (ft)			
Right	6.0[a]	39.3	52.0
Left	6.0[a]	36.7	34.0
Stopping distance (ft)		59.8	69.4

Note: 1 fps = 0.3 m/s; 1 ft = 0.3 m; 1 lbf = 4.4 N.

[a]At time metal tapes failed.
[b]$a = (V_o^2 - V_f^2)/2gs$.
[c]Collision with guide cable anchor masks interaction with net.

Figure 3. Test D1.

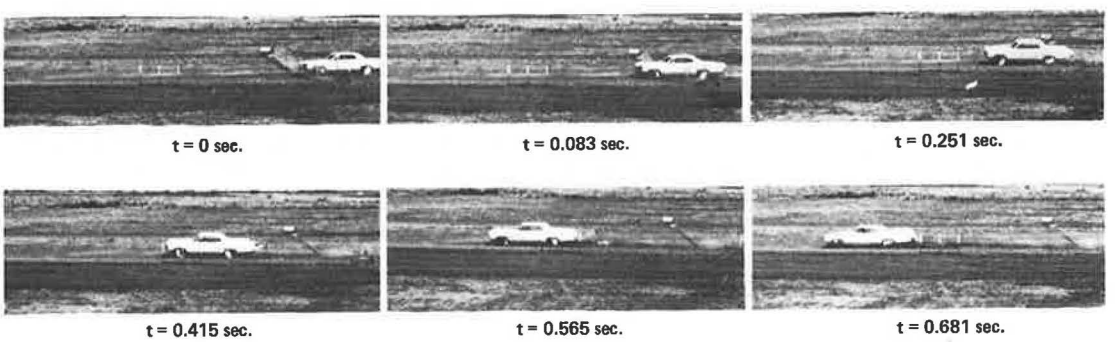

Figure 4. Vehicle after test D1 in which both tapes failed.

Figure 5. Brass bushing placed inside coil of reserve tape.

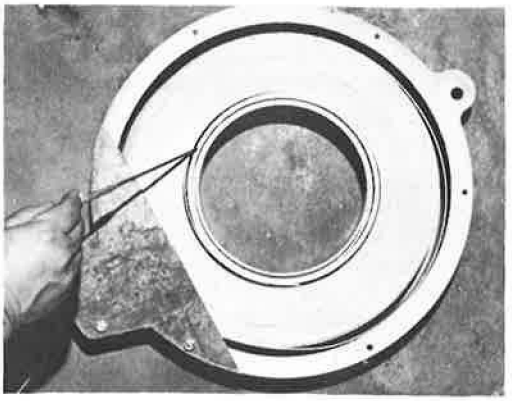

Figure 6. Test D2.

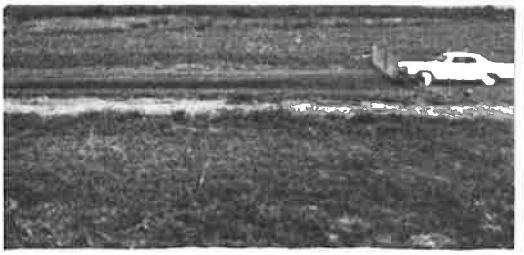

t = 0 sec.

t = 0.186 sec.

t = 0.267 sec.

t = 0.296 sec.

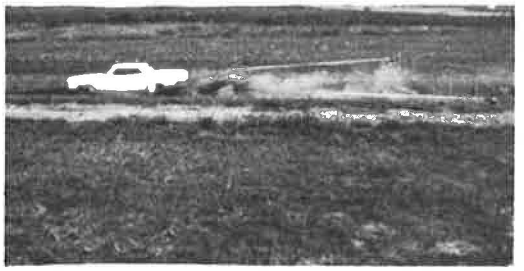

t = 0.916 sec.

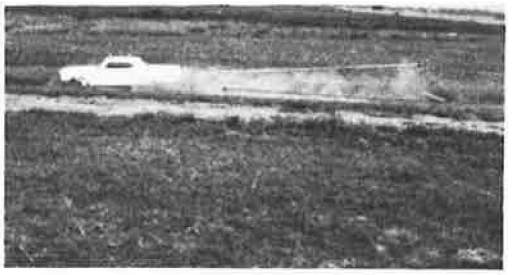

t = 1.786 sec.

about 4 in. (100 mm) above the ground and fastening the two parts together with a lap splice secured by $^{3}/_{16}$-in. (4.7-mm) brass screws (or bolts). The post bent around the front of the car as shown in Figure 9. Note that the net entrapped the nose of the vehicle more securely than it did in test D2 (Fig. 7), and the bent breakaway support seems to serve as a guide in shaping the "pocket." The other posts could have been (and should be) made to break away for noncentric impacts.

DISCUSSION OF RESULTS

This particular dragnet system performed as intended after the bushings had been added to the metal benders to keep the coil of reserve tape from binding. The 4,400-lbm (1995-kg) car was stopped in a straight line from approximately 60 mph (97 km/h) with tolerable decelerations with no noticeable damage in both the head-on and 30-deg impacts.

The stopping distance predictions based on previously developed equations were greater than observed, assuming 4,000 lbf (17 800 N) of tension from each metal bender. The stopping distance in the head-on test was 60 ft (18.3 m) as opposed to the predicted 85 ft (25.9 m), and in the angled test was 69 ft (19.8 m) compared to 92 ft (28 m) predicted.

From analysis of the first test, in which the system failed and allowed the vehicle to go free, an estimate of the vehicle deceleration due to vehicle-ground interaction can be made. Observation of the film data over a period after the tapes broke indicates a deceleration of about 0.15 g. Because the vehicle traveled 60 ft (18.3 m) in test D2 and 65 ft in test D3, this could account for 40 and 43 kip-ft (54 and 58 kJ) of energy respectively. The initial kinetic energy of the vehicle was 480 kip-ft (650 kJ) in the head-on test and 530 kip-ft (720 kJ) in the angled test. Assuming that the energy yet unaccounted for was expended in the metal benders, the equivalent tape tensions can be computed by dividing the initial energy minus the energy lost because of rolling by the total tape pullout distance. In the head-on test, 76 ft (23.2 m) of tape was expended, whereas, in the 30-deg test, 86 ft (26.2 m) was used. This gives equivalent tape tensions of 5.8 and 5.7 kips (25.8 and 25.4 kN) respectively. (In test D3 some energy was lost in the collision with the guide cable anchor.) Less than 1 fps (0.3 m/s) of speed change would account for enough energy to make two equivalent tape tensions equal at 5.8 kips (25.8 kN). It is concluded that in both the head-on and angled test configurations dynamic tape tension forces of about 5.8 kips will give accurate predictions. Friction between the bushing and core and other dynamic effects could account for these observations. There are also other sources of discrepancies, such as stretch in the net and the assumption in the equations that the vehicle has no width, but these sources do not contribute errors of the magnitude seen here. Until further dynamic tests are conducted on these modified metal benders, it would seem that a dynamic load factor of 1.4 would be appropriate for use on metal benders with center holes when vehicle decelerations are being estimated. For estimating vehicle stopping distance, it would be conservative to use the 4,000 lbf (17 800 N) rated tape tension for these metal benders.

The breakaway net-support post seemed to permit better entrapment of the vehicle in test D3 than in test D2. Therefore, it seems desirable to convert all posts to the breakaway type inasmuch as noncentric impacts are likely in the field. These posts can be made breakaway by cutting, overlapping, and fastening with brass screws near the ground.

CONCLUSIONS

The dragnet installation using the Van Zelm metal benders is suitable for certain highway applications. The results of tests reported here show that the system may be installed in V-ditch medians with side slopes of 12:1 ratio, such as those found in wide medians. Certain precautions are necessary to ensure optimum performance of an installation.

1. Bushings must be placed between the axle of the metal bender case and the tape coil so that the coil is free to turn as the tape unwinds from the metal bender (Fig. 5).

Figure 7. Vehicle entrapped in net after test D2.

Figure 8. Test D3.

t = -0.396 sec.

t = -0.138 sec.

t = -0.036 sec.

t = 0 sec.

t = 0.119 sec.

t = 0.199 sec.

Figure 9. Vehicle entrapped in net after test D3.

2. The posts supporting the chain-link fence or other net fencing should be breakaway (Fig. 1), and the ties holding the fence to the posts should be single-strand aluminum wire spaced at approximately 12 in. (30 cm) on center.

3. The posts supporting the metal benders should be similar to standard guardrail posts so that they will break away under direct vehicle impact if their location is such that they might be struck by a vehicle.

4. Until more accurate dynamic load data are determined for this metal bender configuration, the minimum tape length and minimum site dimensions should be determined by using the rated tape force without applying the dynamic load factor.

5. On the other hand, the average decelerations should be estimated by computing the stopping distance by using a dynamic load factor of 1.45.

The redesign of the metal bender so that it may be mounted on a post is a definite improvement for both installation and maintenance. However, there are apparent side effects, such as additional dynamic energy that was not absorbed in earlier configurations. Additional research is needed to determine more precisely the dynamic force and properties of this type of assembly.

ACKNOWLEDGMENT

The contents of this report reflect the views of the authors who are responsible for the facts and the accuracy of the data presented. The contents do not necessarily reflect the official views or policies of the Federal Highway Administration. This report does not constitute a standard, specification, or regulation.

REFERENCES

1. Hirsch, T. J., Hayes, G. G., and Ivey, D. L. Dragnet Vehicle Arresting System. Texas Transportation Institute, Tech. Memo. 505-4, Feb. 1969.
2. Damon, A., Stoudt, H. W., and McFarland, R. A. The Human Body in Equipment Design. Harvard Univ. Press, Cambridge, 1966.
3. Dragnet: Vehicle Safety Barrier System. The Entwistle Co., Boston.

AUTOMOBILES AND HIGHWAY CRASH ATTENUATORS: SYSTEM DESIGN CONSIDERATIONS

Charles Y. Warner, Brigham Young University; and
Donald Friedman, Minicars, Inc., Goleta, California

ABRIDGMENT

Present fixed-object casualties and scheduled future vehicle crashworthiness performance, when compared with trends toward smaller automobiles, allow rough estimation of future requirements for highway crash attenuators. Smaller, stiffer attenuators will be appropriate. They should provide protection for frontal crashes between 40 and 70 mph (64 and 113 km/h). Resulting savings in attenuator costs should allow protection of 2 to 3 times as many hazard sites.

•ALTHOUGH IMPLEMENTATION proceeds slowly and maintenance problems persist, highway crash attenuation devices (HCAD) have proved themselves technically in laboratory tests (1, 2, 3) and both technically and economically in real-world accidents (6).

It is reasonable to predict significant shifts in vehicle factors that have direct bearing on the efficacy and efficiency of the HCAD. Fuel costs will accentuate the already well-established trend toward smaller, lighter vehicles and will temporarily reduce the average traveling speed. More than 40 percent of U. S. cars in 1985 will be subcompacts (15). Lower traveling speeds may reduce the average severity of fixed-object collisions. The trend to smaller, lighter automobiles will very likely increase the average injury level in those crashes that do occur. Federal motor vehicle safety standards and state laws requiring installation and use of effective occupant restraints will significantly improve the built-in crashworthiness of passenger cars. If these measures are effective, vehicle deceleration from a frontal crash can be more than twice the 12-g guideline now used for attenuator design. This will allow installation of attenuators at 2 to 3 times as many hazard sites without cost increases. Occupant restraints planned for the late 1970s will further increase the survivable crash intensity. The structural stiffness of the subcompact will probably increase by that time, in response to federal standards requiring 40-mph (64-km/h) frontal barrier crash survivability and structural compatibility among cars of different mass (7, 8, 9).

ATTENUATORS AND THE FIXED-OBJECT PROBLEM

Analysis of available crash statistics indicates that fixed-object crashes produce between 6,000 and 13,000 fatalities and between 270,000 and 530,000 injuries annually. It is not unreasonable to assume that 6,000 deaths, 300,000 reversible injuries, and 30,000 permanently disabling injuries occur annually in this type of accident. The total annual societal cost is probably in excess of $5 billion (17-22).

It has been shown, however, that crash attenuation systems can provide effective, economical alternatives to this loss (6). Attenuators that are dynamically matched to vehicle crashworthiness levels can provide an even more economical and equally effective crash protection system. Fewer than 10 percent of the automobiles traveling our roadways in 1985 will lack appropriate occupant restraints. Thus the design conditions now in use for crash attenuators will not be cost-effective for that period.

Early attempts to establish attenuator design criteria were hampered by a lack of biomechanical data and the absence of viable automotive occupant restraints. Hence, a 12-g, 40-msec vehicle deceleration limit was established for 60-mph (97-km/h), ±25-deg impacts of 2,000- to 4,000-lbm (907- to 1814-kg) automobiles. It served as a

starting point for attenuator design and allowed appropriate comparisons of prototype systems. It was also employed in the development program initiated in the mid-1960s, under federal sponsorship. The program resulted in the development of several crash attenuators having acceptable crash performance (10, 11).

The attenuator systems that evolved in response to the initial performance criteria have some common characteristics. They range in depth from about 12 to 24 ft (2.7 to 7.4 m), depending on the force-velocity-deflection characteristics, and thus require 70 to 150 ft^2 (6.5 to 14 m^2) of roadside area. Their cost ranges from about $2,000 to about $5,000 for first-installation hardware, but cost per impact varies because some systems are wholly or partially reusable (6).

Thus three very important trends need to be understood for rational prediction of future attenuator needs (16, 17):

1. The total U.S. vehicle population will reach about 150 million by 1985, increasing traffic and accidents by over 50 percent.
2. Emissions, fuel costs, parking, and other economic factors of increasingly urbanized living will drive many purchasers toward smaller automobiles. The subcompact will account for more than 40 percent of all passenger cars by 1985.
3. Enforced active restraint use, factory-installed passive restraints, structural changes, and other vehicle crashworthiness features will greatly reduce the need for crash attenuation along the roadside. This will allow a much more effective implementation of attenuators at those sites where they are needed.

ATTENUATOR-AUTOMOBILE COMPATABILITY

Figure 1 shows the estimated distribution of all U.S. accidental frontal crash fatalities as a function of barrier equivalent velocity (BEV). BEV as used here is defined on the basis of vehicle crush: It is the barrier crash velocity needed to produce about the same vehicle crush as that seen in an actual accident and thus serves as a measure of severity. If account is taken of the distribution of about 38,000 passenger car occupant deaths and 2.8 million occupant injuries that occurred in 1971, it is seen that about 19,000 deaths and 1 million injuries occurred in the frontal mode alone, and almost 7,000 deaths occurred in frontal crashes between 20 and 40 mph (32 to 64 km/h) BEV (9). The dashed line in Figure 1 is an estimate of the upper limit of fatality distribution in fixed-object accidents. Such crashes account for an inordinate number of casualties per accident and may have a distribution that is as much as 10 mph (16 km/h) BEV more intense than average. The precise distributions are unknown. Had crashworthiness standards recently announced for the 1976 to 1980 time frame been in effect, as many as 16,000 of the 38,000 deaths that occurred in 1971 could have been avoided. If these standards take effect according to announced schedule, similar savings can be realized by 1985, independent of attenuator implementation (Fig. 2).

Basically, occupant survival depends on proper control of occupant crash forces, which requires prevention of occupant compartment intrusion and use of stopping distance to limit vehicle forces. The occupant only requires (12) that the acceleration be kept below about 50 to 60 g (with 2,000-g/s onset) and that the area of force application be large enough to prevent pressures from exceeding 50 to 100 psia (3.5 to 7 $\times 10^5$ Pa). Experimental crashes (9) have shown that most cars exhibit sufficient structural integrity to prevent serious occupant compartment collapse in frontal barrier crashes up to about 30 to 35 mph (48 to 56 km/h).

Lap-shoulder belts perform quite well in controlling occupant forces at speeds below 25 to 30 mph BEV. Improved restraints are likely to give good performance at speeds up to 40 mph (64 km/h) BEV (12, 13, 14). Future automobiles will probably be built to meet a federal standard frontal crush force of about 80,000 lbf (356 000 N) to provide improved car-to-car crash protection (8, 9, 15, 16).

DESIGN GUIDELINES

Attenuator design guidelines from the vehicle crashworthiness programs announced by DOT indicate that attenuators should be designed to provide the additional stopping

Figure 1. Estimated distribution of frontal fatalities versus crash severity.

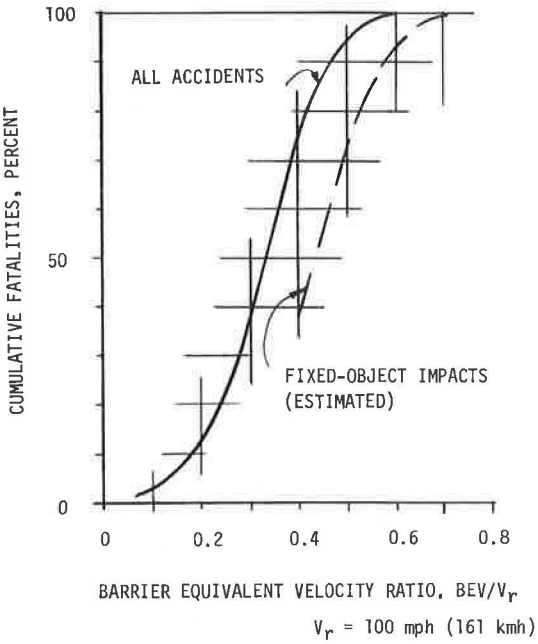

Figure 2. Estimated effectiveness of announced FHWA standards for frontal impacts.

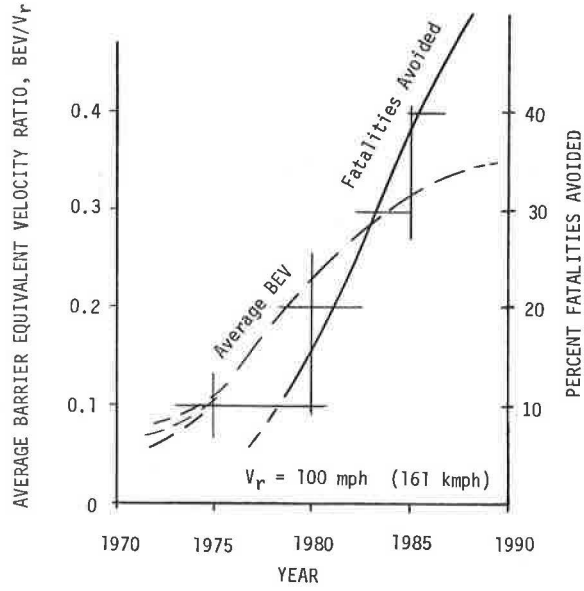

Figure 3. Minimum attenuator stroke versus fixed-object crash velocity ratio.

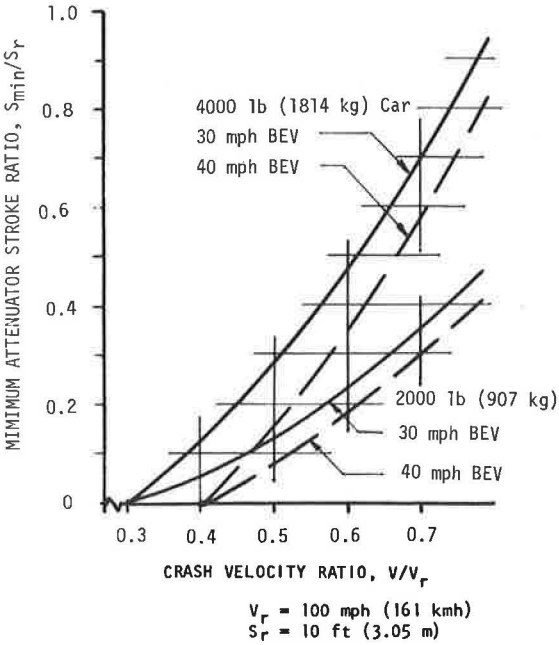

Figure 4. Recommended stiffness profiles for 40-mph BEV car crash attenuators.

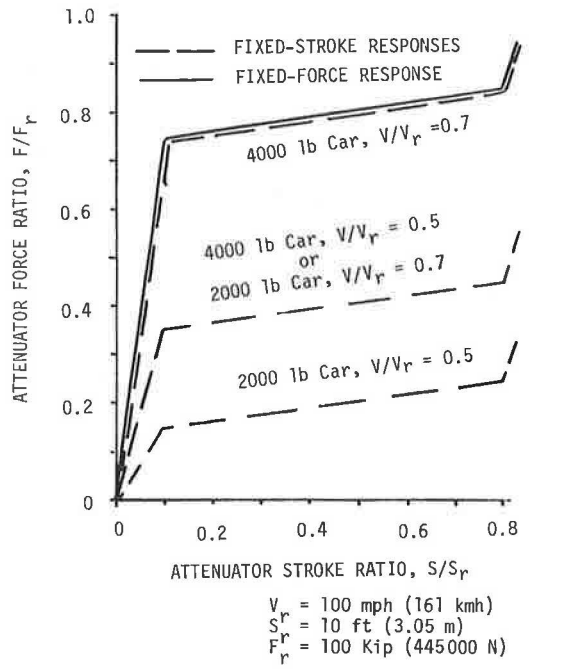

distance needed for crashes above 35 to 40 mph (56 to 64 km/h) and should provide a stopping force near, but slightly less than, the design frontal crush force on the vehicle. Hence, the majority of the crush provided by a crash attenuator should be near but less than 80,000 lbf for maximum total occupant stroke efficiency.

As shown in Figure 1, the fatality benefits achievable above 40 mph (64 km/h) BEV are essentially all contained below 70 mph (113 km/h) and most of these are below 60 mph (97 km/h) BEV. Figure 3 is a plot of required attenuator depth versus BEV performance, assuming a 75,000 lbf (334 000 N) crush force and 30- or 40-mph (48- or 60-km/h) BEV frontal crashworthiness of all cars between 2,000 and 5,000 lbm (907 and 2260 kg).

As may be seen from Figure 3, about 5 ft (1.52 m) of properly designed attenuator may be expected to give acceptable 60-mph performance for all 40-mph crashworthy passenger vehicles. Even when nonideal conditions encountered in practice are considered, a depth of 8 ft (2.44 m) would be adequate. A device this short can be much less expensive than present attenuators, for not only less space is needed but less complexity, less concern about buckling, redirection hardware, and the like.

Although these estimates were derived on the basis of constant attenuator forces, the ideal attenuator would probably include a moderate "ramp" force characteristic over the first foot of deflection and should exhibit constant-stroke behavior if this can be achieved at low cost (2, 3). These features would reduce losses in low-speed collisions and skidding side impacts. Suggested force-deflection characteristics are given in Figure 4. For a fixed-force attenuator, the upper curve would hold for all car weights and impact velocities.

Hence, the realization of 40-mph (64-km/h) automobile frontal crashworthiness could allow a reduction in HCAD length to one-third the present values, without compromise of effectiveness. This should make costs more reasonable inasmuch as attenuator complexity will be greatly reduced. Far greater overall safety can result without increased highway cost.

CONCLUSIONS

Significant changes in highway safety will result from automobile improvements that are now being introduced into public use. Appropriate crashworthiness measures scheduled for implementation in all new cars by 1980 will provide built-in safety for most fixed-object crashes at speeds between 30 and 40 mph. Attenuators designed for fixed-object impacts with those vehicles should concentrate on high-velocity impacts and may therefore be more compact. An attenuator depth of 8 ft (2.4 m) will be adequate for survival of frontal crashes at speeds up to 70 mph (113 km/h) in 1980+ vehicles, and will improve crashworthiness of lower speed impacts, if appropriately designed. Whereas a constant-stroke attenuator is preferable for the same space constraints, a fixed-force system having a gradually increasing force can also provide good performance. Attenuator force for the 70-mph impact should be 75,000 to 85,000 lbf (334 000 to 378 000 N). The highway crash attenuator will thus fill an important gap in the future safety problem; it will provide a means to prevent casualties that vehicle systems are not able to prevent economically.

REFERENCES

1. Viner, J. G. Recent Developments in Roadside Crash Cushions. Transportation Engineering Jour., Proc. ASCE, Feb. 1972, pp. 71-87.
2. Walker, G. W., Warner, C. Y., and Young, B. O. Angle and Small-Car Impact Tests of an Articulated Gore Barrier Employing Lightweight Concrete Energy-Absorbing Cartridges. Published in this Record.
3. Development of Safer Roadside Structures and Protective Systems. Highway Research Record 259, 1969.
4. Design of Traffic Safety Barriers. Highway Research Record 343, 1971.
5. Traffic Safety Barriers, Lighting Supports, and Dike Slopes. Highway Research Record 386, 1972.
6. Viner, J. G., and Boyer, C. M. Accident Experience With Impact Attenuation

Devices. Federal Highway Administration, Rept. FHWA-RD-73-71, April 1973.
7. Program Plan for Motor Vehicle Safety Standards. National Highway Traffic Safety Administration, NHTSA Docket 69-7.
8. Speech by James Beggs, Special Representative of the Secretary of Transportation, at 4th Internat. Conf. on Experimental Safety Vehicles, Kyoto, Japan, March 1973.
9. Carter, R. L. Passive Protection at 50 Miles per Hour. 2nd Internat. Conf. on Passive Restraints, Detroit, SAE Paper 720445, May 1972.
10. Proposed Full-Scale Testing Procedures for Guardrails. Highway Research Correlation Service, HRB Circular 482, Sept. 1962.
11. The 4-S Program: Structural Systems in Support of Safety. Federal Highway Administration, 1969.
12. Warner, C. Y. Belt Occupant Restraint Effectiveness. Proc. 17th Annual Meeting of American Association of Automotive Medicine, Oklahoma City, Nov. 1973.
13. Warner, C. Y., et al. An Assessment of the Performance of Belt Restraint Systems in Automobile Crashes. ASME, Paper 73-1CT-107, Sept. 1973.
14. Warner, C. Y., et al. Effectiveness of Automotive Occupant Restraints. Presented at National Transportation Engineers Meeting, Tulsa, ASCE, July 1973.
15. Advanced Passive Restraint System for Subcompact Car Drivers. Minicars, Inc., in progress.
16. Strother, C., and Krauss, R. Study of Passive Restraint Requirements for High Speed Protection. National Highway Traffic Safety Administration, 1973.
17. Safety Benefits of the Occupant Crash Protection Standard. National Highway Traffic Safety Administration, Jan. 1971.
18. IIHS Status Report. Insurance Institute for Highway Safety, 1972.
19. Accident Facts, 1972. National Safety Council, 1973.
20. A Study of Auto Accidents in Washenaw County, Michigan. Office of Accident Investigation, National Highway Traffic Safety Administration.
21. Societal Costs of Motor Vehicle Accidents. National Highway Traffic Safety Administration, preliminary rept., 1972.
22. Warner, C. Y. Presentation to HRB Committee A2A04, Jan. 1974, unpublished.

DEVELOPMENT OF A NEW MEDIAN BARRIER TERMINAL

Maurice E. Bronstad and Jarvis D. Michie, Southwest Research Institute

Traffic barrier terminals or end treatments have been shown by test and in the field to be more hazardous than the downstream or typical barrier installation. New end treatments are needed to improve the performance of the barriers when they are impacted end-on. Accordingly, new traffic barrier concepts were formulated and two were evaluated by crash tests. A guardrail breakaway cable terminal (BCT) developed previously was subjected to more extensive testing, and modifications were incorporated as indicated by test results. A new median barrier terminal that incorporated breakaway cable features was also developed and evaluated; this terminal is the subject of this paper. Because the purpose of barrier terminals is to provide longitudinal and lateral restraint for downstream impacts without being a hazard for end-on impacts, the test terminals were subjected to both angular and end-on impacts. Impact conditions included both standard (4,000-lbm) and subcompact (2,000-lbm) vehicles, moderate (40-mph) and high-speed (60-mph) velocities, and angles of 0 and 25 deg. Sixteen crash tests were conducted on the median barrier BCT. Crash events were documented by photography and electronic transducers. Results of the tests indicate that these new terminals provide a significant improvement in performance over other currently specified terminals. The median barrier BCT elements that collapse in accordian-like manner when impacted end-on could be used at sites requiring crash cushions (e.g., at elevated gores). The cost is substantial, but the increase in cost over existing terminal designs diminishes as the length of the barrier increases.

•APPROACH ENDS of guardrails and median barriers have long been recognized (8) as formidable roadside obstacles with which traffic must contend. The W-beam in upright terminals has penetrated the passenger compartment in numerous end-on impacts, whereas ramped terminals have caused impacting vehicles to be launched, rolled, and tumbled. A guardrail terminal was developed, evaluated, and then refined in a recent NCHRP program (7). This breakaway cable terminal (BCT) features a horizontally flared end to introduce flexural loading in the end-beam panel for end-on impacts.

The median barrier terminal is exposed to a wider range of vehicle collisions (e.g., being struck from either side) than a typical guardrail terminal; hence, the guardrail BCT is not directly applicable to median barriers. Accordingly, it was deemed desirable to develop a symmetrical median barrier BCT in contrast to the unsymmetrical (i.e., flared) guardrail BCT.

The objective of this research was to develop and evaluate a new median barrier terminal concept by a series of crash tests.

Inasmuch as the dual purposes of traffic barrier terminals are to present minimal hazard for end-on impacts and to anchor the installations for downstream impacts, the terminal concepts were evaluated for both end-on and angular impacts. Both 2,000-lbm (900-kg) and 4,000-lbm (1800-kg) vehicles were used to provide a range of vehicle sizes. Impact conditions included both 40- and 60-mph (64- and 97-km/h) velocities and 0- and 25-deg angles.

TERMINAL DEVELOPMENT

Preliminary Designs

Based on the success of the guardrail BCT, it was concluded that the BCT could be used for the median barrier terminal. Because the horizontal flare in the guardrail BCT is used to reduce longitudinal resistance of the standard W-beam element, another method was needed for the symmetrical (no flare) median barrier end. A design using flat plates in the terminal length to reduce the longitudinal resistance for end-on impacts was formulated. These plates serve as redirection panels for angular impacts within the terminal length. A number of preliminary tests were conducted (Fig. 1) before a finalized configuration was determined. Although a steel post system was tested, most of the preliminary tests were conducted with the blocked-out W-beam median barrier, wood post (5). These early tests were characterized by a relatively smooth deceleration of the vehicle as the flat plates collapsed, followed by launching of the vehicle as it approached the more rigid W-beam elements (Fig. 2).

Finalized Configuration

A major redesign of the median barrier BCT was undertaken with the following primary objectives:

1. Decelerating a 4,000-lbm (1800-kg) vehicle impacting end-on at 60 mph (97 km/hour) to stop in contact with the barrier using a minimum of terminal length (the vehicle must be brought to a stop before contacting the rigid barrier elements; i.e., the terminal must be of sufficient length to stop the vehicle and to keep decelerations within tolerable limits);
2. Redirecting a 4,000-lbm vehicle impacting downstream of the end at 60 mph and at an angle of 25 deg; and
3. Minimizing the terminal length for economic and hazard-exposure conditions.

The finalized BCT configuration as shown in Figures 3 and 13 (Appendix) is characterized by the following features and components: terminal length, beams, posts, nose, and BCT hardware.

Terminal Length—A 24-ft (7.3-m) terminal length was selected based on the loads developed in the preliminary end-on tests and the expression

$$s = \frac{V^2}{2ag} \tag{1}$$

where

s = vehicle stopping distance, ft (m);
V = vehicle impact velocity, fps (m/s);
a = average vehicle deceleration, g; and
g = gravitational constant = 32.2 ft/s^2 (9.8 m/s^2).

If we assume a constant decelerating force of F = 20 kips (89 kN) (based on preliminary tests), the deceleration level for a vehicle of W = 4,000 lb (1800 kg) would be

$$a = \frac{F}{W} = \frac{20}{4} = 5 \text{ g} \tag{2}$$

or 10 g for a 2,000-lbm (900-kg) vehicle. From Eq. 1

$$s = \frac{(88 \text{ fps})^2}{(2)\ (5 \text{ g})\ (32.2 \text{ ft/s}^2/\text{g})} = 24 \text{ ft}$$

The 10-g level for the 2,000-lbm (900-kg) vehicle is in conformance with current FHWA crash cushion criteria, which specify a maximum of 12 g based on stopping distance (9).

Beams—Launching of the vehicle in preliminary tests was partially attributed to the

Figure 1. Preliminary median barrier terminal test installations.

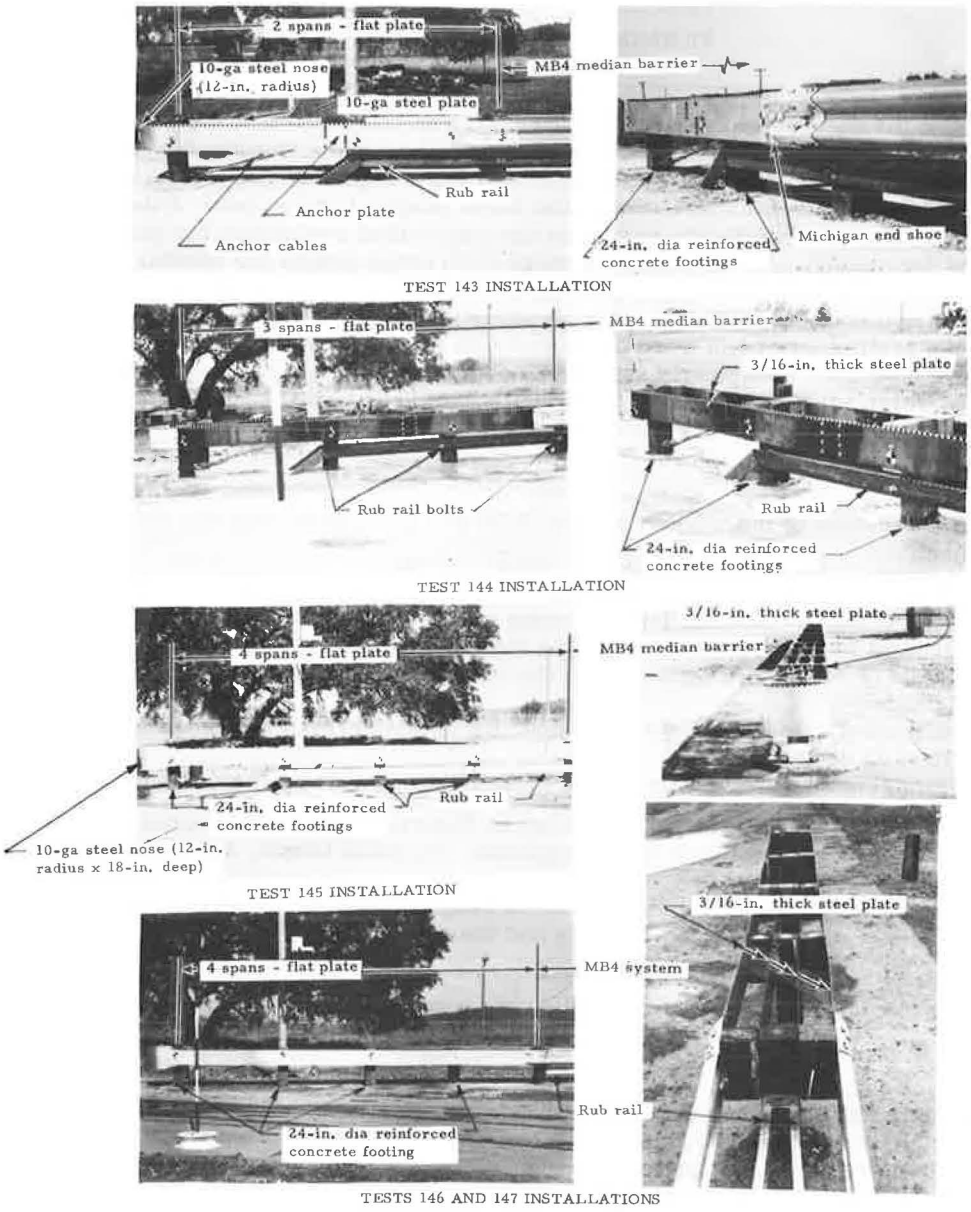

Figure 2. After impacting BCT, vehicle is launched by rigid W-beam.

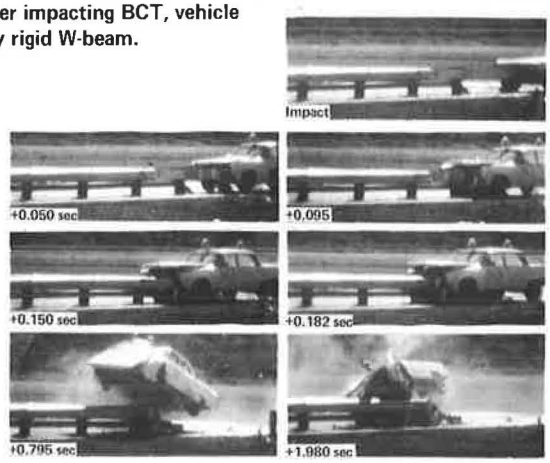

32-in. (813-mm) height of the terminal. This elevation permitted the vehicle to climb atop the deformed terminal in later stages of a test. This height was modified to 42 in. (1.1 m) for the final terminal design; an outer beam width of 30 in. (0.7 m) was used to prevent vehicle underride for angular impacts. Interior beams 12-in. (0.3-m) wide were placed between the posts and blocks at 42-in. elevation to help minimize launching.

Posts—Both steel and timber posts were used in the final configurations. Because breakaway performance of the terminal posts is essential, steel posts are welded to base plates only on the traffic sides. Both W6 × 8.5 and TS6 × 8 × 0.1875 steel posts were tested in the finalized design configurations. Terminal posts of 6- × 8-in. (150- × 200-mm) timber with a $2\frac{3}{8}$-in. (60-mm) diameter hole bored through the neutral axis were tested in a finalized configuration.

Rigid foundations are considered basic to the breakaway post concept inasmuch as brittle fracture is desirable; posts that lean in soil have launched vehicles. The reinforced concrete footings used in the work provide adequate support for design performance.

Nose—A steel barrel was selected as the terminal nose for the final configuration. Tests of the barrel crash cushion have demonstrated that the front barrels fold over and under the vehicle front forming a mechanical "lock" on the vehicle. This lock is considered desirable because it helps to prevent a vehicle from vaulting over the installation.

BCT Hardware—BCT hardware consisted of anchor plates, anchor cables, and end posts. The steel end post was reinforced locally to increase the anchor load capacity.

TEST PROGRAM

Nine crash tests were conducted on the finalized BCT configuration (Table 1). Test installations included the median barrier BCT installed with the following systems:

1. MB3—box beam median barrier,
2. MB4S—blocked-out W-beam on steel posts, and
3. MB4W—blocked-out W-beam on timber posts.

Terminal posts were of the same material as the system. A design drawing of the BCT installed with the MB4S system is shown in Figure 13. Also shown in the Appendix are photographs of the test series.

End-On Performance

End-on performance of the finalized configuration was demonstrated with both steel and timber terminal posts by using standard-sized and subcompact vehicles. Three terminal post designs were evaluated for end-on performance:

1. W6 × 8.5 post welded to base plate with a $\frac{3}{8}$-in. (9.5-mm) fillet weld on the traffic side of the flanges only,
2. TS6 × 6 × 0.1875 box-beam post welded to base plate with a $\frac{3}{8}$-in. fillet weld on the traffic side of the flanges only, and
3. Timber posts 6 × 8 in. (150 × 120 mm) with a hole drilled through the neutral axis.

The median barrier BCT with W6 × 8.5 steel posts was impacted end-on with a standard vehicle at 62 mph (100 km/hour) as shown in Figure 4b. The vehicle was decelerated to a stop in contact with the barrier with an effective stopping distance of 30 ft (9 m). A subcompact car impacted an identical installation end-on at 41.5 mph (67 km/hour) and was decelerated to a stop in contact with the barrier as shown in Figure 4a with an effective stopping distance of 13 ft (4 m). The end-on test of the BCT with TS6 × 6 × 0.1875 box-beam posts was conducted with a subcompact vehicle impacting at 62.4 mph (100 km/hour) as shown in Figure 5. The vehicle was decelerated to rest in contact with the barrier with an effective stopping distance of 16 ft (4.9 m).

In test 158, the five terminal posts were 6- × 8-in. (150- × 200-mm) southern pine members embedded in concrete footings; an MB4W system was installed downstream of the terminal. A standard-sized vehicle impacted the barrier end-on at a speed of 64.8 mph (104 km/hour) and was decelerated to rest in contact with the barrier as shown in Figure 6. The effective stopping distance was 22 ft (6.7 m).

Figure 3. BCT installations on three types of median barriers.

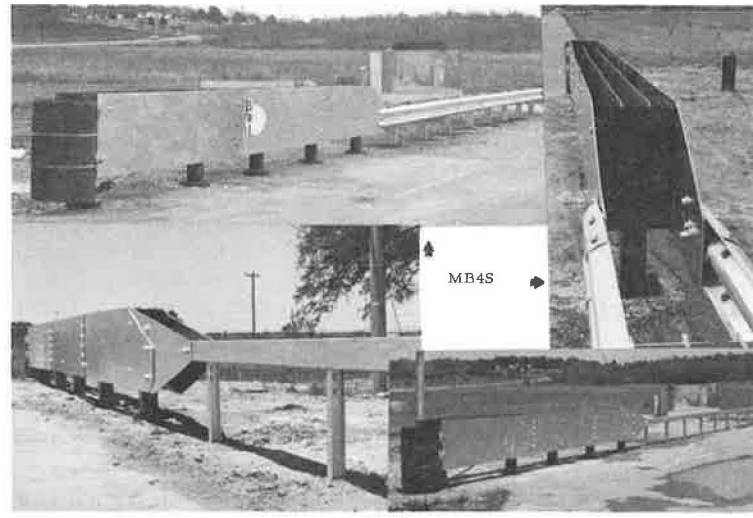

MB3

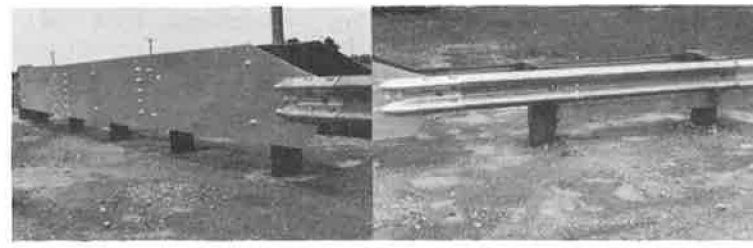

MB4W

Table 1. Summary of finalized median barrier BCT tests.

Barrier System[a]	Terminal Length (ft)	Terminal Post[b]	Terminal Beam Elements (in.)	Terminal Rail Height (in.)	Vehicle Weight (lbm)	Vehicle Speed (mph)	Impact Angle (deg)	Max Average Deceleration[c] (g) Long.	Lat.	Remarks
D, E, F	25	W6 x 8.5 steel	3/16 x 30	42	3,800	63.0	0.5	7.2 (4.4)	1.2	Vehicle smoothly decelerated in contact with barrier (30-ft stopping distance).
D, E, F	25	W6 x 8.5 steel	3/16 x 30	42	2,200	41.5	0.4	5.7 (4.4)	2.4	Vehicle smoothly decelerated in contact with barrier (13-ft stopping distance).
D, E, F	25	W6 x 8.5 steel	3/16 x 30	42	3,900	57.0	27	6.2	2.5	Vehicle impacted rail just upstream of second post; no redirection was evident as vehicle penetrated the system. Local anchorage failure occurred.
D, F, G	25	TS6 x 6 x 0.1875	3/16 x 30	42	4,000	54.5	26.7	7.0	3.3	Vehicle impacted rail 2 ft upstream of second post; little redirection occurred as vehicle penetrated the system. Local anchorage failure occurred.
D, F, G	25	TS6 x 6 x 0.1875	3/16 x 30	42	4,000	61.1	26	7.1	7.6	Vehicle impacted at third post and was smoothly redirected.
D, F, G	25	TS6 x 6 x 0.1875	3/16 x 30	42	2,400	62.4	1.5	13.3 (8.1)	2.7	Vehicle came to rest in contact with barrier with little change in direction (16-ft stopping distance).
D, F, G	25	TS6 x 6 x 0.1875	3/16 x 30	42	3,800	60	25	—	—	Vehicle was redirected although unanchored box beam spans disengaged from posts.
D, F, G	25	TS6 x 6 x 0.1875	3/16 x 30	42	3,900	58	25	8.5	6.4	Vehicle was redirected, noticeable roll away from barrier was evident in redirection. Vehicle impacted rail upstream of third post.
A, C, F	25	6 x 8 timber posts with hole through neutral axis	3/16 x 30	42	3,900	64.8	1.2	11.6 (6.4)	5.0	Vehicle decelerated in contact with barrier; stopping distance 22 ft.

Note: 1 ft = 0.3 m; 1 in. = 25.4 mm; 1 lbm = 0.45 kg; 1 mph = 1.6 km/h.

[a]Barrier systems: A = timber post W beam median barrier, B = rub rail terminated at second post, C = rub rail terminated at sixth post, D = steel post W beam median barrier with no rub rail, E = W6 x 8.5 terminal posts welded to base plate at grade, F = 55-gal drain added to end, interior terminal beams 12 in. wide and placed at top of outside rail elevation, and G = TS6 x 6 x 0.1875 steel posts welded to base plate at grade.

[b]All terminal posts set in 24 in. diameter reinforced concrete footing at 41 in. deep.

[c]Maximum deceleration averaged over 50-msec duration obtained from high-speed cine. Parenthesis indicates deceleration based on stopping distance.

Angular Impact Tests

Crash test evaluation of the finalized median barrier BCT configuration was conducted with standard sedans impacting the barrier upstream of the third terminal post with standard impact conditions [i.e., 4,000-lbm (1800-kg) vehicle, 25 deg, 60 mph (97 km/hour)]. Tests were conducted with the BCT installed with the MB3 and MB4S. The transition from the BCT to the box-beam median barrier was effected as shown in Figure 7. Although significant rolling occurred, which caused the test vehicle to ride up the barrier, the vehicle was redirected (Fig. 8). The BCT-MB4S system installation was impacted upstream of the third post, and the vehicle was then redirected as shown in Figure 9.

CONCLUSIONS

Performance

Performance of this design was demonstrated for terminals constructed with the MB3, MB4S, and MB4W systems. The median barrier BCT behaves as a crash cushion for end-on impacts; i.e., it decelerates the vehicle to a stop in contact with the terminal length. The 25-ft (7.6-m) BCT length appears to be adequate for safely attenuating the energy of a 4,000-lbm vehicle impacting end-on at 60 mph. Although penetration of the system is likely for large-angle impacts near the nose, the terminal is an effective redirection barrier for standard test impacts within the terminal length. The breakaway steel post assembly provides sufficient installation anchorage to redirect vehicles impacting downstream of the third post at standard test conditions. The vehicle deceleration ratings assigned to individual tests correspond closely to those ratings (5) determined for general performance of the length of need.

Economics

The median barrier BCT design is considerably more expensive than many other terminals being used (i.e., $1,263 as compared to $355 for the G4 terminal shown in NCHRP Report 118). (These costs were developed from information obtained from barrier manufacturers.) However, the effect of the additional cost is diminished when the normal length of median barriers is considered. Although a continuous effort was made to keep the design simple and inexpensive, there are features of the median barrier BCT where cost reductions may be appropriate; these are the post and block out, concrete footings, and outer plate thickness.

ACKNOWLEDGMENTS

The work reported was conducted at Southwest Research Institute by the Department of Structural Research as part of an NCHRP project. The crash test program was conducted with the assistance of C. E. Kimball, G. W. Deel, R. P. Guillot, and T. H. Conard, Jr. C. A. Walker was responsible for crash test photography, and R. C. DeHart, Director, served in the capacity of technical and administrative advisor.

A special ad hoc committee offered continuous support of the program through their advice and recommendations; their help is gratefully acknowledged. This group consisted of William A. Goodwin (Chairman), University of Tennessee; John L. Beaton, California Division of Highways; Malcolm D. Graham, New York Department of Transportation; Paul C. Skeels (deceased), General Motors Proving Ground; and John Viner, Federal Highway Administration.

The assistance and cooperation of many persons in the state highway departments, manufacturing firms, and government agencies are gratefully acknowledged. In particular, cooperation from the California Division of Highways, the Federal Highway Administration, Syro Steel Company, and Armco Steel Corporation is recognized.

The work discussed in this report was sponsored by the American Association of State Highway Officials, in cooperation with the Federal Highway Administration. The opinions, findings, and conclusions expressed in this paper are those of the authors and not necessarily those of the sponsoring agencies.

Figure 4. (a) Subcompact and (b) standard-sized vehicles impacting same BCT-barrier configuration.

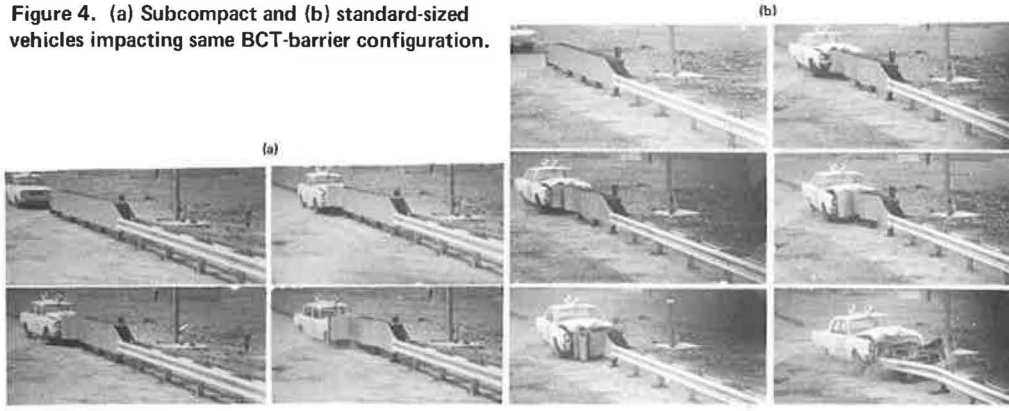

Figure 5. Subcompact car impacting BCT box-beam post configuration.

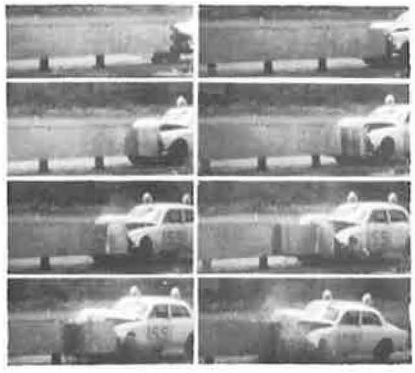

Figure 6. End-on impact of BCT-MB4W configuration.

Figure 7. BCT transition details for MB3 box-beam system.

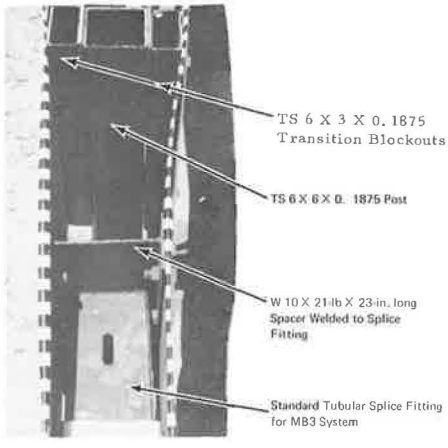

Figure 8. Angle impact of BCT-MB3 configuration.

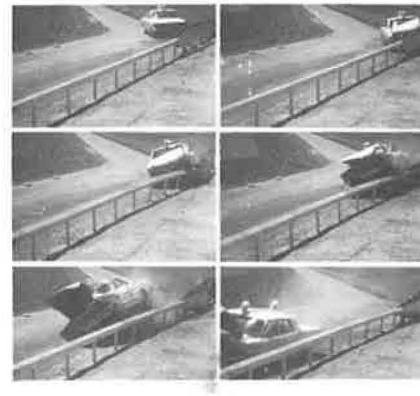

Figure 9. Angle impact of BCT-MB4S configuration.

REFERENCES

1. Deleys, N. J., and McHenry, R. R. Highway Guardrails—A Review of Current Practice. NCHRP Rept. 36, 1967.
2. Michie, J. D., and Calcote, L. R. Location, Selection, and Maintenance of Highway Guardrails and Median Barriers. NCHRP Rept. 54, 1968.
3. Olson, R. M., Post, E. R., and McFarland, W. F. Tentative Service Requirements for Bridge Rail Systems. NCHRP Rept. 86, 1970.
4. Michie, J. D., Calcote, L. R., and Bronstad, M. E. Guardrail Performance and Design. NCHRP Rept. 115, 1971.
5. Michie, J. D., and Bronstad, M. E. Location, Selection, and Maintenance of Highway Traffic Barriers. NCHRP Rept. 118, 1971.
6. Michie, J. D., and Bronstad, M. E. Guardrail Crash Test Evaluation: New Concepts and End Designs. NCHRP Rept. 129, 1972.
7. Evaluation of Breakaway Cable Terminals for Guardrails. NCHRP, Research Results Digest 43, 1972.
8. Highway Design and Operational Practices Related to Highway Safety. Special AASHO Traffic Safety Committee rept., 1967.
9. Federal Highway Administration Instructional Memorandum 40-1-71, 1971.

APPENDIX

TEST PHOTOGRAPHS AND INSTALLATION DRAWING

Figure 10. Photographs after end-on tests.

Figure 11. Photographs after angle impacts.

Test 154

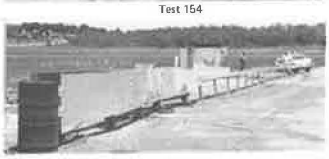

Test 157

Figure 12. Vehicle damage.

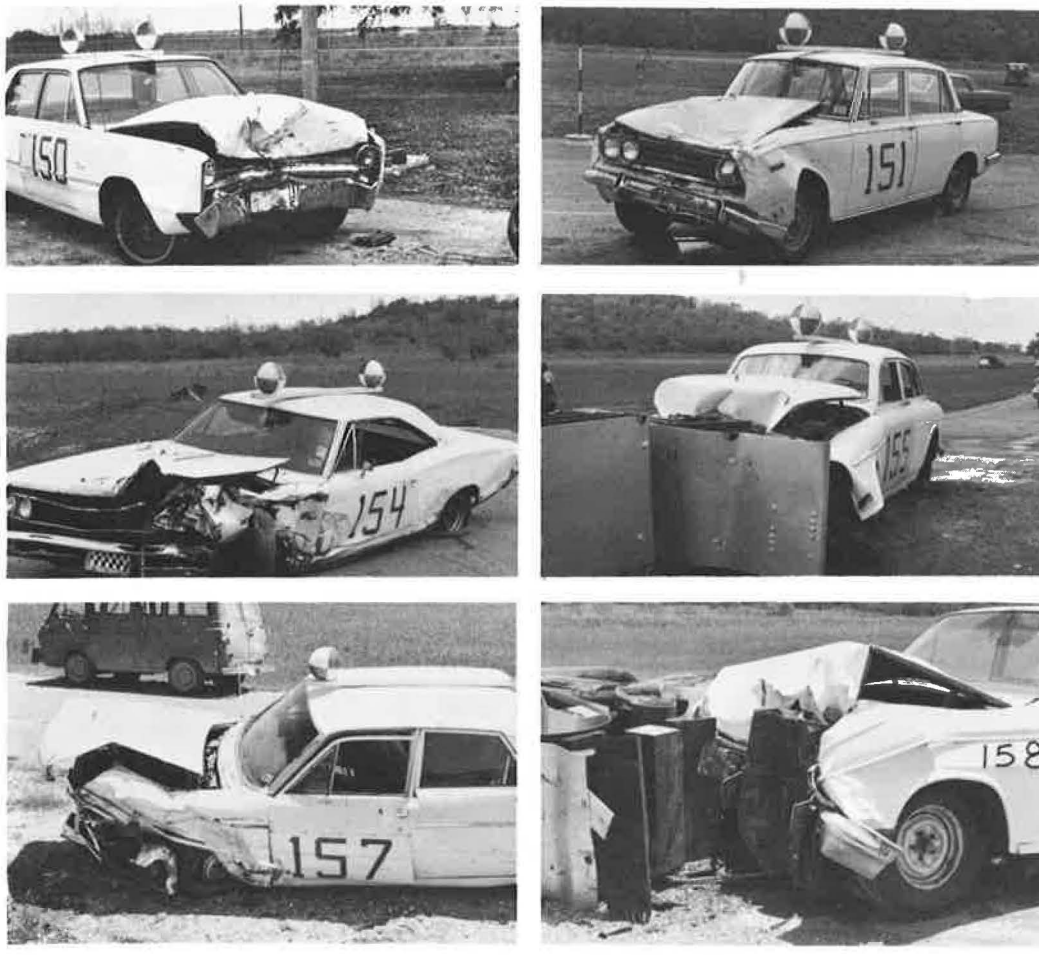

Figure 13. Median barrier BCT design drawing.

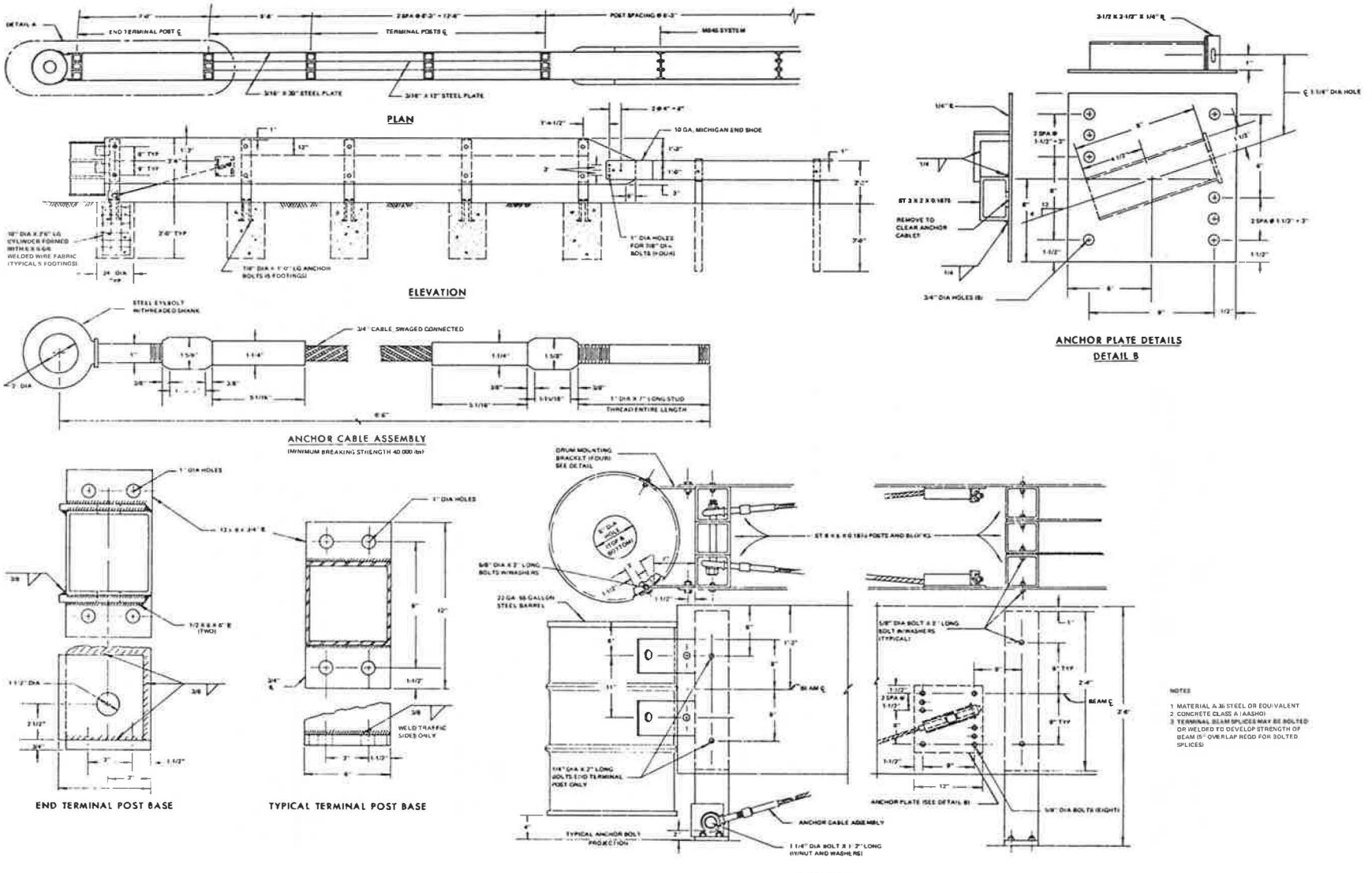

CRASH TEST EVALUATION OF THRIE BEAM TRAFFIC BARRIERS

M. E. Bronstad and J. D. Michie, Southwest Research Institute;
J. G. Viner, Federal Highway Administration; and
W. E. Behm, Anderson Safeway Guard Rail Corporation

Since its general nationwide adoption, the standard W-beam or flex-beam has been widely used as a traffic barrier element; its performance has been proved in crash tests and field use. However, the mounting height of the W-beam has been shown to be critical in tests as well as field installations. Background information on the conception and development of a configuration known as the Thrie beam is presented in this paper along with findings of a crash test series (five tests) on this new barrier element. Basically, the Thrie beam can be described as a triple corrugated beam as compared to a double corrugated W-beam. It is 1½ times the width of the W-beam, but the corrugation geometry and 3¼-in. (83-mm) depth are similar. The crash test series was conducted on blocked-out steel post median barrier and guardrail systems. Test conditions included 4,500- to 2,200-lbm (2.0- to 1.0-Mg) vehicles with speeds ranging from 54 to 67 mph (87 to 108 km/h) and impact angles varying from 16 to 29 deg.

• THE NEED for a rail element deeper than the 12-gauge U. S. standard steel W-beam (12¼ in. or 311 mm deep) was recognized by the Federal Highway Administration as a result of problems experienced with one particular guardrail system and crash test results of other traffic railing designs. This guardrail system, using the New York weak-post W-beam design, was originally installed with the top of the rail 27 in. (0.7 m) above the ground (1, 2). Field experience with this design disclosed that a surprising percentage of vehicles were going over the installation during collision (2, 3). After further examination of this problem, the mounting height of this system was increased to 33 in. (0.8 m) (3; 4, Table 6). Tests conducted on this design showed problems with small cars contacting the posts at the 33-in. mounting height (5).

About this time, a test (T1-D) was conducted on a bridge rail that used two standard W sections overlapped (6). This 18-in. (0.5-m) deep rail is shown in Figure 1a after a 60-mph (97-km/h), 25-deg impact with a 3,600-lbm (1.6-Mg) vehicle (test T1-D), and the vehicle is shown in Figure 1b. The results of a similar test (T1-B) with a normal 12-gauge W section without the second overlapping section are shown in Figure 2. In this case, the 18-in. (0.5-m) deep overlapped W rails clearly reduced both vehicle damage and barrier damage (6). Thus, FHWA staff speculated that such an 18-in. deep section might help solve the problems noted in the G2 guardrail system.

Following the tests conducted on the Texas T-1 bridge rail, Walker and Warner (7) developed and tested a guardrail-bridge rail transition that used a lapped W-beam similar to that used in test T1-D. Energy-absorbing cartridges between the rail section and the posts were used, and the investigation concluded that, for the conditions examined, "overall acceleration loads and velocity changes are reduced while postcrash controllability is increased, as compared to the performance of G-4 guardrail systems." At this point it appeared that a new 18-in. deep section would be helpful in the guardrail-bridge rail design developed by Warner and Walker, and the following potential uses for such a shape were identified:

Figure 1. Barrier and vehicle damage after test T1-D.

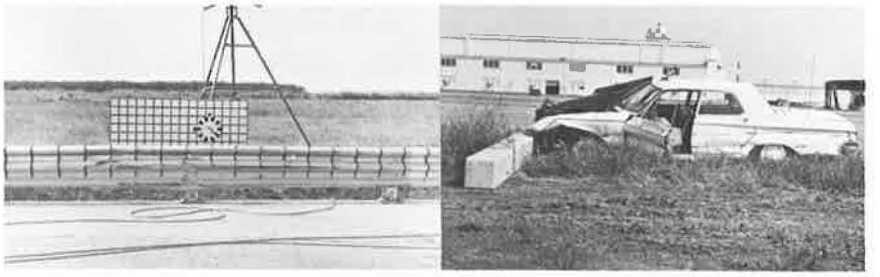

Figure 2. Barrier and vehicle damage after test T1-B.

Figure 3. Thrie beam geometry.

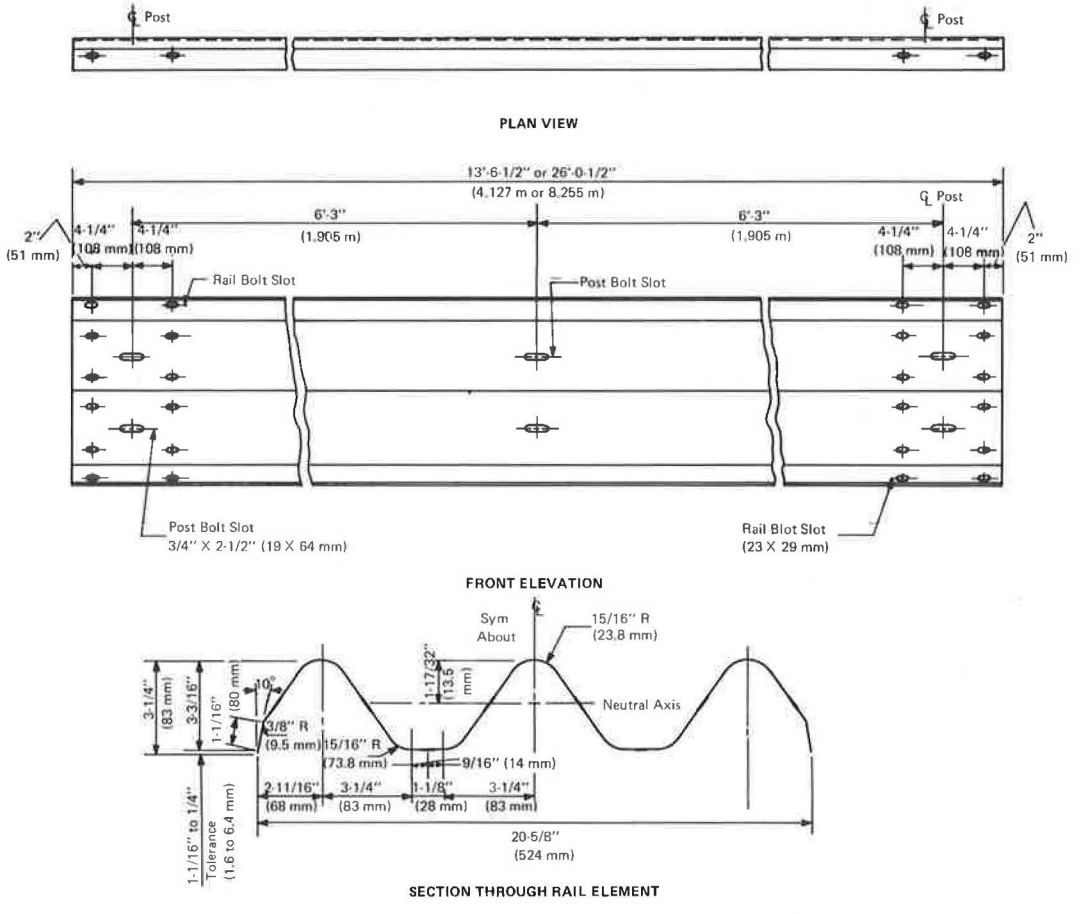

1. Weak-post guardrail designs with improved performance for vehicles ranging from subcompacts through standard-sized passenger cars,
2. Upgrading of the safety performance of existing bridge rail designs,
3. Guardrail-bridge rail transitions,
4. Elimination of the rub rail in the California blocked-out W-beam median barrier (MB4W) design, and
5. New guardrails, median barriers, bridge rails, and guardrail-bridge rail transitions capable of improved performance for both large vehicles (buses and trucks) and small subcompact automobiles.

Several guardrail suppliers were contacted to see whether it would be feasible to produce such a rail section. The Anderson Safeway Guard Rail Corporation produced such a shape, and, at the suggestion of the staff of FHWA, the elimination of the rub rail of the MB4W was selected as the first objective of the test program. The cost of such a design would be significantly less than that of the MB4W, possibly making it economical to retool to produce a new deep rail section. This would make the section available for development and use for all of the other applications listed. A drawing of the Thrie beam element as produced by Anderson Safeway is shown in Figure 3. Photographs in Figure 4 show the advantages of the Thrie beam over the current W-beam regarding vehicle bumper-barrier interface. [The vehicles are a 1969 Ford 2-ton (1814-kg) truck, a 1972 subcompact car, and a 1973 medium-sized car.]

CRASH TEST EVALUATION

The objective of this research was to evaluate by crash test Thrie beam barrier systems. A program consisting of five tests examined the dynamic performance of guardrail and median barrier installations composed of 12-gauge (2.8-mm thick) Thrie beam elements and W6 × 8.5-lb steel posts and blocks. The specific objectives and test conditions are discussed by test number.

Test AS-1

Early test results from the California Division of Highways (8) indicate that the maximum mounting height of the 12-in. (304-mm) wide flex-beam that could be used without a rub rail was 27 in. (0.69 m) for the strong-post systems; at higher mounting heights, impacting vehicles tend to wedge under the beam and snag on the posts. A 30-in. (0.76-m) high rail system with rub rail is used for the MB4W, whereas a 27-in. high rail with no rub rail is specified for guardrail (G4W). It is worth noting that California tests median barriers at 65 mph (105 km/h) instead of the standard 60 mph (97 km/h). Most states that specify the MB4W system use the C6 × 8.2 structural steel channel for the rub rail element; however, Michigan and others use a W-beam element.

The cost of the channel rub rail element is significant—as much as 25 percent more than the W-beam element. The function of the rub rail could also be served by increasing the depth of the W-beam. Accordingly, AS-1 test conditions (Fig. 5) were formulated to permit comparison of the Thrie beam installation with California test 103, which featured the standard W-beam mounted on 8 × 8 timber posts with a channel rub rail (8).

Test AS-2

There are still a number of guardrail installations that have a W-beam mounting height of 24 in. (0.6 m) or less. Work reported by California (8) included the following conclusions and observations:

1. A high incidence of vehicle vaulting with 24-in. (0.6-m) mounting height (blocked-out W-beam on 8 × 8 timber posts with 12½-ft or 3.81-m spacing),
2. Recommendation that all future beam barriers be designed with an overall height of at least 26 in. (0.66 m) above the ground, and
3. Less pocketing in tests with 6¼-ft (1.91-m) post spacing with 27-in. (0.69-m) mounting height than with 24-in. mounting height.

Figure 4. Bumper-beam interface.

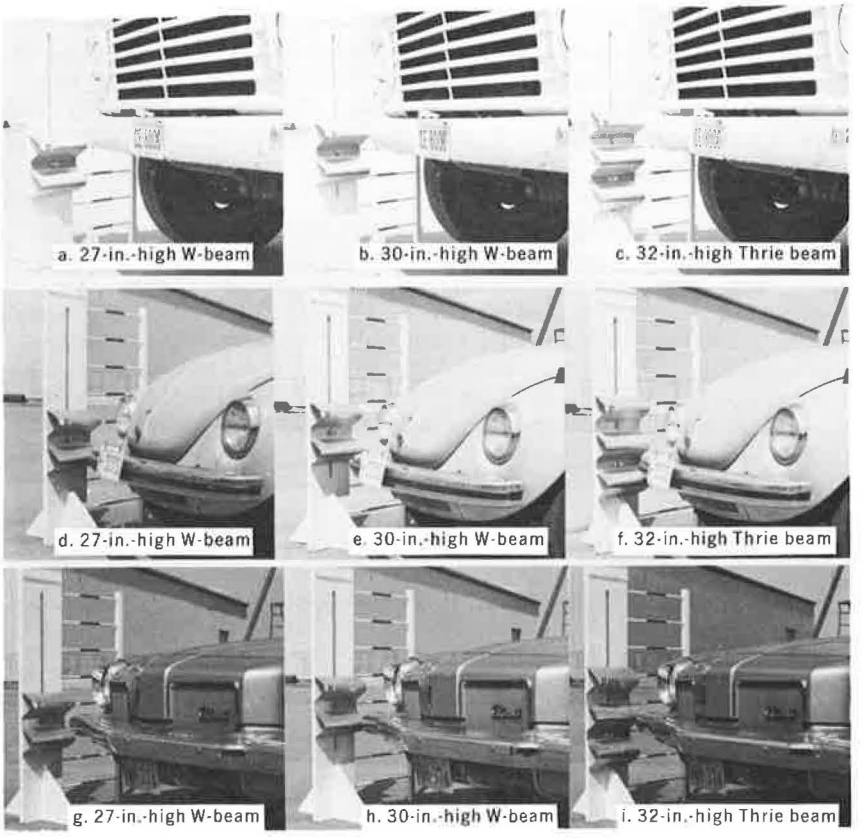

Figure 5. Installation for test AS-1.

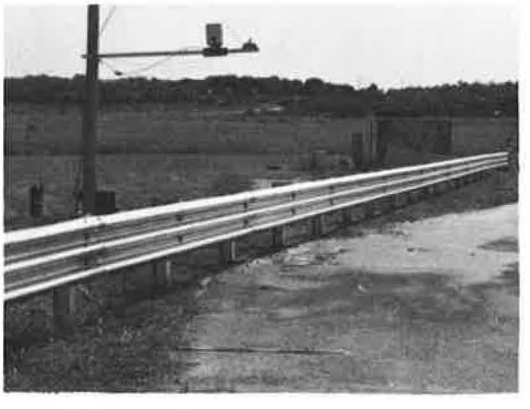

Figure 6. Installation for test AS-2.

The Thrie beam is proposed as a higher warranty barrier, affording better protection for a greater range of vehicles. Because 24-in. or less barriers warrant upgrading, it would be desirable to salvage as much of existing installations as possible in an upgrading program. Hence, test AS-2 was devised to evaluate performance of the 32-in. (0.8-m) Thrie beam system mounted on short posts (Fig. 6) as would occur with upgrading an existing installation by using the in-place posts. Of particular interest was the effect of the block-out projecting 6 in. (150 mm) or more above the top of the post.

Test AS-3

The standard test conditions originally outlined in HRB Circular 482 (9) characterized by a 4,000-lbm (1.8-Mg) vehicle and 60-mph (97-km/h), 25-deg impact are considered to constitute a strength test of the barrier; i.e., these conditions permit evaluation of the capacity of the barrier to restrain and redirect a vehicle impacting at these conditions. It is conjectured that impact angles of 15 deg or less represent the preponderance of actual impact angles. Test AS-3 was designed to evaluate dynamic performance of the 32-in. (0.8-m) Thrie beam median barrier system when impacted by a 2,000-lbm (0.9-Mg) subcompact car at 60 mph from an angle of 15 deg. The installation for test AS-3 is shown in Figure 7

Test AS-4

The purpose of the test was to evaluate the performance of a 32-in. high Thrie beam guardrail system when impacted at 60 mph and 15 deg by a 4,000-lbm (1.8-Mg) vehicle. The test installation for AS-4 is shown in Figure 8.

Test AS-5

The objective of this test was to evaluate the effectiveness of 14-in. (0.36-m) spacer used with 10-gauge (5.5-mm) Thrie beam in a guardrail installation. The M14 $\times$17.2 spacer element was selected because of its compatible flange width with the standard W6 $\times$8.5 post (Fig. 9). Standard crash test conditions were selected to evaluate performance of this increased spacer block depth; a goal of this test was to prevent wheel contact with posts.

TEST RESULTS

Results of the test series are given in Table 1 with a detailed description of each test.

Test AS-1

A 4,500-lbm (2.0-Mg) vehicle impacted the barrier downstream of post 10 (posts are numbered consecutively beginning upstream) with a speed of 66 mph (106 km/h) and an angle of 26.8 deg. The vehicle was redirected as shown in Figure 10; evidence of wheel contact with posts 12 and 13 was noted. Maximum dynamic deflection of 3.17 ft (0.97 m) occurred between posts 12 and 13.

Damage to the installation included two rail sections between posts 10 and 14, spacer blocks at posts 11 and 12, and post 12. Maximum permanent rail deflection of 22 in. (0.56 m) occurred between posts 12 and 13. Vehicle damage was severe at the left front corner as shown in Figure 11.

Test AS-2

The 4,000-lbm (1.8-Mg) vehicle impacted the barrier downstream of post 10 at a speed of 67.1 mph (106 km/h) and an angle of 28.7 deg. The vehicle was redirected at a large exit angle as shown in Figure 12. Vehicle stability appeared to be good until the vehicle left the pavement. As the vehicle dropped off the pavement, the damaged left wheel plowed into the rain-soaked ground causing complete vehicle rollover; there was evidence of some wheel snagging on post 13.

The barrier maximum dynamic deflection of 3.4 ft (1.04 m) occurred between posts 12 and 13.

Figure 7. Installation for test AS-3.

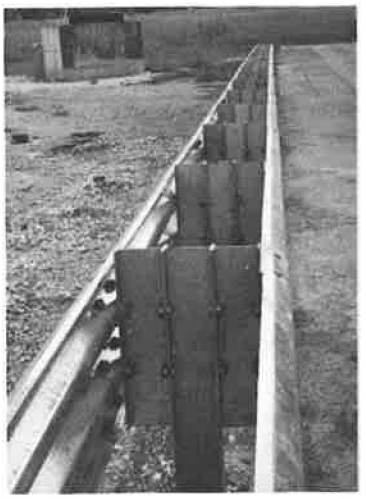

Figure 8. Installation for test AS-4.

Figure 9. Installation for test AS-5.

Table 1. Summary of Thrie beam tests.

Test	Beam Height (in.)	Post Embedment (in.)	Vehicle Weight (lbm)	Vehicle Speed (mph)	Impact Angle (deg)	Maximum Average Decelerations[a] (g)		Remarks
						Long.	Lat.	
AS-1	33	48	4,500	66.1	26.8	6.6	6.3	Median barrier test; vehicle redirection; no damage to passenger compartment
AS-2	32	42	4,000	67.1	28.7	5.9	7.4	Guardrail test; beam installed on short posts; vehicle redirected at large exit angle, relatively stable before crossing roadway where underside of vehicle plowed into ground causing vehicle upset
AS-3	32	48	2,200	54.1	16.8	2.0	5.3	Vehicle redirected with little damage to barrier or vehicle; vehicle was driveable after test
AS-4	32	48	4,500	59.1	15.9	2.9	4.1	Vehicle redirected with little damage to barrier or vehicle; left rear tire was split by off-site object; otherwise vehicle was driveable
AS-5	32	48	4,000	56.4	25.2	3.9	7.9	Vehicle redirected with no wheel-to-post contact.

Note: 1 in. = 25.4 mm; 1 lbm = 0.45 kg; 1 mph = 1.6 km/h.
[a]Highest 50-msec average obtained from high-speed cine analysis.

Figure 10. Test AS-1.

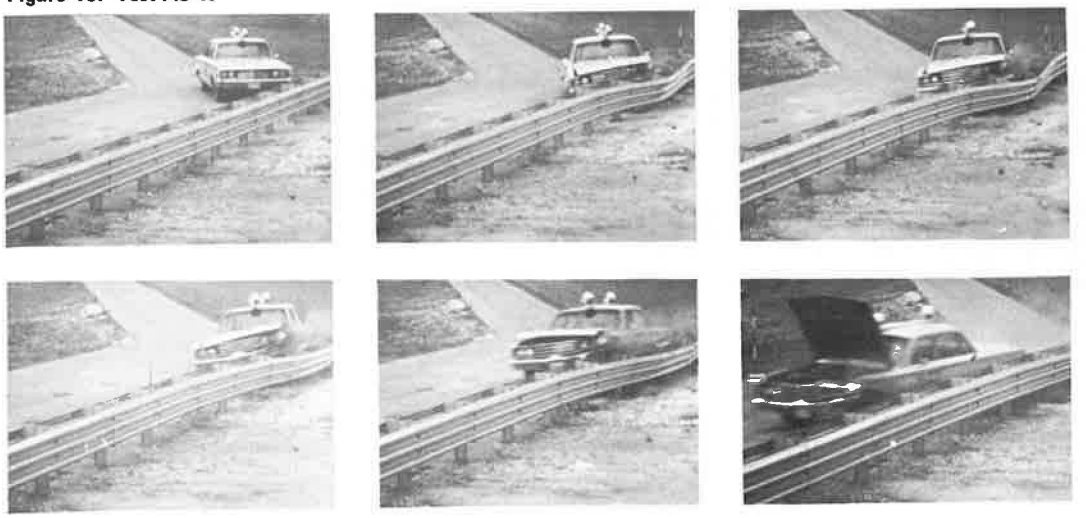

Figure 11. Beam and vehicle damage after test AS-1.

Figure 12. Test AS-2.

Damage to the barrier (Fig. 13) included two beam sections between posts 10 and 14. Although locally deformed near grade by the vehicle, post 12 was reusable. All posts and spacer blocks were judged to be reusable. There was no evidence of distress

Vehicle damage was severe because of the rollover; however, the passenger compartment was not deformed badly. Evidence of severe damage to the left corner of the vehicle (Fig. 13) is typical for strong-post guardrail systems under standard test conditions.

Test AS-3

A 2,200-lbm (1.0-Mg) vehicle impacted the barrier 0.1 ft (30 mm) upstream of post 9 at a speed of 54.1 mph (87 km/h) and an angle of 16.8 deg. The vehicle was smoothly redirected as shown in Figure 14. Barrier maximum dynamic deflection of less than 4 in. (100 mm) occurred between posts 9 and 10. No evidence of wheel contact with posts was noted.

Barrier damage as shown in Figure 15 was insignificant. The vehicle was driven from the test site with minimal front-end damage.

Test AS-4

The 4,500-lbm (2.0-Mg) vehicle impacted the barrier 0.1 ft upstream of post 9 at a speed of 59.1 mph (95 km/h) and an angle of 15.9 deg. The vehicle was redirected as shown in Figure 16. No evidence of wheel contact with posts was noted, and the vehicle was very stable throughout the impact. Maximum dynamic deflection of 7 in. (180 mm) occurred between posts 9 and 10. Damage to vehicle and barrier was very moderate (Fig. 17). The left rear vehicle tire was cut during the post impact trajectory; otherwise, the vehicle was driveable and was driven back to the impact zone.

Test AS-5

The 4,000-lbm (2.0-Mg) vehicle impacted the barrier 2.3 ft (0.7 m) downstream of post 9 at a speed of 56.4 mph (90.7 km/h) and an angle of 25.5 deg. The vehicle was redirected with no wheel-to-post contact (Fig. 18). Maximum dynamic deflection of 1.5 ft (0.56 m) occurred between posts 10 and 11. Damage to the barrier was limited to two rail sections inasmuch as most of the energy absorbed by the barrier was dissipated in beam flexure (plastic deformation) and translation of posts in soil (Fig. 19). No crushing or buckling of the 14-in. (0.35-m) spacers occurred. Damage to the vehicle was confined to the left front quarter; significant frame and suspension damage did not occur.

DISCUSSION OF RESULTS

The Thrie beam barrier systems tested in this program are proposed as a higher warranty system than the current W-beam systems. Because of the greater depth of this new element, the sensitivity of installation height is less than that of the standard 12-in. (305-mm) wide W-beam. In addition, the higher mounting height of the Thrie beam system will make it more compatible for impacts of vehicles with high centers of gravity.

Specifically, the findings of this program are as follows:

1. Use of the Thrie beam element eliminates the need for a rub rail in median barrier installations, thus effecting a substantial cost reduction. The capacity of the Thrie beam system to restrain a 4,500-lbm (2.0-Mg) vehicle impacting at 65 mph (105 km/h) and 25 deg on this system was demonstrated in test AS-1.
2. The Thrie beam can be mounted to existing posts of systems requiring upgrading. No structural problems developed in the details of this retrofit in test AS-2.
3. After impacts of both a 2,200-lbm (1.0-Mg) subcompact at 54 mph (87 km/h) and 17 deg with the Thrie beam median barrier design (test AS-3) and a 4,500-lbm (2.0-Mg) standard sedan impact at 59 mph (95 km/h) and 16 deg with the Thrie beam

Figure 13. Beam and vehicle damage after test AS-2.

Figure 14. Test AS-3.

Figure 15. Beam and vehicle damage after test AS-3.

Figure 16. Test AS-4.

Figure 17. Beam and vehicle damage after test AS-4.

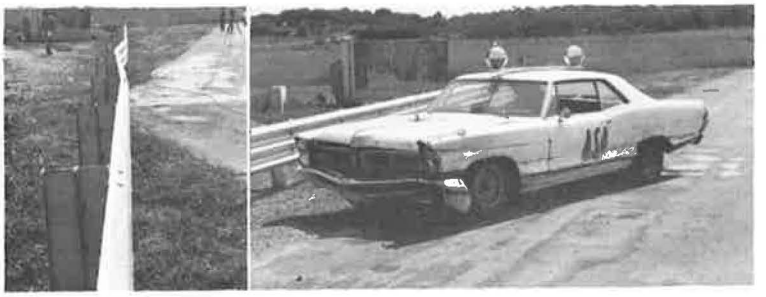

Figure 18. Test AS-5.

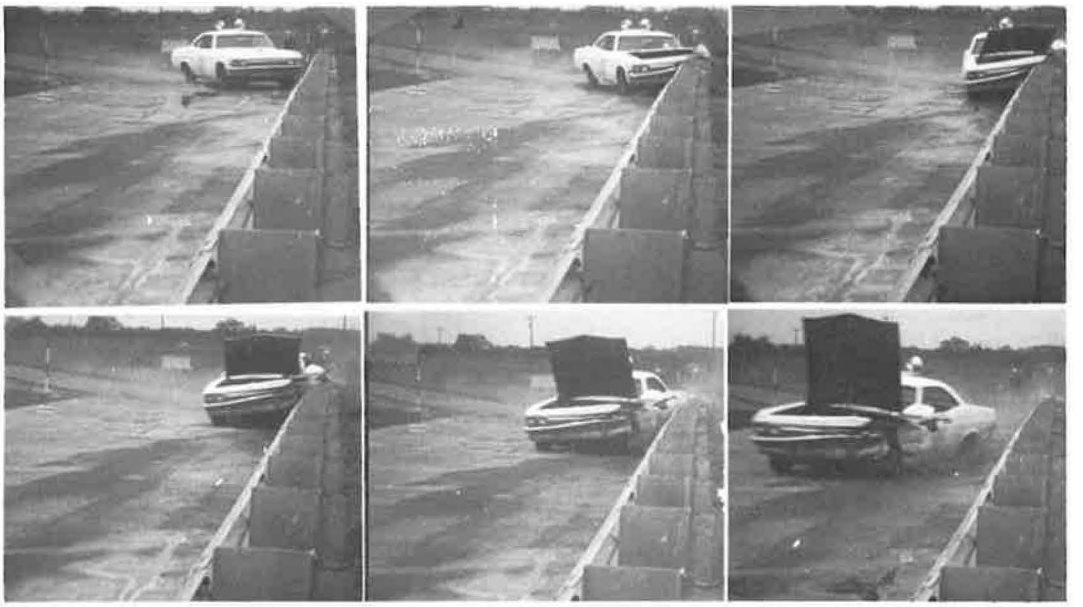

Figure 19. Beam and vehicle damage after test AS-5.

guardrail design (Test AS-4), the vehicles were driveable.

4. Use of 10-gauge (5.5-mm) Thrie beam element with 14-in. (356-mm) spacers prevented wheel contact with posts in test AS-5.

ACKNOWLEDGMENTS

The work reported was conducted at Southwest Research Institute by the Department of Structural Research and was sponsored by the Anderson Safeway Guard Rail Corporation of Flint, Michigan.

The crash test program was conducted with assistance from C. E. Kimball, G. W. Deel, R. P. Guillot, Roland Guerra, and T. H. Conard, Jr. C. A. Walker was responsible for the crash test photography, and R. C. DeHart served in the capacity of technical and administrative adviser.

Assistance was provided by Douglas Chisholm of the Structures and Applied Mechanics Division of FHWA in selecting the method of forming the prototype test railing sections. The valuable suggestions regarding the railing design details and test program formulation provided by Eric Nordlin of the California Division of Highways are gratefully acknowledged. Finally, for his continued interest and support, the authors are grateful to William C. Shapiro, President of Anderson Safeway Guard Rail Corporation.

The opinions, findings, and conclusions expressed in this paper are those of the authors and not necessarily those of the sponsor or other agencies with which the authors are affiliated.

REFERENCES

1. Graham, M. D., Burnett, W. C., Gibson, J. L., and Freer, R. H. New Highway Barriers: The Practical Application of Theoretical Design. Highway Research Record 174, 1967, pp. 88-183.
2. Van Zweden, J. Performance of Highway Barriers. New York State Dept. of Transportation, final report, June 1972.
3. Graham, D. Progress Report on New York State's Highway Barrier Research Program. Presented to the AASHO Design Committee, Oct. 29, 1969.
4. Michie, J. D., and Bronstad, M. E. Location, Selection, and Maintenance of Highway Traffic Barriers. NCHRP Rept. 118, 1971.
5. Whitmore, J. L., Snyder, W. A., and Picciolca, J. G. Highway Barriers and Safety Accessories. New York State Dept. of Transportation, final report, June 1972.
6. Olson, R. M., Smith, H. L., Ivey, D. L., and Hirsch, T. J. Texas T1 Bridge Rail Systems. Texas Transportation Institute, Tech. Memo. 505-10, April 1971.
7. Walker, G. W., and Warner, C. Y. Crash Tests Evaluation of Strong-Post, Energy-Absorbing Guardrail Using a Lapped W-Beam for Transitions and Median Barriers. Highway Research Record 386, 1972, pp. 78-87.
8. Field, R. N., and Prysock, R. H. Dynamic Full Scale Impact Tests of Double Block-Out Metal Beam Barriers and Metal Beam Guard Railing—Series X. California Division of Highways, Feb. 1965.
9. Proposed Full-Scale Testing Procedures for Guardrails. Highway Research Correlation Service, HRB, Circular 482, Sept. 1962.

PROPORTIONS FOR IMPROVED STIFFNESS OF BOX SECTION BEAMS USED AS LONGITUDINAL ROADSIDE GUARDRAIL BARRIERS

W. V. Brewer, University of Tulsa

ABRIDGMENT

•DIMENSIONS for barrier beam sections cannot be specified in an optimum way without a detailed consideration of the system using the beam. Proportions, however, may be examined with a minimum of information about the system. It is here assumed that the beam is part of a strong-beam, weak-post, high-performance system designed to accept high-speed vehicles with low deceleration rates. As performance requirements increase, a cost-effective system must use greater barrier spans to absorb vehicle energy (1). A high specific stiffness is desirable. The second moment of cross-sectional area about the major section axis divided by the cross-sectional area squared is the stiffness ratio used for comparisons because it is not dependent on section size. Similar ratios are used for minor axis and torsional stiffness.

AISC specifications limiting width-thickness ratios for structural plate elements are used wherever applicable. Simply supported plate conditions are assumed throughout so that all proportions are conservative to this extent. Nomenclature is as shown in Figure 1. Pertinent formulas are as follows:

1. (second moment of area about the major section axis)/(half depth)^4

$$\frac{I}{h^4} = 4\,\frac{a_2}{h}\,\frac{b_2}{h}\left(\tfrac{1}{2}\,\frac{a_1}{a_2}\,\frac{b_1}{b_2}\left(\frac{z_1}{h}\right)^2 + \left[\frac{(z_1/h)^2 + (z_2/h)^2}{2}\right]\left\{1 + \tfrac{1}{3}r\left[\frac{(z_1/h)^3 + (z_2/h)^3}{(z_1/h)^2 + (z_2/h)^2}\right]\right\}\right)$$

for $\frac{z_2}{h} = 2 - \frac{z_1}{h}$ and $\frac{z_1}{h} = \dfrac{1}{1 + \frac{1}{2}\,\frac{a_1}{a_2}\,\frac{b_1}{b_2}\left(\frac{1}{1+r}\right)}$.

2. (second moment of area about the minor section axis)/(half depth)^4

$$\frac{i}{h^4} = 4\,\frac{a_2}{h}\left(\frac{b_2}{h}\right)^3\left[\tfrac{1}{6}\,\frac{a_1}{a_2}\left(\frac{b_1}{b_2}\right)^3 + r\left(1 + \frac{1}{3r}\right)\right]$$

for $r = \dfrac{\frac{j_2}{a_2}}{\frac{b_2}{h}}$.

3. (torsional stiffness for a thin walled tube)/(cross-sectional area)^2

$$\frac{J}{A^2} = \left(\frac{2h}{j_2}\right)\frac{r}{\left(\frac{1}{2}\,\frac{a_1}{a_2}\,\frac{b_1}{b_2} + 1 + r\right)^2\left(1 + \frac{1}{1 + a_1/a_2} + 2\,\frac{a_2}{j_2}\,\frac{h}{b_2}\right)}$$

As a point of reference, consider a box section structural tube of uniform wall thickness, compact about its major axis. The maximum width-thickness ratio for flanges (2, p. 102) is

Figure 1.

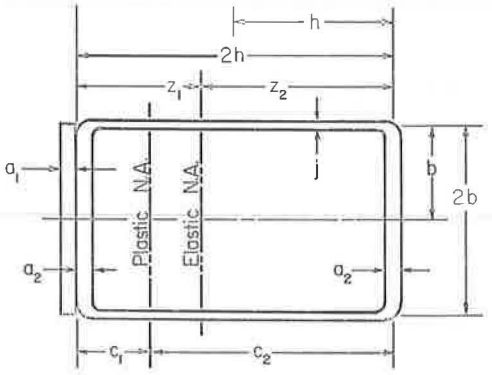

$$\frac{2b}{a} \leq \frac{6,000}{f^{1/2}}$$

and for webs is

$$\frac{2h}{j} \leq \frac{13,300}{f^{1/2}}$$

where f is the yield or plastic stress in psi.

Stiffness for this section is a function of ratio r. The function maximizes for r = 3.

$$r = \left(\frac{j}{a}\right)\Big/\left(\frac{b}{h}\right)$$

$$\frac{I}{A^2} = \frac{2h}{j}\,\frac{r(1 + \frac{1}{3}r)}{8(1 + r)^2}$$

Maximum stiffness about the major section axis is produced at a flange ratio less than the allowable; however, increasing 2b/a to the limit does not significantly change this performance. Minor axis and torsional stiffness are substantially increased as b/h = 1/r = 0.451.

$$\frac{I}{A^2} = \frac{619}{f^{1/2}}$$

$$\frac{i}{A^2} = \frac{185}{f^{1/2}}$$

$$\frac{J}{A^2} = \frac{443}{f^{1/2}}$$

Elastically designed sections have more desirable stiffness characteristics but cannot be used in guardrail applications because of the prohibitive expense of preventing plastic hinge in the vehicle impact area. It is in this area that the roadside flange is in compression and must be capable of performing plastically without local buckling. The opposite outside flange need not meet the same requirements. It is in tension throughout the plastic impact zone of maximum moment and is therefore stable. Zones of second largest bending moment occur on either side of the vehicle impact area. The discussion that follows applies only to roadside barriers and not to median barriers, which must have identical performance from both flanges. Further, the discussion assumes that the barrier system has been designed to prevent plastic flexure in these areas. (Our studies lead us to believe that this would minimize initial costs as well as reduce replacement costs for high performance systems.) Outside flanges may then be designed elastically to take advantage of superior overall stiffness. Resulting cross sections have only one axis of symmetry.

An asymmetric section that is relatively easy to fabricate from a strip of uniform thickness (by folding or possibly roll forming) has one flange double the thickness of the other. Elastic design of the outside flange to meet AISC specification (2, p. 100) requires a width-thickness ratio somewhat more conservative than the perfect plate theory:

$$\frac{2b}{a} \leq \frac{8,000}{f^{1/2}}$$

The doubled roadside flange exceeds plastic plate requirements.

Plastic requirements for stability of the webs subjected to combined tension and bending are less severe than for pure bending. Any reasonable estimate of this ratio must depend on relative magnitudes of tension and bending or alternatively on the location of the neutral axis for a plastic section. This cannot be known without specifying section proportions that require the desired ratio 2h/j. An iterative solution is necessary. Values thus obtained produce the following results for the proposed asymmetric section:

$$\frac{a_1}{a_2} = 1 \qquad \frac{j}{a_2} = 1 \qquad \frac{b}{h} = 0.455 \qquad \frac{2b}{a_2} = \frac{8,000}{f^{1/2}}$$

$$\frac{I}{A^2} = \frac{765}{f^{1/2}} \qquad \frac{i}{A^2} = \frac{197}{f^{1/2}} \qquad \frac{J}{A^2} = \frac{479}{f^{1/2}} \qquad \frac{2h}{j} = \frac{17,600}{f^{1/2}}$$

Stiffness ratios have improved in every category for this section when compared with a symmetric box section structural tube of uniform wall thickness. In volume production fabrication cost would be little if any more than for a symmetric box section. Lighter sections could be used to obtain the same performance levels.

A second asymmetric section that is relatively easy to fabricate consists of a box section tube of uniform wall thickness with the roadside flange augmented by a plate. The tube flanges satisfy the elastic criterion. Thickness a_1 of the plate augmenting the roadside flange can be adjusted so that the plastic criterion is satisfied where the possibility of different maximum stress levels in the component parts has been taken into account.

$$\frac{a_1}{2b} = \frac{f_1^{1/2}}{6,000} - \frac{f_2^{1/2}}{8,000}$$

for $f_1 \geq f_2$. When $f_1 > f_2$, then a_1 is sized conservatively as if the entire composite roadside flange would develop plastic stress f_1.

If component parts are made of the same material and the largest elastic stress is equal to the plastic stress, then

$$\frac{2b}{a_2} = \frac{8,000}{f^{1/2}} \qquad \frac{i}{A^2} = \frac{246}{f^{1/2}} \qquad \frac{a_1}{a_2} = \frac{1}{3}$$

$$\frac{I}{A^2} = \frac{665}{f^{1/2}} \qquad \frac{2h}{j} = \frac{14,800}{f^{1/2}} \qquad \frac{j}{a_2} = 1$$

$$\frac{2b}{a_1} = \frac{24,000}{f^{1/2}} \qquad \frac{J}{A^2} = \frac{552}{f^{1/2}} \qquad \frac{b}{h} = 0.542$$

Stiffness ratios are improved in every respect when compared with symmetric section but are superior to the single-component asymmetric section only about the minor axis and in torsion.

Performance about the major axis is enhanced as a result of a shift in the plastic neutral axis. The greater shift in single-component section is a result of greater augmentation of material to the roadside flange. A more pronounced effect can be obtained by increasing the strength of the augmenting material. As an example in the extreme, let $f_1 = 2f_2$.

$$\frac{a_1}{a_2} = 0.886 \qquad \frac{2b}{a_2} = \frac{8,000}{f_2^{1/2}} \qquad \frac{i}{A^2} = \frac{188}{f_2^{1/2}}$$

$$\frac{j}{a_2} = 1 \qquad \frac{I}{A^2} = \frac{936}{f_2^{1/2}} \qquad \frac{2h}{j} = \frac{20,800}{f_2^{1/2}}$$

$$\frac{b}{h} = 0.384 \qquad \frac{2b}{a_1} = \frac{9,030}{f_2^{1/2}} \qquad \frac{J}{A^2} = \frac{492}{f_2^{1/2}}$$

SUMMARY

Asymmetric box beam cross sections, formed by adding material to the roadside flange, have superior specific stiffness characteristics when compared with symmetric sections designed to meet similar stability criteria. Stiffness about the major section axis can be increased by as much as 50 percent while minor axis and torsional stiffness are maintained at levels comparable to a symmetric section. Alternatively minor axis and torsional stiffness can both be increased 25 percent by accepting a marginal 7 percent increase about the major axis.

CONCLUSIONS

Current barrier systems employing box section beams use unnecessarily conservative section proportions. A roadside barrier system designed to employ asymmetric box sections could translate superior stiffness into reduced overall cost for a high-performance system.

ACKNOWLEDGMENTS

This investigation was supported by the National Science Foundation and by the University of Tulsa.

REFERENCES

1. Brewer, W. V. Energy-Absorbing Barrier Beams Suspended From Linear Supports (Abridgment). Highway Research Record 460, 1973.
2. Brackenbrough, R. L., and Johnston, B. G. Steel Design Manual, 2nd Ed. United States Steel Corp., Nov. 1968.

DEVELOPMENT OF APPROACH RAIL-BRIDGE RAIL TRANSITION USING ALUMINUM BALANCED SYSTEM

J. D. Michie and M. E. Bronstad, Southwest Research Institute; and
G. Alison, The Aluminum Association

ABRIDGMENT

A series of four vehicle crash tests was performed during the development of an approach rail-bridge transition using the Aluminum Association balanced rail system. Nominal impact conditions for the 4,000-lbm (1800-kg) cars were 60 mph (97 km/h) and 25 deg; the point of impact was immediately upstream from the bridge rail end. After each test, design modifications were incorporated in the installation to improve its performance. Features that were varied during the test series include the bridge curb, transition post spacing, soil reaction plates for posts, rail cross section geometry, and rail splice details. The final design, tested in the fourth test, exhibited acceptable vehicle redirective performance. Vehicle decelerations of 6.6 (long.) and 7.8 (lat.) g are moderately high but are judged acceptable.

•A SIGNIFICANT number of fatal highway accidents occur near, at, or on bridges. Olson and others (1) showed that approximately 22 percent of fatal single-vehicle accidents involve these bridge sites. An analysis of these fatal accidents by location shows that 73 percent of errant vehicles impact the approach guardrail and bridge end and 27 percent collide with the bridge railing. Performance of the barrier systems in the accidents has been inadequate as evidenced by the fact that 16 percent of the vehicles either vaulted or penetrated the installation and 52 percent pocketed or snagged.

As a result of these statistics, highway engineers recognized the need for structural continuity between approach guardrail and bridge rail installations in the 1969 AASHO bridge specification. However, the design of safely performing schemes has been slow because of the difficulty of achieving a gradual and nonsnagging transition from the more flexible approach guardrail to the stiffer bridge rail installations.

The Aluminum Association balanced system traffic barrier offers a unique situation because the barrier is used as both guardrail and bridge rail. Accordingly, a research program was undertaken to develop an effective transition for the AA balanced system. The finalized system is shown in Figures 1 and 2.

PROGRAM

The program consisted of four full-scale crash tests with nominal impact conditions of a 4,000-lbm (1800-kg) vehicle impacting at 60 mph (97 km/h) and 25 deg. The point of impact was immediately upstream from the bridge rail end, the most vulnerable area of a traffic barrier. During the test series, installation features were modified to improve dynamic performance; the modified features were bridge curb, transition post spacing, soil reaction plates, rail cross section, and splice bar length.

FINDINGS

A summary of results for the four tests is given in Table 1. Because tests AA-2, AA-3, and AA-4 were preliminary tests, the primary interest of this paper is directed to test AA-5.

Figure 1. Pretest photographs of test installation.

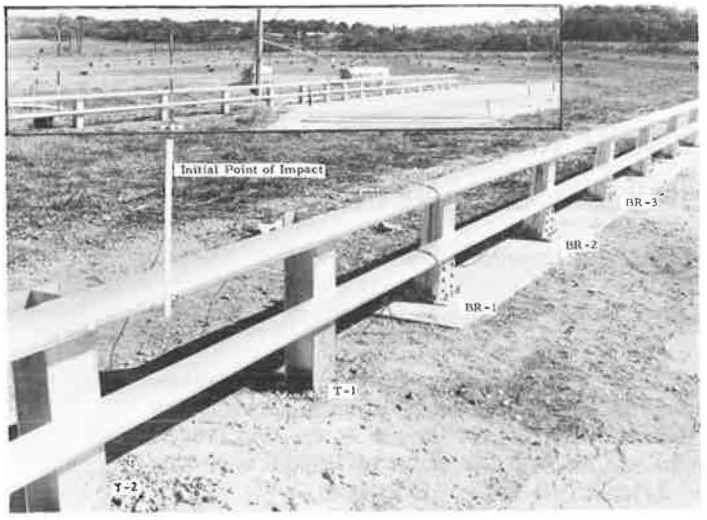

Figure 2. Details of approach rail-bridge rail test installation.

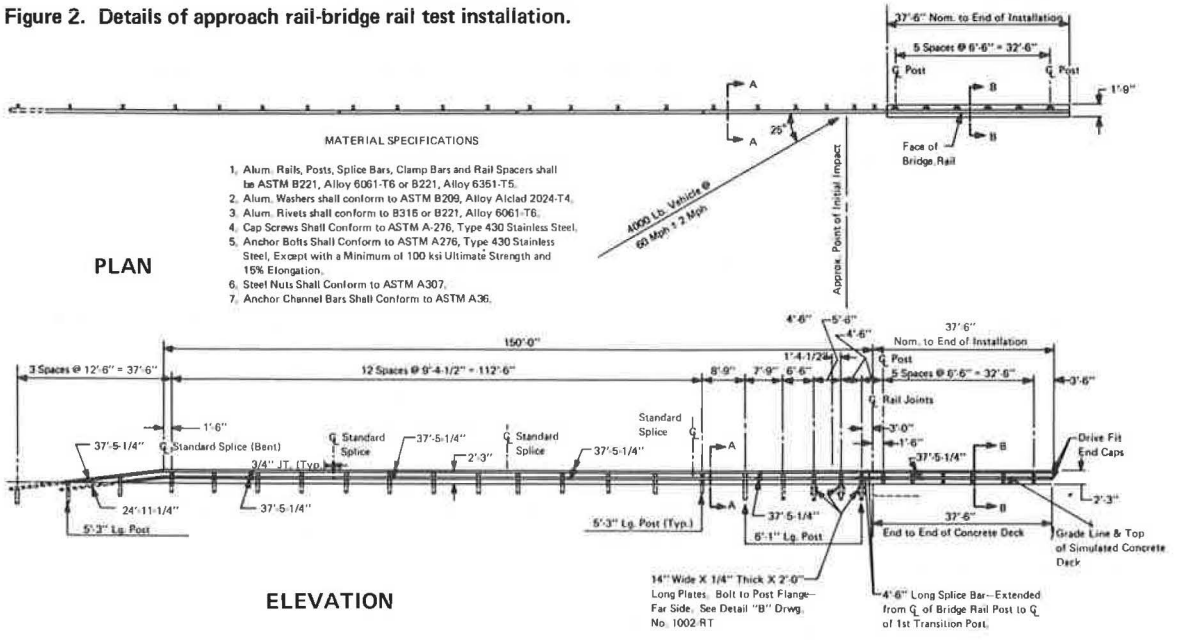

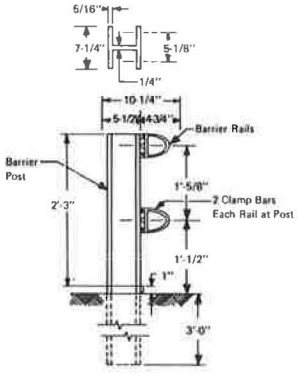

SECTION A-A

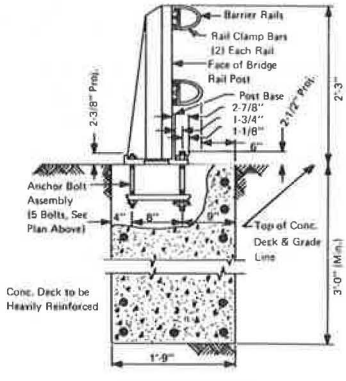

SECTION B-B

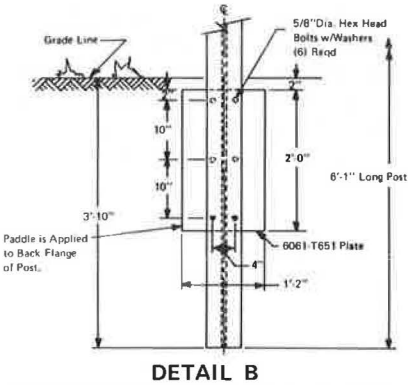

DETAIL B
REINFORCING PADDLES TO POSTS

Table 1. Summary of test results.

Test	Impact Conditions				Vehicle Decelerations (g)[a]		Remarks
	Vehicle Weight (lbm)	Speed (mph)	Angle (deg)	Location	Long.	Lat.	
AA-2	3,997	58.2	26.7	8.5 ft upstream of bridge post 1	15.5	13.0	Vehicle snagged on concrete curb; both rails broke at end of transition connection splice bar
AA-3	4,050	63.7	25.0	1.0 ft downstream from transition post T3	14.2	14.0	Vehicle snagged on transition post; both rails failed at splice connection; excessive lateral deformation of transition post
AA-4	4,017	68.1	25.5	2.5 ft downstream from transition post T2	9.1	8.0	Vehicle redirected although snagging on transition post T1 occurred; top rail was severed after redirection
AA-5	3,965	58.0	23.0	0.8 ft downstream from transition post T2	6.6	7.8	Vehicle redirected although snagging on post T1 occurred

Note: 1 lbm = 0.45 kg; 1 mph = 1.6 km/h; 1 ft = 0.305 m.
[a]50 msec average.

Figure 3. Views of impacted rail showing (a) vehicle position after impact and (b) vehicle approach.

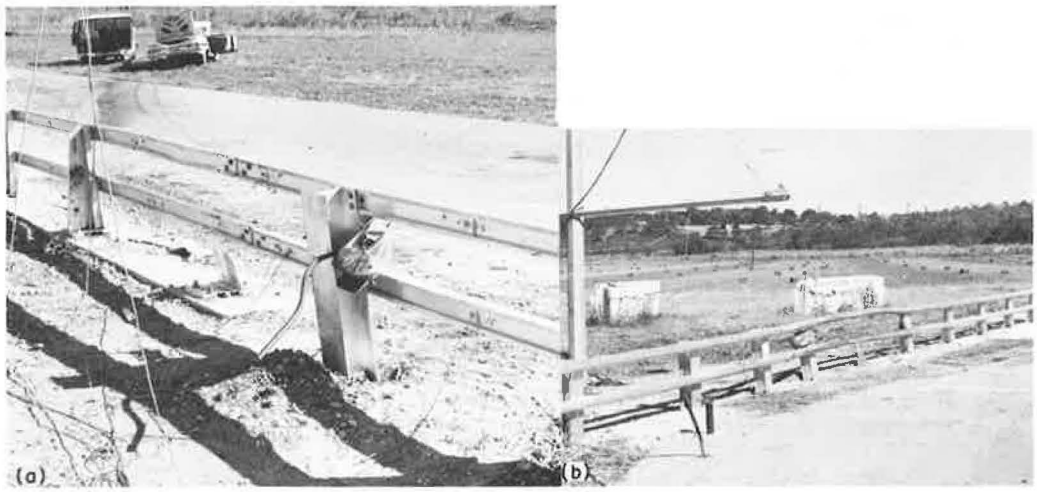

Figure 4. AA-5 test vehicle (a) before and (b) after impact.

After impacting the rail 0.8 ft (0.2 m) downstream from transition post T-2 (Fig. 1) at 58 mph (94 km/h) and 23 deg, the 3,965-lbm (1798-kg) AA-5 test vehicle was redirected at 20 deg after being in contact with the rail for 0.51 sec. Maximum lateral dynamic deflection of the system was 1.4 ft (0.45 m) and occurred between transition post T-1 and bridge post BR-2 (post BR-1 was taken out). Maximum vehicle accelerations were -6.6 (long.) and -7.8 (lat.) g. Installation damage is shown in Figure 3; vehicle damage is shown in Figure 4.

CONCLUSIONS

From the results of this test, the following conclusions are drawn:

1. The overall performance of the balanced system transition section was judged satisfactory considering the accepted performance criteria (2) and present traffic barrier technology.
2. Vehicle decelerations during redirection were moderate. It is conjectured that passengers restrained with lap belt and shoulder straps would probably have survived with only minor to moderate injuries.
3. The vehicle's 20-deg exit angle was relatively high and could possibly be a hazard to adjacent or following traffic.
4. Vehicle damage was extensive but is characteristic of damage for the severe test conditions involving relatively rigid traffic barrier systems.
5. The displacement of bridge post BR-1 could be a hazard, especially in urban areas where the bridge rail is installed on an overpass. The bridge post falling off the structure could endanger vehicular or pedestrian traffic below.

ACKNOWLEDGMENT

The research was sponsored by the Aluminum Association and performed at Southwest Research Institute. The opinions, findings, and conclusions expressed are those of the authors and not necessarily those of the sponsoring and performing agencies.

REFERENCES

1. Olson, R. M., Post, E. R., and McFarland, W. F. Tentative Service Requirements for Bridge Rail Systems. NCHRP Rept. 86, 1970.
2. Michie, J. D., and Bronstad, M. E. Location, Selection, and Maintenance of Highway Traffic Barriers. NCHRP Rept. 118, 1971

FULL-SCALE EMBANKMENT TESTS AND COMPARISONS WITH A COMPUTER SIMULATION

Hayes E. Ross, Jr., and Edward R. Post, Texas Transportation Institute, Texas A&M University

Criteria have been published identifying embankments that need guardrail protection. Some of the criteria, related to embankment severity, were based on output from the Texas Transportation Institute's version of the highway-vehicle-object simulation model (HVOSM). Because HVOSM had not been validated for embankments with relatively steep side slopes and because implementation of the criteria would require changes in current Texas Highway Department design procedures, a limited validation study was undertaken. Six full-scale automobile tests were conducted on an embankment of an in-service roadway. The embankment had a side slope of approximately 3.5:1 and a flat-bottom ditch approximately 20 ft below the roadway. The grassy slope, ditch bottom, and back slope were well compacted. A wide variety of encroachment conditions were obtained in the six tests. In addition, suspension failures and, in one case, an attempt to steer back on the side slope created special test conditions. This range of test conditions encompasses many of the conditions that occur in run-off-the-road accidents. Each test was simulated by the HVOSM, and the results were then compared with the measured test results. Three basic types of data were compared: vertical accelerations, vehicle paths, and vehicle attitudes.

• A STUDY at the Texas Transportation Institute (TTI) developed need criteria (1, 2) for a steel W-beam guardrail with 6-ft 3-in. post spacing. The criteria indicate where guardrail should be used to prevent an automobile from going over a given embankment configuration. The embankment geometry consisted of a side slope with a flat-bottom ditch. The criteria were established by comparing the severity of an automobile leaving the road and going down an embankment with the severity of an automobile striking the guardrail. In this manner, we could identify embankment geometries in which the severity of traversing them is less than that of striking a guardrail. To quantify severity, we used automobile accelerations with which a severity index was compared.

The severity of striking a guardrail was determined primarily from full-scale test results, whereas the severity of traversing an embankment was determined by use of TTI's version of the highway-vehicle-object simulation model (HVOSM). Previous validation studies have shown that HVOSM can accurately predict the dynamic motion of an automobile in many types of maneuvers (3, 4, 5, 6, 7). However, no reported full-scale tests have been conducted to establish the validity of HVOSM in predicting the behavior of an automobile traversing embankments similar in geometry to those considered in the aforementioned studies (1, 2).

The criteria (1, 2) indicate that guardrail protection is not warranted for side slopes that are 3:1 or flatter with ditches less than 50 ft deep. If adopted, this criterion would require changes in current Texas Highway Department (THD) highway design specifications. A limited number of full-scale tests were therefore considered necessary to substantiate the results of HVOSM and to aid in the decision on revisions to the specifications.

A series of tests was conducted on an in-service roadway to provide data with which the HVOSM predictions could be compared. This paper summarizes the tests, the comparisons, and their implications. Complete details cannot be given here; however, full details of the study are available in a TTI report (8).

FULL-SCALE TESTS

Test Site

An effort was made to locate an embankment with a side slope of approximately 3:1 (3 lengths laterally to 1 length vertically) and with considerable depth inasmuch as the criteria (1,2) indicated that such was the "critical" slope. In other words, it was determined that the severity of traversing 3:1 and flatter slopes was less than that of striking a guardrail.

With the assistance and cooperation of THD personnel, a site was located on Texas-21 (Fig. 1). The slope and depth of the embankment were very close to the desired values.

The test section extended 400 ft along the roadway and approximately 140 ft laterally from the edge of the pavement. A grid layout of the test section is shown in Figure 2. Eleven stations, spaced on 40-ft centers, were established on a control line along the edge of the unpaved 10-ft shoulder. At each station, wooden stakes were set at ground level on 10-ft horizontal centers along a line perpendicular to the control line. Figure 3 shows profiles of stations 1, 2, and 3.

Chalk lines were placed on the embankment grid to provide a reference for determining vehicle path from film analysis and visual observations of tire tracks.

Test Vehicle

A 1963 Ford Galaxy was used in the test because TTI had all the parameters needed in its simulation by HVOSM.

The hazardous nature of the planned tests precluded the use of a test driver. Guide cables could not be used to control the vehicle, for this would have required blocking traffic on Texas-21 for an unreasonable time period. The only alternative was to design and build a remote-control system for the test vehicle. Its basic features were closed-loop (controlled) proportional steering or open-loop (free-wheeling) steering, proportional acceleration, and brake and clutch control. Commands to the test vehicle were transmitted from a trailing vehicle.

Data Measurement

Accelerations, attitude, and path are important parameters that affect the relative severity of a vehicle traversing an embankment. To measure these quantities, we used accelerometers, high-speed photography, and visual observation of tire tracks.

Encroachment speed was determined from the high-speed movie film by observing the time required for the vehicle to traverse a known distance between stadium poles (see Fig. 6). The vehicle position and attitude as a function of time could also be determined from the movie film by observing the vehicle's path with respect to the grid lines.

Three accelerometers were mounted in a cluster near the vehicle's center of gravity to measure longitudinal, lateral, and vertical accelerations. The accelerometer cluster was located at the intersection of the longitudinal and lateral center-of-gravity axes and approximately 7 in. below the vertical position of the center of gravity. Acceleration output was telemetered back to an instrumentation trailer for recording on magnetic tape.

A thin layer of dirt was placed along the shoulder where the test vehicle left the roadway. Tire tracks on the dirt provided a simple means of determining the encroachment angle.

As the vehicle traversed the embankment, distinct tire tracks were made. After each test, the position of the tracks was measured with respect to the grid system and then recorded.

Figure 1. Test site viewed from ditch bottom.

Figure 2. Embankment grid layout.

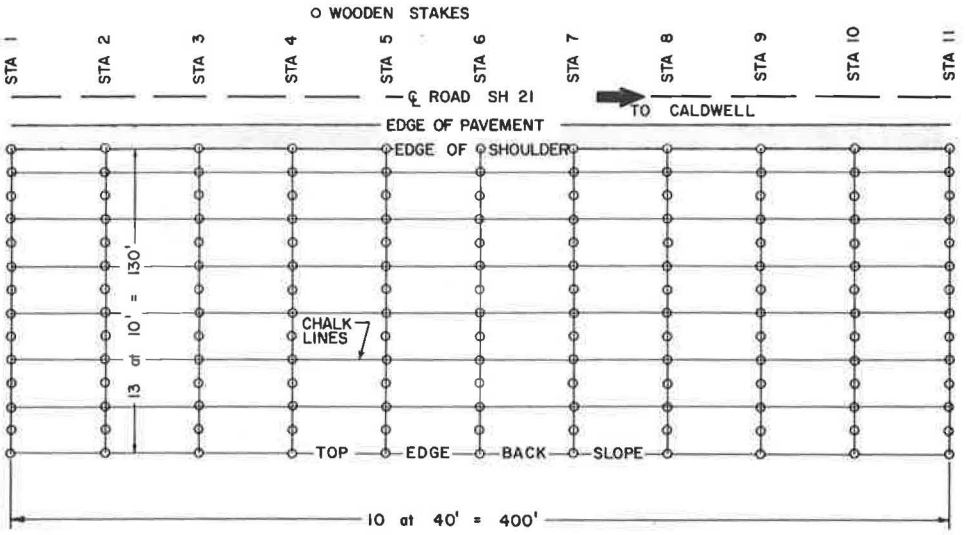

Figure 3. Embankment profiles.

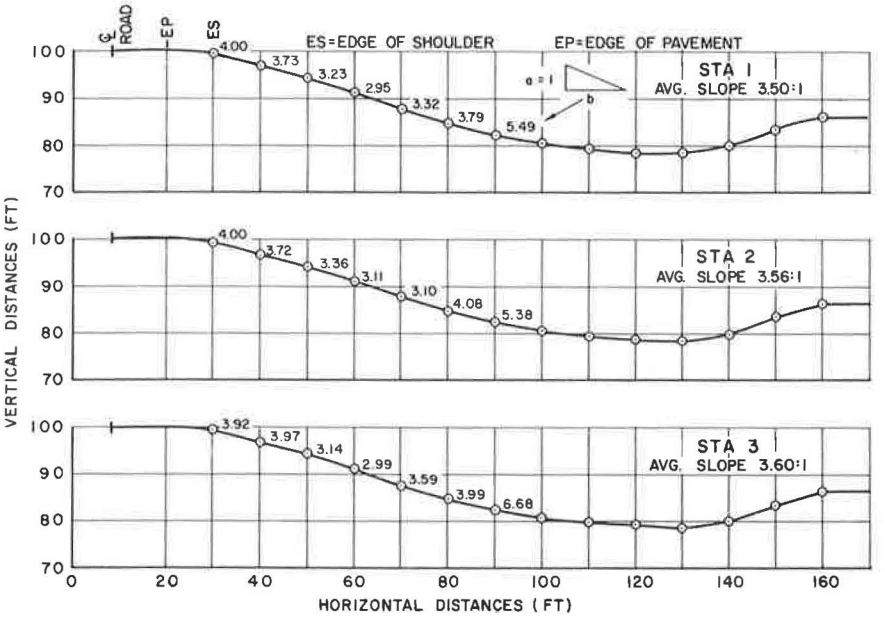

Test Procedure

Figure 4 shows a plan view of the test setup. Just before each test, traffic was halted approximately ½ mile from the test site. The test car was then accelerated to the desired speed and guided off the road from the trailing vehicle. Traffic cones were used as guides to aid the remote-control operator in steering the car off the road at the desired location and encroachment angle.

Upon leaving the roadway, the test car was allowed to traverse the embankment in a free-wheeling condition. After it reached the bottom of the slope, steer control was regained and an attempt was made (not always successfully) to prevent the car from going over the back slope.

TEST RESULTS AND COMPARISONS WITH HVOSM

A total of six tests were conducted for various encroachment conditions. Table 1 gives the details of each test. The primary reason for the tests was to provide a wide variety of conditions to simulate. In addition, the tests provided valuable full-scale test data on an actual in-service roadway site. Other than tie-rod failures, the test car sustained no significant structural damage and was still in running condition at the conclusion of the tests.

HVOSM Input

Each test was simulated by HVOSM. Input to the program consisted of embankment geometry, vehicle parameters, and test conditions. Vehicle parameters for the test car were obtained at TTI on another study (5). Sears Supertread tires were used on the test car, and their properties were available from the literature (4). A friction coefficient between the tire and the grassy slope was not available. However, skid tests were conducted at the Texas A&M Research Annex on grass and sod similar to that at the test site and a coefficient of 0.5 was determined.

Comparisons

Three types of comparisons were made between test results and HVOSM output. These were plots of the right front tire track (Fig. 5), computer-generated perspective drawings of the simulated vehicle at selected times adjacent to prints of frames from the high-speed movie film at the same times (Figs. 6 and 7), and plots of vertical acceleration versus time (Fig. 8). These figures show comparisons for test 1. The grid lines shown on the HVOSM tire track plots correspond to the chalked grid lines at the test site. Data given in Table 2 show a comparison of the measured peak and average vertical accelerations and those from the HVOSM simulation for the six tests. It is important to note that these accelerations are below tolerance limits established for an unconstrained occupant (1).

Generally good agreement was obtained between measured and predicted values for tests 1, 3, 4, and 5. Vehicle path and attitude comparisons for these four tests were very good. Although there were some variations in the acceleration time comparisons, the differences in the measured and predicted peak and average accelerations were within acceptable accuracy, given that several factors can contribute to their differences:

1. Terrain irregularities—Local irregularities such as bumps and eroded areas, whose simulation is not feasible, can cause small fluctuations in the accelerations;
2. Type and location of accelerometer support—The degree to which the automobile's structural vibration contributes to the measured values is unknown; and
3. Tire rutting—Although the slope and ditch bottom were well compacted, some minor rutting was observed (the effects of rutting cannot be accounted for in TTI's version of HVOSM without prior knowledge of its occurrence).

Tie-rod failures, which locked the right front tire in a full right-turn position, in tests 2 and 6 created special test conditions in that HVOSM is not currently capable of predicting such failures and their subsequent effects. It is not known to what extent the previous tests (same car used in all tests) contributed to these failures, i.e., by

Figure 4. Plan view of test setup.

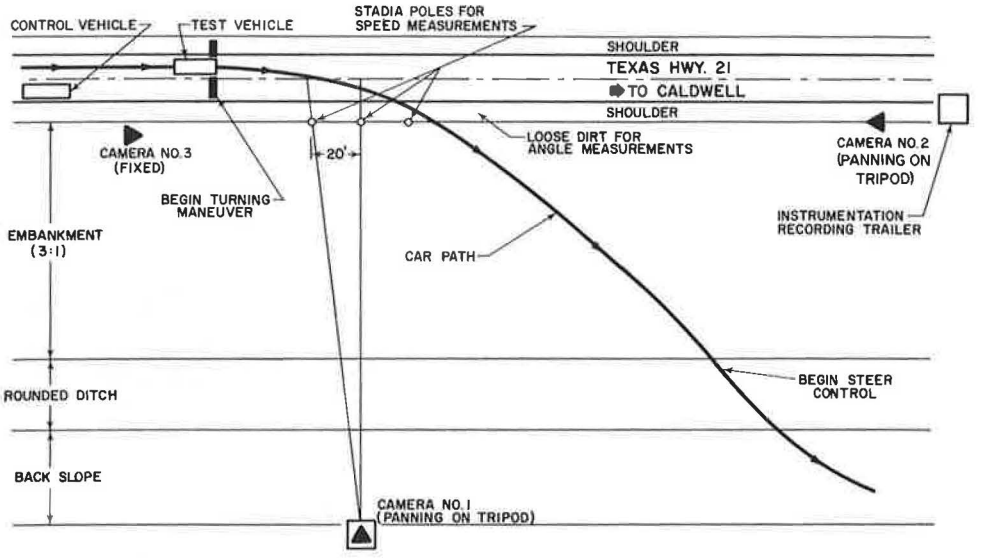

Table 1. Test conditions.

Test No.	Encroachment Angle (deg)	Encroachment Speed (mph)	Comments
1	9.7	55.7	No problems.
2	13.8	45.1	Tie-rod failure locked right front tire in full right steer position. Steer control lost and car went over back slope. No other vehicle damage occurred.
3	9.8	45.3	No problems.
4	20.4	47.0	Instrumentation trailer failed, causing loss of accelerometer data. Also, because of large encroachment angle, sufficient time and space were not available to steer car back after reaching ditch bottom, and car went over back slope. No vehicle damage occurred.
5	8.6	59.9	No problems. However, remote-control operator attempted to steer test vehicle back up slope before it reached the ditch bottom.
6	13.3	63.6	Tie-rod failure locked right front tire in right steer position. Steer control was partially lost and car went over back slope. No other vehicle damage occurred.

Figure 5. Right front tire track, test 1.

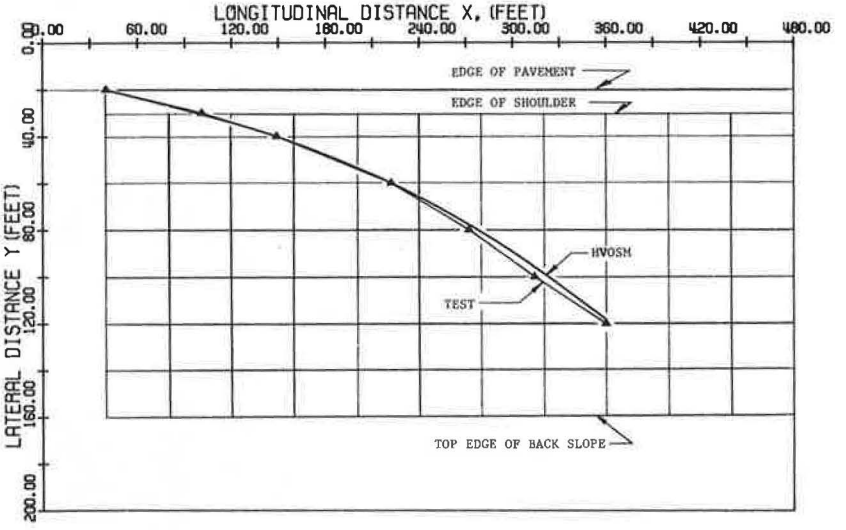

Figure 6. HVOSM versus test results for test 1 (camera position 1).

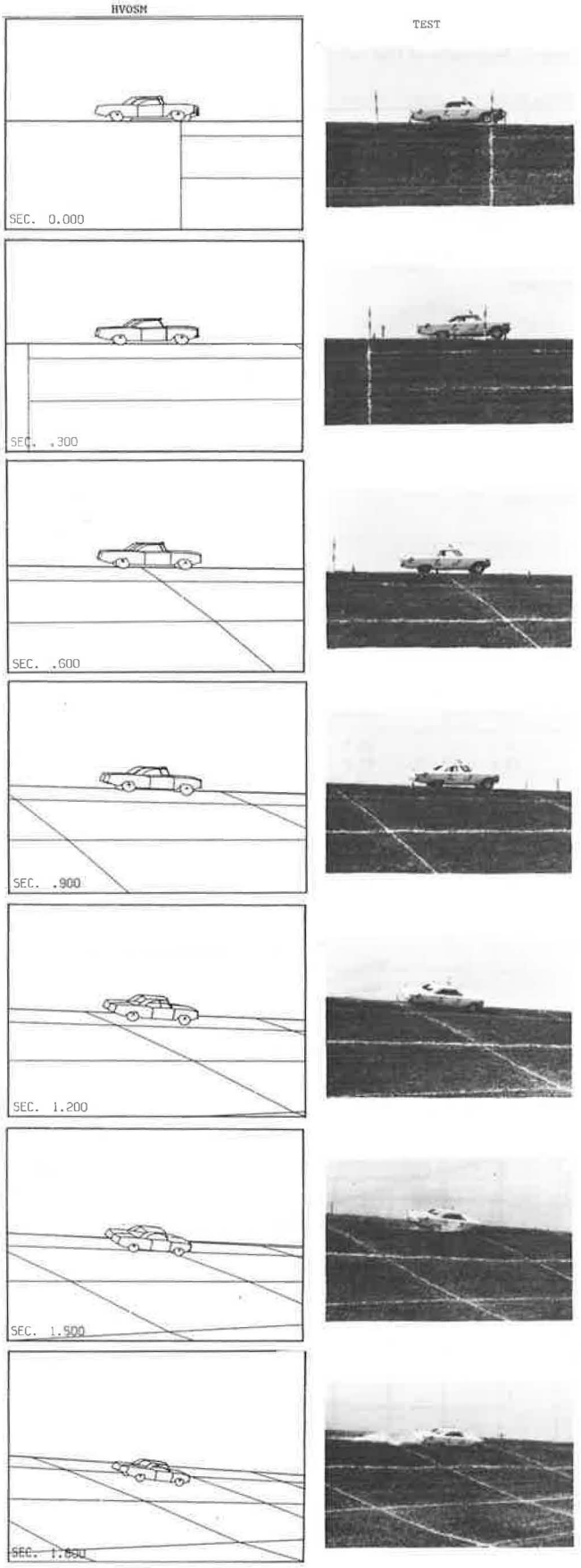

Figure 6. (Continued).

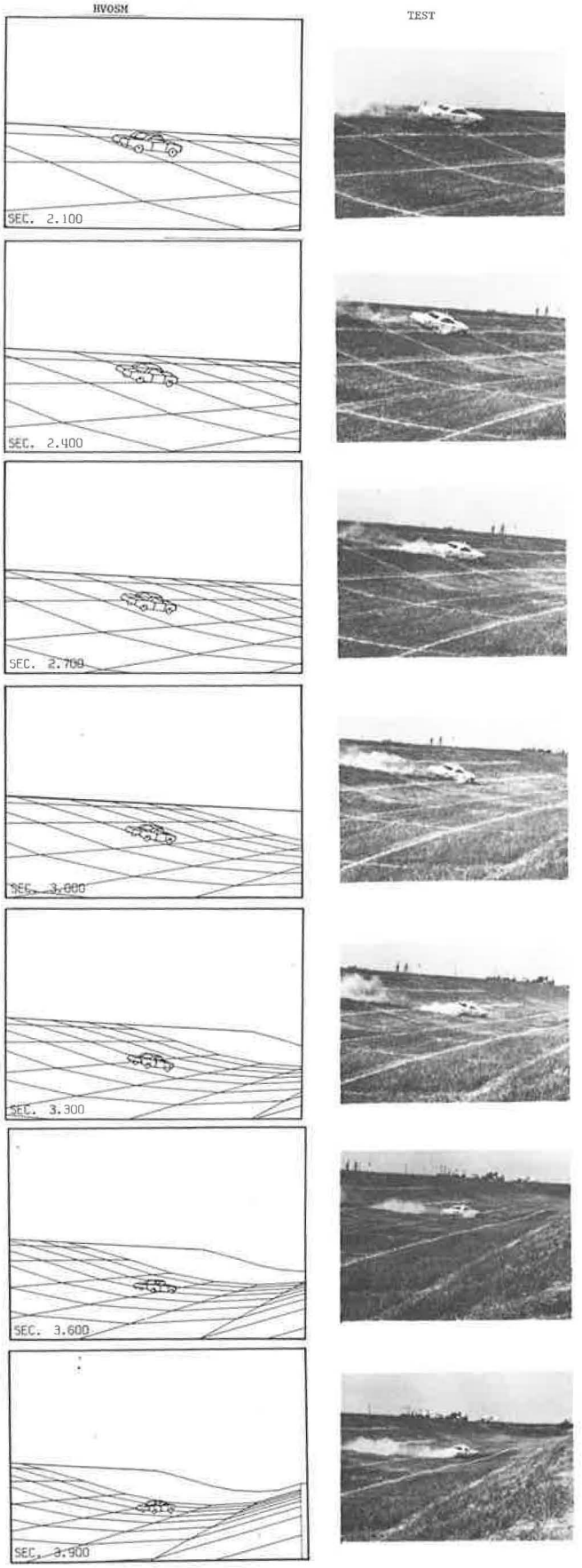

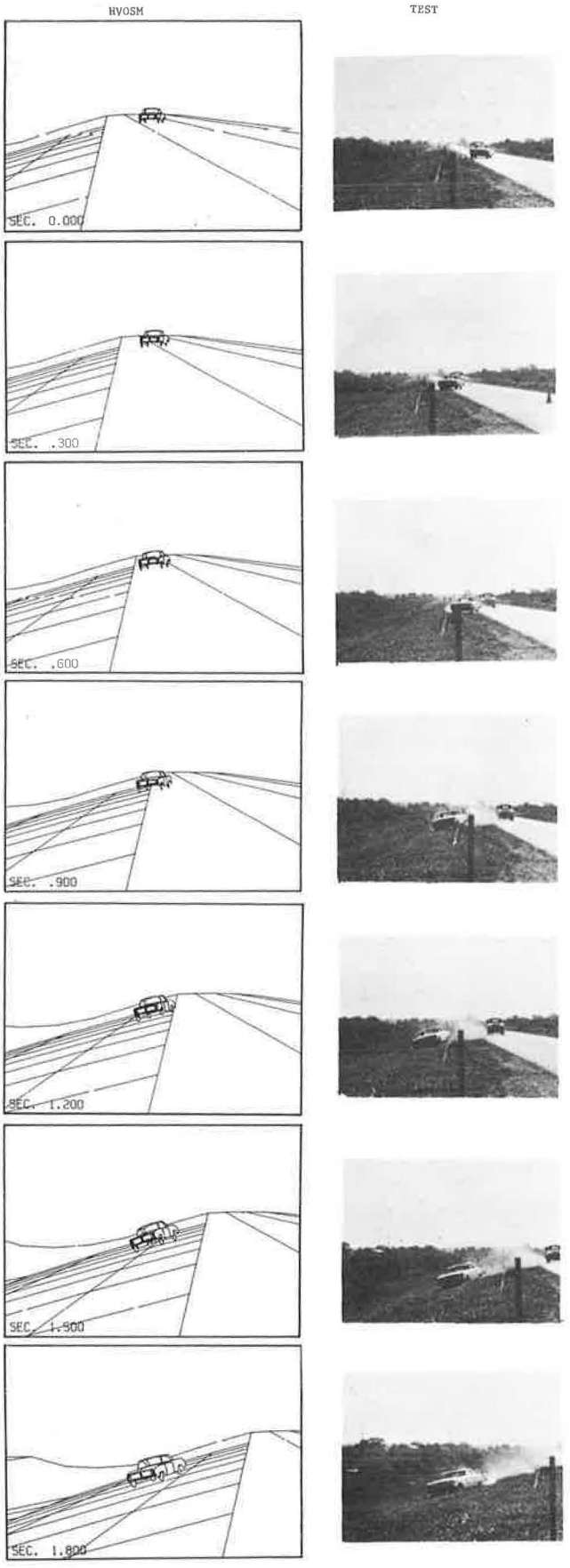

Figure 7. HVOSM versus test results for test 1 (camera position 2).

Figure 7. (Continued).

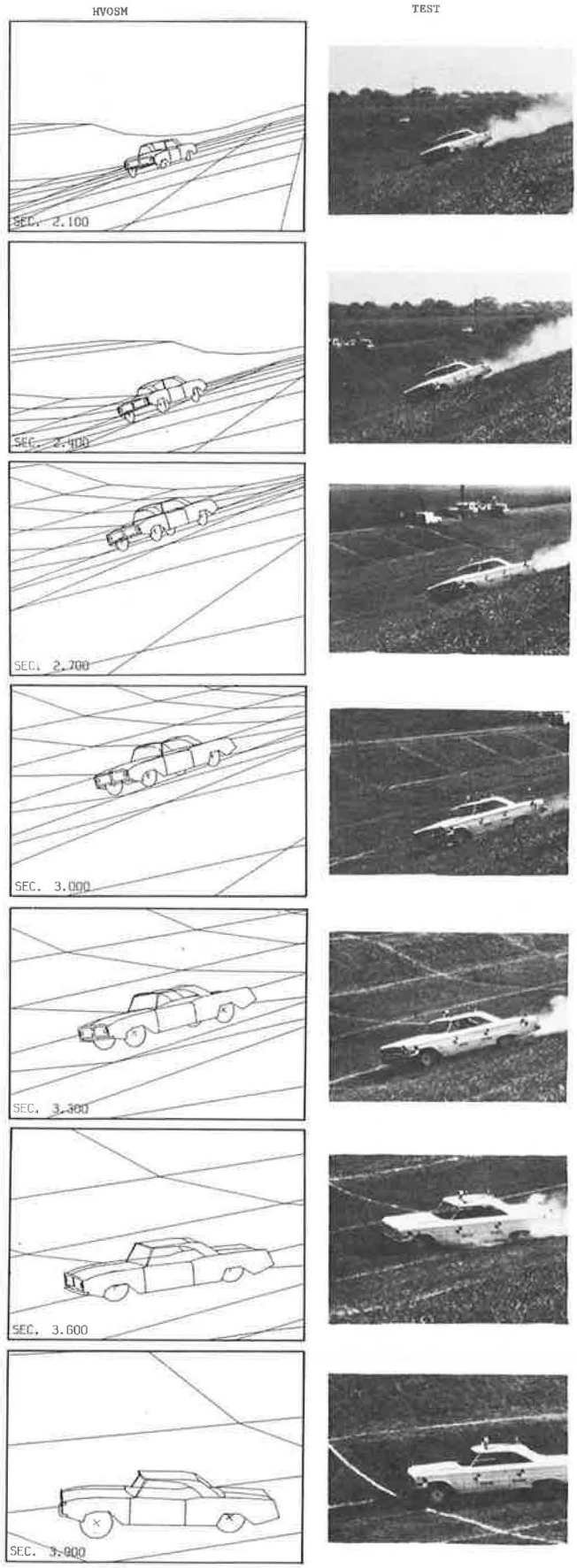

Figure 8. Vertical acceleration versus time for test 1.

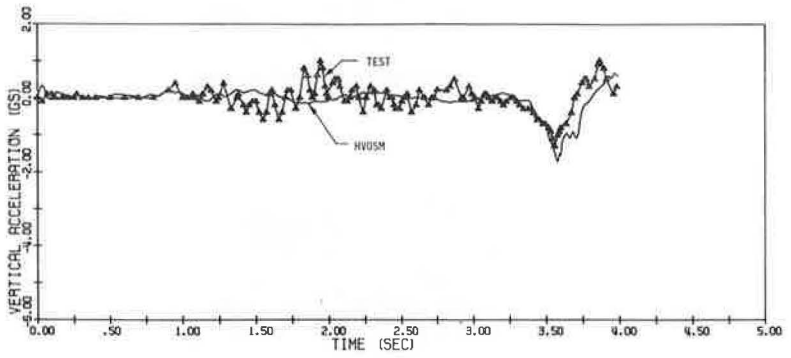

Table 2. Vertical accelerations.

Test No.	Speed/Angle (mph/deg)	Vertical Acceleration (g)			
		Peak		Average[a]	
		Test	Simulation	Test	Simulation
1	55.7/9.7	1.3	1.7	1.0	1.5
2	45.1/13.8	3.9	4.1	3.3	2.7
3	45.3/9.8	1.6	0.8	1.3	0.8
4	47.0/20.4	—[b]	5.6	—[b]	4.0
5	59.9/8.6	1.3	1.8	1.0	1.6
6	63.6/13.3	4.1	5.4	3.2	4.3

[a]Averaged over 50 msec. [b]Not available.

weakening the suspension system. An attempt was made to simulate the effects of these failures by programming in a full right turn coinciding with the time of failure in the test. The comparisons thus obtained for tests 2 and 6 were not so good as the other tests but were still considered reasonable under the circumstances.

In summary, a wide variety of encroachment conditions were encountered in the study. Encroachment speeds ranged from 45.1 to 63.6 mph, and encroachment angles ranged from 8.6 to 20.4 deg. In addition, suspension failures (tests 2 and 6) and the steer back on the side slope (test 5) created special test conditions. This range of test conditions is believed to encompass many of the conditions that occur in run-off-the-road accidents. It is significant that for these conditions both test and simulation results showed that a car could traverse the embankment with no tendency to roll over. It is also significant that in all six tests both measured and predicted accelerations were below tolerable limits for unrestrained occupants (1).

CONCLUSIONS

1. The highway-vehicle-object simulation model can accurately predict the dynamic behavior of an automobile traversing an embankment, with the exception of those instances when mechanical failures occur in the vehicle.
2. Consequently, the criteria on guardrail need (1, 2) have been substantiated.
3. An automobile and its occupants can traverse a 3.5:1 side slope with a flat-bottom ditch 20 ft below the roadway with relative ease and tolerable accelerations for a wide variety of encroachment conditions.
4. HVOSM is incapable of predicting mechanical failures that may occur in an automobile and the subsequent effects of such failures. The suspension failures that occurred in two of the six tests were attributed in part to the fact that the test car's suspension system degenerated with each test.

5. Although vehicle control was lost because of mechanical failures in two of the six tests, the vehicle remained in a stable attitude and traversed the embankment without any serious problems.

ACKNOWLEDGMENTS

The writers sincerely appreciate the cooperation and support of Texas Highway Department District 17 personnel during the full-scale tests. Special thanks are extended to Joe G. Hanover, Billy G. Bockmon, and Michael L. McClure of District 17. John Nixon and Dave Hustace of THD D-8 and Edward V. Kristaponis of FHWA worked closely with the TTI researchers during the study, and their valuable input is acknowledged.

The cooperation of the TTI support service personnel at the Research Annex is appreciated. Lionel Milberger, with assistance from Dick Zimmer and George Shute, designed and implemented the remote-control system used in the test car. Don Cangelos directed the preparation of the test car.

The contents of this paper reflect the views of the authors who are responsible for the facts and the accuracy of the data presented. The contents do not necessarily reflect the official views or policies of the Federal Highway Administration. This report does not constitute a standard, specification, or regulation.

REFERENCES

1. Ross, H. E., Jr., and Post, E. R. Criteria for Guardrail Need and Location on Embankments—Volume 1: Development of Criteria. Texas Transportation Institute, Texas A&M Univ., Res. Rept. 140-4, April 1972.
2. Ross, H. E., Jr., Post, E. R., Nixon, J. F., Hustace, D., and Kristaponis, E. V. Warrants for Guardrails on Embankments. Highway Research Record 460, 1973.
3. McHenry, R. R., and Segal, D. J. Determination of Physical Criteria for Roadside Energy Conversion Systems. Cornell Aeronautical Laboratory, Rept. VJ-2251-V-1, July 1967.
4. McHenry, R. R., and Deleys, N. J. Vehicle Dynamics in Single Vehicle Accidents: Validation and Extension of a Computer Simulation. Cornell Aeronautical Laboratory, Rept. VJ-2251-V-3, Dec. 1968.
5. Weaver, G. D., Marquis, E. L., and Luedecke, A. R., Jr. Vehicle Dynamics on Roadway Slopes. Texas Transportation Institute, Texas A&M Univ., Rept. 626A-1, Oct. 1971.
6. Young, R. D., Post, E. R., and Ross, H. E., Jr. Simulation of Vehicle Impact With the Texas Concrete Median Barrier: Test Comparisons and Parameter Study. Highway Research Record 460, 1972, pp. 61-72.
7. Weaver, F. D., Ross, H. E., Jr., Post, E. R., and Olson, R. M. Effect of Curb Geometry and Location of Vehicle Behavior. Texas Transportation Institute, Texas A&M Univ., Oct. 1972.
8. Ross, H. E., Jr., and Post, E. R. Comparisons of Full-Scale Embankment Tests With Computer Simulations. Texas Transportation Institute, Texas A&M Univ., Res. Rept. 140-7, Dec. 1972.

A BREAKAWAY CONCEPT FOR TIMBER UTILITY POLES

G. K. Wolfe, M. E. Bronstad, and J. D. Michie, Southwest Research Institute; and J. Wong, Insurance Institute for Highway Safety

The feasibility of modifying existing timber utility poles so that they will readily break away upon impact was investigated. Various drilled holes and groove patterns were experimentally examined during 13 pendulum tests of full-size class 4-40 poles by using a 4,000-lbm (1814-kg) mass striking the specimens at 20 mph (32 km/h). Two weakened zones, located 6 in. (152 mm) above grade and 6 ft (1.8 m) from the pole top, facilitated the detachment of the 27-ft (8.2-m) center section. Based on Federal Highway Administration criteria [400 16·s (1780 N·s) for pendulum tests], linear impulse test results of weakened and unweakened poles indicate that poles with a large probability of being struck by an errant vehicle may be easily modified to a breakaway structure. Vehicle crash tests are recommended as the next step in breakaway concept development.

• ROADSIDE STRUCTURES that readily break away when impacted by an errant vehicle have been used for several years. Roadside sign structures (1) and lighting supports (2) have been of breakaway design since mid-1960, and their worth has been clearly demonstrated by the reduction in injuries and fatalities in highway accidents involving them. In general, these breakaway structures employ a weakened shear plane located near grade level. Designs such as a three- or four-bolt slip base or a frangible aluminum base member readily disengage or fracture when impacted by a vehicle yet have adequate strength to resist sign or luminaire environmental loads. The design criteria for these structures require that (a) they disengage during vehicle impact without producing hazardous forces in the car and (b) the broken parts and elements not present a hazard to vehicle occupants or other traffic. That is, the pole should break easily and should be thrown clear of the impacting car and other traffic.

CONCEPT

When the breakaway concept is applied to timber poles, one of the self-imposed constraints is to develop a scheme whereby existing as well as new poles can be easily and economically modified in the field. Furthermore, because poles are connected by lines to adjacent poles, a second weakened zone is required immediately below these lines so that the center section of the pole will detach from the top, line-carrying section. This approach minimizes the weight supported by the adjacent poles after a collision and hence minimizes the possibility of broken lines and loss of electrical or communication service.

The method used in this program to effect a weakened zone in the timber specimens is to drill and cut a pattern of holes and grooves at two selected elevations (3). This approach can be accomplished in actual service by maintenance personnel using standard equipment. A possible drawback of this method is that the integrity of the preservative treatment may be violated in most modifications, leaving the pole vulnerable to rot. However, field application of preservatives offers protection.

TEST PROGRAM

The program objective was to determine the technical feasibility of modifying timber utility poles so that they will break away when impacted by errant vehicles with minimum injuries to passengers while maintaining a high degree of structural integrity to sustain service loads under design environmental conditions. The FHWA linear impulse value of 400 lb·s (1780 N·s) for luminaire supports tested by a pendulum was selected as the evaluation criterion for this program (4).

The program consisted of a series of 13 pendulum impact tests of timber poles and pole assemblies of a typical pole configuration. Initial effort was concentrated on effecting a fracture near grade level (phase I), and then attention was directed to poles modified for both top and bottom fracture planes (phase II). For comparison, a baseline test was conducted on an unmodified pole. Experimental procedures are presented in the Appendix.

FINDINGS

Typical Utility Pole

There is a wide range in physical properties of existing timber utility poles. Basically, poles are categorized into nine general classes with each class having an average of 12 lengths. In addition, there are seven wood species and five preservative treatments. Hence, there is a possibility of nearly 3,800 unique combinations of these features (i.e., $9 \times 12 \times 7 \times 5$). For this program, a representative utility pole was defined for use as a model in evaluating the feasibility of the breakaway concept. To define this model, we selected the most predominant characteristics of existing poles by surveying telephone and other utility companies. Electric power (utility) companies prefer classes 2, 3, and 4 poles, whereas telephone companies use more class 4 and class 5 poles. Because 80 percent or more of the telephone company poles are used jointly with a utility company, class 4 is the most common group. The length most often specified is 40 ft (12.2 m) with 34 ft (10.4 m) extending above grade and a 6-ft (1.8-m) embedment. A description of the model utility pole used for all of the tests is given below.

Characteristic	Value
Species	Southern yellow pine fiber
Class	4
Stress	8,000 psi (55 MPa)
Minimum circumference	
At 6 ft (1.83 m) from butt end	33.5 in. (0.85 m)
At top	21 in. (0.5 m)
Length	40 ft (12.2 m)
Surface treatment	10-lbm (4.53-kg) creosote

Lower Pole Break Zone (Phase I)

A breakaway section height of 6 in. (152 mm) above grade was selected because it would provide undercarriage clearance for virtually all standard cars and still have sufficient length above grade to attach the equipment to modify the poles without excessive excavation.

As a starting point for the lower break zones, one $3\frac{5}{8}$-in. (92-mm) diameter hole was drilled through the pole 6 in. above grade; the hole axis was approximately 90 deg to the pendulum velocity vector. This hole configuration was selected after work performed by the California Division of Highways (4) on timber sign posts. Linear impulse results of the first test (Table 1) and test 2, 5-in. (12.7-cm) diameter hole of 798 (3550) and 980 lb·s (4359 N·s) respectively, showed that the single-hole pattern would not satisfy the 400-lb·s (1779-N·s) requirement.

After tests 1 and 2, there was concern about whether the utility pole could be modified to break within the 400-lb·s (80-N·s) linear impulse region. This concern was

based on the fact that a class 4-40 pole weighs almost 1,000 lbm (450 kg), and the linear impulse required just to accelerate the pole to impact speed could possibly exceed 400 lb·s. Test 3, therefore, was conducted to experimentally ascertain the impulse required to accelerate the pole. Pole NP-1 was used with the lower fractured section removed. The pole was held in a vertical position by an overhead crane so that it rested on but was not embedded in the ground. In this configuration, there was no fracture energy expended during impact, and momentum was transferred from the pendulum mass to the pole. The momentum change for this test serves as a lower bound for modified class 4-40 poles. As shown in Table 1, the maximum recorded acceleration was 7.6 g; linear impulse was 151.5 lb·s (673.9 N·s), well below the 400-lb·s guideline.

As an alternate method to improve the pole fracture characteristics, two holes were drilled through the pole and oriented 90 deg apart (Fig. 1). Theoretically, the two-hole pattern presents a constant section modulus regardless of impact orientation. This layout removed material needed to reduce the shear area while providing the maximum section modulus for bending strength required for line loads. Tests 4 through 6 were conducted to examine this hole pattern. As shown in Table 2, linear impulse values ranged from a low of 304 (1352) to a high of 612 lb·s (2722 N·s) for the three tests; because these values were close to the target value of 400 lb·s, we decided to proceed to phase II experimentation.

Modified Pole Evaluation (Phase II)

In phase II, pole specimens were evaluated as a part of a utility line system. That is, a three-pole utility line was erected, with the center pole being the specimen; line tension was adjusted to 190 lbf (845 N) (normal installation tension) for the four-line configuration. An upper breakaway zone, similar in design to the lower zone (i.e., two holes spaced 90 deg apart), was located 6 ft (1.8 m) from the top of the pole. The hole diameter was scaled down from 3½ (89) to 2 in. (51 mm) based on sectional areas of the pole specimen at the lower and upper points.

Results of phase II testing are given in Tables 2 and 3. Tests 7 and 8 showed that the complete system installation reacted differently from the single-pole test as evidenced by the relatively high linear impulse values, i.e., 792 (3523) and 747 lb·s (3323 N·s) respectively. The extra end support provided by the utility lines apparently added shear rigidity to the structure causing an increase in linear impulse. Also, analysis of the highspeed films showed a marked increase in the "toughness" of the pole; much fiber tearing (green fracture) was noted in the tests in contrast to a desired brittle fracture.

To decrease the green fracture tendency, a ½-in. (12.7-mm) deep V groove was routed all around the lower test section; the V groove concept was evaluated at the upper breakaway zone in test 8. The two holes at the lower zone were reduced from 3½ (89) to 3 in. (76 mm) in diameter to maintain approximately the same shear area. The final hole and groove configuration is shown in Figure 2. Although electronic data were not recorded for the first test with this configuration (test 9), high-speed film indicated excellent results; therefore, the next test was scheduled with the same configuration. In test 10, the lower zone fractured readily, but the upper fracture did not occur. After review of the high-speed movies and data, it was concluded that the utility lines were stretched from previous tests and did not provide sufficient pole restraint; hence, the desired flexural moment at the upper weakened zone could not develop.

Tests 11 and 12 were repeats of tests 9 and 10 with the exception that tension of each of the four utility lines was adjusted to 190 lbf (845 N) prior to each test, and slightly more area was removed from the lower section to lessen the linear impulse. Figure 3 shows photographs of test 12 before and after impact; Figure 4 shows sequential photographs of test 12.

Normal Load Capacity of Utility Pole

The modified pole was analyzed to determine its capacity to sustain normal forces. Generally, a pole is subjected to the following forces:

Table 1. Phase I test data summary.

Test	Specimen	Description	Test Section Area ($in.^2$)	Moment of Inertia About X-Y Axis ($in.^4$)	Section Modulus ($in.^3$)	Impact Velocity (ft/sec)	Maximum Acceleration (g)	Linear Impulse (lb·s)	Final Velocity (fps)	Impact Duration (msec)	Fracture Energy (ft-lb)	Peak Force (lbf)	Average Force (lbf)	Comments
1	NP-1	Single 3.62-in. diameter hole through at 6 in. above groundline oriented 90 deg to impact	52.46	286	53.0	30	12.3	798	23.57	62.3	21,400	49,100	12,820	
2	NP-2	Single 5-in. diameter hole through at same location as NP-1	44.17	202	35.6	30	14.2	980	22.11	76.4	25,500	56,800	12,810	
3	NP-1A	Fractured section of NP-1 cut off, and pole suspended just touching ground	0	–	–	30	7.6	152	28.78	16.0	4,540[a]	30,350	9,655	Test used to determine lower limit of impulse obtainable
4	NP-4	Two 3.62-in. diameter holes oriented 90 deg apart located 6 in. above ground level	31.50	318	56.3	30	9.8	304	27.55	31.4	8,750	39,350	9,684	
5	NP-5	Same as NP-4	29.43	287	51.6	30	10.5	612	25.07	85.5	16,950	42,000	7,201	Specimen appeared to lift out of sand at impact
6	NP-6	Same as NP-4	32.03	326	57.5	30	11.7	466	26.24	39.2	13,100	46,600	11,884	

[a]Inertial energy.

Figure 1. Two-hole breakaway pole concept.

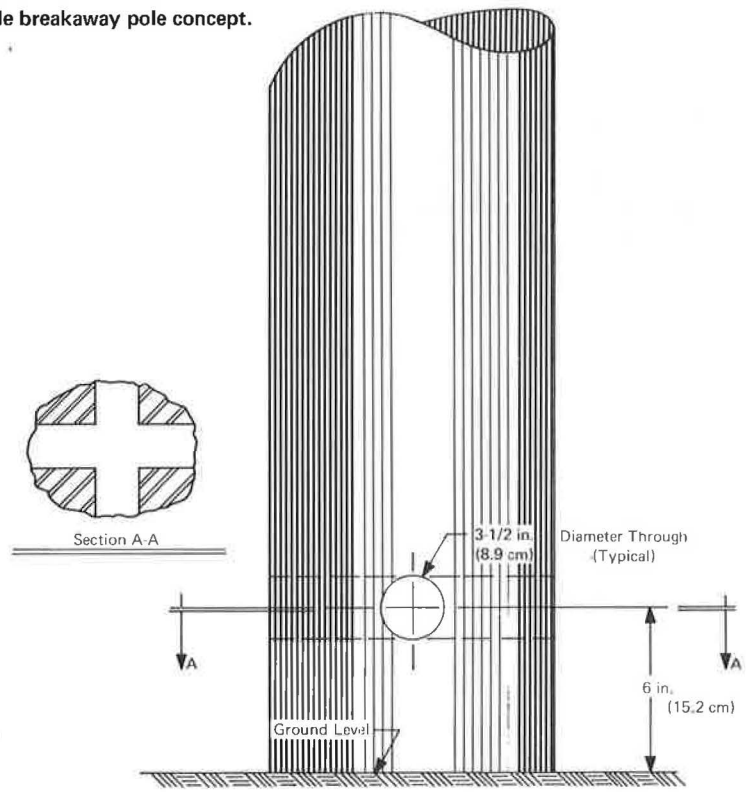

Table 2. Description of specimens for phase II testing.

Test	Specimen	Description	
		Pole 1	Pole 2
7	NP-7	Two 3.62-in. diameter holes drilled 90 deg apart at 6.5 ft from butt	Single 3.62-in. diameter hole through at 6 ft from top
8	NP-8	Same as NP-7	Two 2-in. diameter holes 6 ft from top plus ½-in. deep groove cut all around at test section
9	NP-10	Two 3-in. holes oriented 90 deg apart at 6.5 ft from butt plus ½-in. deep V groove all around	Same as NP-8
10	NP-11	Same as NP-10	Same as NP-10
11	NP-14	Same as NP-10 except holes are 3½ in. in diameter	Same as NP-10
12	NP-12	Same as NP-14	Same as NP-14
13	NP-13	No weakened section	No weakened section

Table 3. Phase II test data summary.

Test	Pole 1			Pole 2			Impact Velocity (fps)	Max Acceleration (g)	Linear Impulse (lb-s)	Final Velocity (fps)	Impact Duration (msec)	Fracture Energy (ft-lb)	Peak Force (lbf)	Average Force (lbf)	Comments
	Test Section Area ($in.^2$)	Moment of Inertia About X-Y Axis ($in.^4$)	Section Modulus ($in.^3$)	Test Section Area ($in.^2$)	Moment of Inertia About X-Y Axis ($in.^4$)	Section Modulus ($in.^3$)									
7	31.82	323	57.0	24.97	65	15.4	29.8	10.3	792	23.40	77.4	21,147	41,080	10,266	Upper section did not fracture.
8	31.50	318	56.2	18.96	85	19.7	29.4	12.1	747	23.40	56.0	19,676	48,560	13,385	Fractured section started to kick out but dug into sand causing upper pole to fall forward.
9	30.52	255	45.1	22.87	115	25.3	–	–	–	–	–	–	–	–	Good break; premature release; no electronic data. Film data acceptable.
10	28.91	235	42.1	25.36	136	29.0	29.8	8.8	575	25.2	69.2	15,714	35,000	8,270	Upper section did not break; extreme slack in lines indicates stretch of wire.
11	30.90	299	49.5	22.69	113	24.9	29.8	11.2	424	26.40	17.4	11,868	44,880	24,320	All data acceptable; tightened lines before test.
12	22.02	178	31.9	18.96	85	19.7	29.7	10.5	277	27.50	12.4	7,816	42,160	22,039	All data acceptable.
13	97.47	754	135.3	75.27	450	91.8	29.8	12.2	2,134	–	155.0	–	48,960	–	Test specimen did not fracture.

Note: See Table 2 for specimen descriptions.

Figure 2. Test configuration.

Figure 3. Test 12 before and after impact.

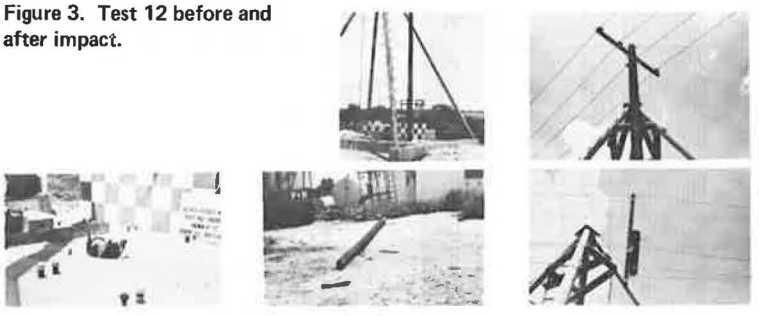

Figure 4. Impact sequence of test 12.

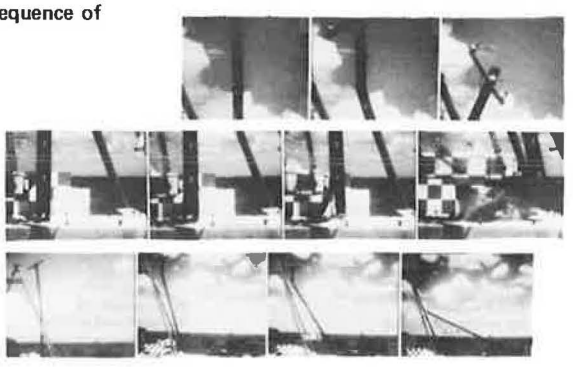

1. Vertical forces due to weight of pole, wires, ice, and downward pull of guys;
2. Lateral horizontal forces due to wind across line on pole and wire;
3. Longitudinal horizontal forces due to unbalanced pull of wires; and
4. Torsional forces due to unbalanced pull of wires.

A pole is strong in respect to the vertical forces but weak for horizontal forces, and the cross arms are weak for the torsional forces (5, 6, 7). In practice, calculations for strength of poles are ordinarily limited to the effects of side wind.

Minimum section moduli of poles located in the three territorial divisions of the United States were determined. The findings show that a class 4-40 pole, embedded 6 ft in the ground with characteristics of the model pole, requires a minimum section modulus of 32.4 in.^{3} (531 cm^3) for the most severe environmental loading areas. Because the maximum section modulus for the breakaway concept is approximately 50 in.^{3} (819 cm^3), it is apparent that the modified pole can support its normal load in any region in the United States.

DISCUSSION OF RESULTS

Concept Performance

Results of pendulum tests are shown in Figure 5 in the form of linear impulse versus shear area of the lower test section. Phase I tests 1, 2, 4, 5, and 6 were performed on pole specimens that were unrestrained or not loaded by service lines; results are indicated by open circles. The origin point (i.e., zero shear area) was determined in test 3 by impacting a detached but suspended pole segment; the linear impulse measured in this case is that required to accelerate the pole segment to pendulum mass speed.

In phase II tests, the pole specimens were under typical service line restraints and loads; results are shown in Figure 5 by squares. The importance of the groove cut around the test pole is illustrated by comparing tests 7 and 8 (ungrooved specimens) with tests 10, 11, 12, and 14 (grooved specimens). Although insufficient testing was performed to quantify the curves, two definite trends are shown in Figure 5. From this evidence, it seems apparent that shear area alone is an insufficient parameter to control the fracture mechanism; the geometry of the weakened section including stress risers such as grooves is also a prime factor.

As might be expected, there was a marked change in fracture mechanism between the single-pole tests (phase I) and the system tests (phase II). Principally the simulated lines in phase II tests introduced a vertical load in the test specimen. More importantly, these lines provided considerable constraint at the pole top. From analysis of high-speed movies, this constraint approximated a rigid fixity, at least instantaneously, from the cross-arm connection down to the single-wire connection. Flexural loads due to this constraint were introduced in the upper weakened section after the lower section had sheared. This sequence is shown in Figure 6. In one test (test 10), the utility lines were atypically slack and did not provide the necessary fixity; hence, the upper section failed to break.

As indicated in Figure 5, a net shear area of approximately 30 in.^{2} (190 cm^2), with proper consideration of geometry, appears to constitute an adequate design of a lower weakened section for the breakaway timber utility pole concept; however, this finding should be investigated with vehicle crash tests before a finalized value is established.

Concept Practicality

The primary objective of the program was to determine whether a typical timber utility pole could be modified so that it would break away upon vehicle impact such that the occupants could survive, preferably uninjured. Obviously, for the scheme to be practical, the modified pole must sustain surface loads (i.e., wind, ice, etc.). As presented in the findings, a class 4-40 pole geometry must be reduced to a section area of 30 in.^{2} or less at the lower break section in order to limit the breaking linear impulse to 400 lb·s (80 N·s) or less. When the pole section modulus required to support wind, ice, and dead load from the four utility lines was calculated, it was determined that a section modulus of 32.4 in.^{3} (5447 cm^3) was sufficient. Linear impulse values of

the pendulum tests are shown in Figure 7 as a function of section modulus of the modified poles. Also shown are the FHWA linear impulse recommendation and the minimum section modulus requirement for normal loads. It can be seen that a section modulus "window" exists from 32 to 50 in.^{3} (524 to 819 cm^3) where the functions of both breakaway and normal load-supporting capabilities are met.

It should be emphasized that the findings of this program are applicable to one particular timber utility pole: a class 4-40, creosote-treated southern pine with a 6-ft (1.8-m) cross arm and four lines. However, it is believed that the concept is applicable to a large percentage of all timber poles.

CONCLUSIONS

1. The concept of modifying a timber utility pole so that it breaks away upon vehicle impact without subjecting vehicle occupants to undue hazard appears technically feasible. Furthermore, the suggested modification can be easily performed by routine equipment and personnel and, hence, is economically attractive.
2. A class 4-40 timber utility pole, typical of poles found in service today, is converted to a breakaway structure by reducing the lower break zone to a sectional area of approximately 30 in.^{2} (190 cm^2) by means of two drilled holes intersecting at 90 deg at the pole center and a ½-in. (13-mm) groove cut around the pole perimeter. The ½-in. groove appears to change the break from a high-energy "green" fracture to a low-energy brittle fracture.
3. A center section of the class 4-40 pole can be made to detach from the upper pole by providing a second weakened zone immediately below the bottom utility line connection; hence, adjacent poles and lines are required to support only the top section of the detached pole. The upper weakened section is similar to the lower section but scaled according to a ratio of pole diameters. Because the upper break involves a flexure mechanism, the utility lines must be sufficiently taut, say 190-lbf (845-N) tension, to provide an end fixity restraint that in turn induces the failure moment.
4. The breakaway modification reduces the normal load capacity of a utility pole. Under conditions of high winds or icing, failure may occur at one or both weakened sections, although design calculations indicate that the modified pole is adequate for these loads. It would seem reasonable that only a selected number of the most vulnerable poles are candidates for modification.
5. The probability of a severe injury or fatality is almost certain in a car-unmodified pole crash for unrestrained occupants even for impact speeds as low as 15 mph (24 km/h), whereas the potential hazard to other traffic from the detached pole missile from a modified system is problematical.
6. Finally, it is recognized that, although the breakaway timber utility pole concept appears feasible from a technical and practical viewpoint, the investigation has proceeded through only the first of two or more steps. Before the concept is validated for in-service trial use, vehicle crash tests should be conducted to demonstrate concept performance under actual conditions.

REFERENCES

1. Olson, R. M., Rowan, N. J., and Edwards, T. C. Break-Away Components Produce Safer Roadside Signs. Highway Research Record 174, 1967.
2. Edwards, T. C., Martinez, J. E., and Ross, H. E., Jr. Development of Design Criteria for Safety Luminaire Supports. NCHRP Rept. 77, 1969.
3. Tamanini, F. J. Designing Fail-Safe Structures for Highway Safety. Federal Highway Administration, 1970.
4. Nordlin, E. F., Ames, W. H., and Field, R. N. Dynamic Tests of Wood Post and Timber Post Supports for Roadside Signs—Series XV. California Division of Highways, Rept. M&R 636398, Dec. 1967.
5. Pender, H., and Del Mar, W. Electrical Engineers' Handbook: Electrical Power, Fourth Ed. John Wiley, New York, 1949.
6. Abbett, R. W., American Civil Engineering Practice, Vol. II. John Wiley, New York, 1956.

Figure 5. Linear impulse versus shear area.

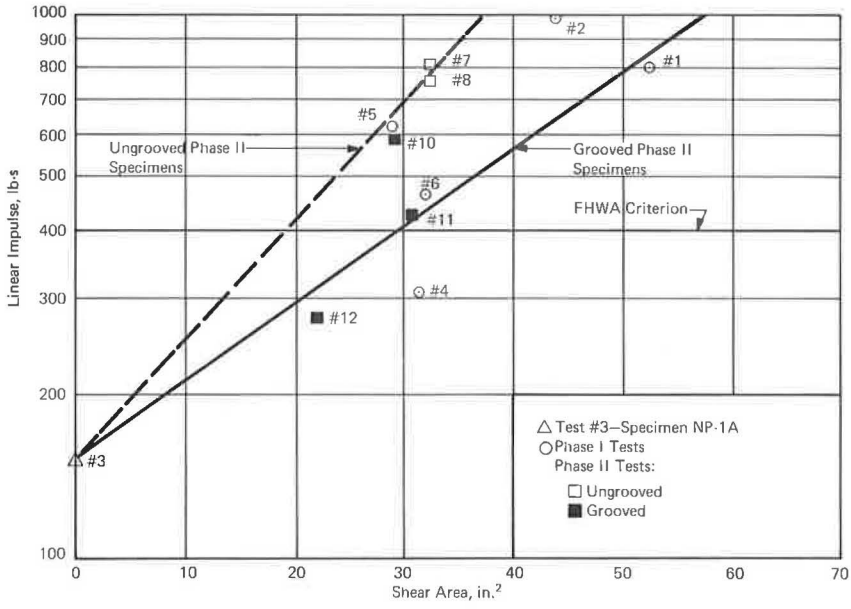

Figure 6. Utility pole fracture sequence: (a) before impact, (b) lower section fracture, and (c) complete fracture.

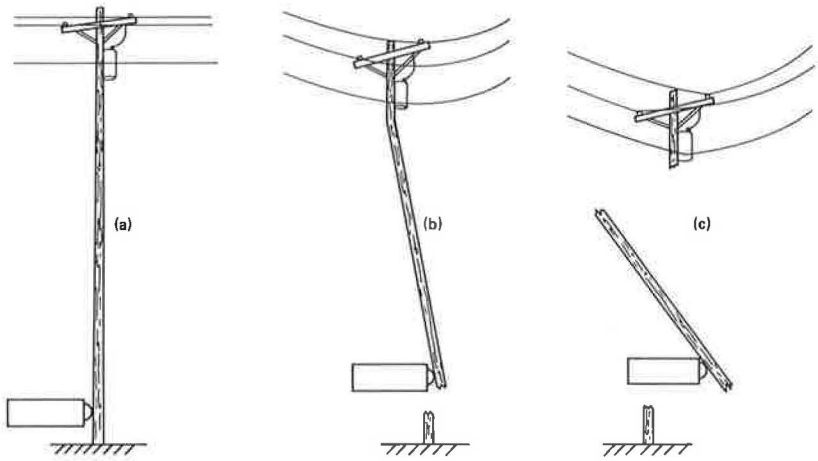

Figure 7. Linear impulse versus section modulus.

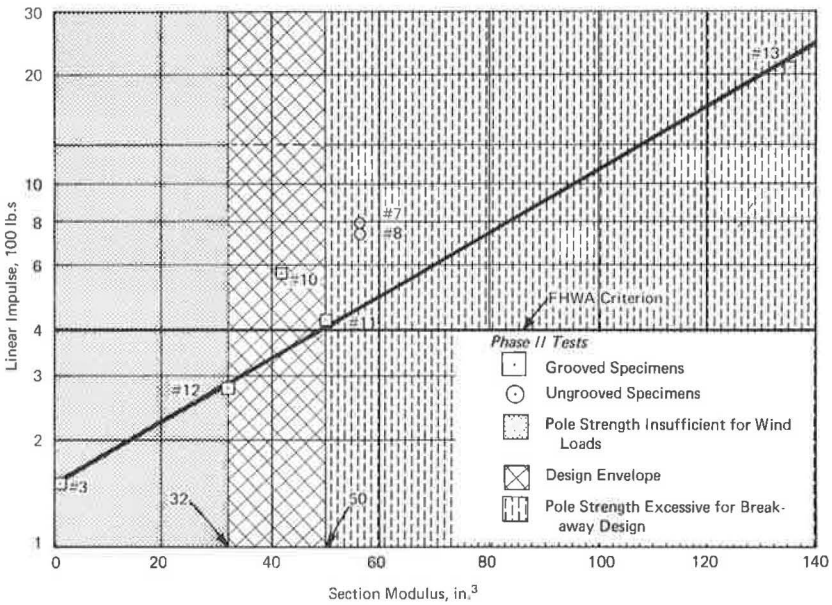

7. Pender, H., and McIlwain, K. Electrical Engineers' Handbook: Communication Electronics, Fourth Ed. John Wiley, New York, 1950.

APPENDIX

EXPERIMENTAL PROCEDURES

The facility consists of a pendulum, operating equipment, and test control and data acquisition instrumentation. An overall view of the facility is shown in Figure 8. A 4,000-lbm (1800-kg) mass is suspended in such a manner that it remains horizontal throughout the normal swing arc of 26-ft (7.92-m) radius and strikes the specimen 20 in. (0.5 m) above grade. The 3- × 6- × 1.5-ft (0.9- × 1.8- × 0.4-m) mass is faced with a steel bumper fabricated from 8-in. (203-mm) diameter extra heavy pipe and filled with concrete. A 1-in. (25-mm) thick, 70 durometer neoprene pad attached to the steel bumper provides the impact surface of the mass.

Impact velocity is programmed by adjusting the vertical fall of the mass, and it is calculated by the expression

$$V_I = \sqrt{2gh}$$

where

V_I = impact velocity,
g = acceleration due to gravity, and
h = mass drop height.

Impact velocities ranging from 0 to 40 fps (0 to 12.19 m/s) are obtainable within the available 25-ft (7.62-m) drop height.

Test specimens are stationed at the lowest point of the pendulum arc where the kinetic energy (i.e., velocity) of the mass is a maximum. The specimens were inserted 6 ft (1.8 m) into a 24-in. (0.6-m) diameter steel-cased hole. A damp, uniformly graded sand was then tamped into the void between the pole and casing.

Mechanics of the test were simple. Instrumentation systems were energized and calibrated. The mass was pulled away from the impact point until its elevation provided the proper drop height. On signal from the test engineer, the mass was released by means of a quick-release mechanism.

Signals from an accelerometer, mounted at the rear of the mass, were continuously recorded throughout impact by a high-speed magnetic tape recorder operating at 60 in./s (1.5 m/s). The recorded data were later replayed through an oscillograph without electronic filters at various tape deck and oscillograph speeds. Frequency response of the system, as determined by the M-400 oscillograph galvanometer, was 0 to 240 Hz. A typical data trace is shown in Figure 9. The accelerometers were subjected to a calibrated 2.8-g, 100-Hz acceleration before and after each test; the recorded signal served as a calibration standard for data processing. Signals from a break-wire speed trap provided impact velocity data.

High-speed cameras were used to record events on 16-mm color film. A Red Lake-HYCAM 400-ft (122-m) × 16-mm high-speed camera operating at 1,000 fps (305 m/s) recorded the events. A timing pulse of 60 pps was recorded on the film edge and used to establish the exact camera frame rate.

Figure 8. Southwest Research Institute pendulum impact tester.

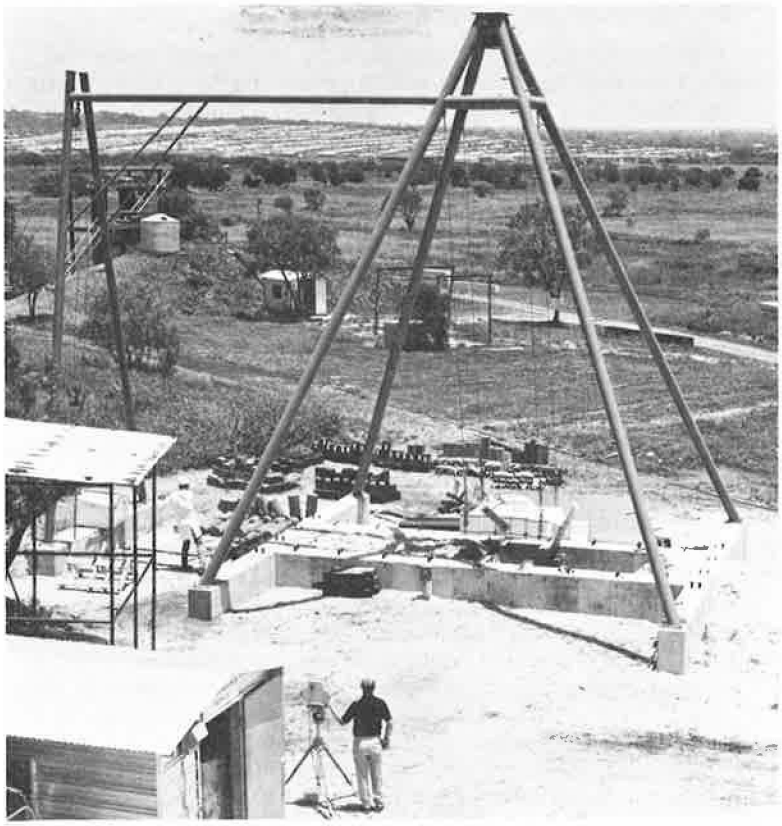

Figure 9. Typical force-time data for pole test.

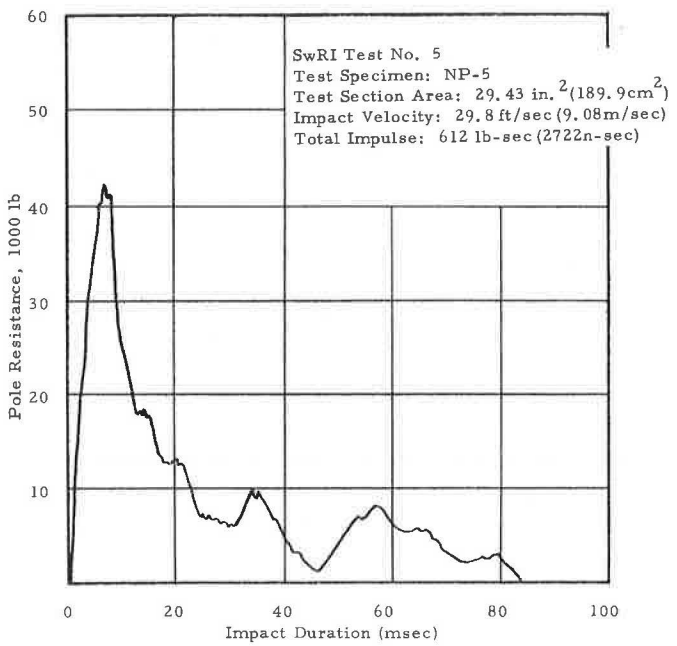

DISCUSSION

John M. Peacock, American Telephone and Telegraph Company

The paper presents the results of analysis and preliminary tests to evaluate the feasibility of field modifications to existing timber utility poles to convert them into structures that would readily break away on impact. The authors suggest that, pending further evaluation and testing, this may be a practical means of reducing roadside hazards.

There can be no responsible argument against the need to minimize roadside hazards, particularly those structures in vulnerable locations. Weakening selected utility poles by removing material, as suggested, may indeed be feasible in some cases, but the resultant reduced load-carrying capacity would have to be evaluated very carefully in each case. The authors state that the cross-sectional area and section modulus of a class 4-40 pole can be reduced by factors more than three to one and that the pole will still support wind, ice, and dead load "for the most severe environmental loading areas." They further state that the concept is applicable to a large percentage of all timber poles. This implies a very generous factor of safety for the typical pole. Our experience with the design and performance of pole lines in the Bell System would not support such conclusions.

Design calculations on pole lines take into account the strength of the various poles (after aging) and also depend on assumptions on loading. Normal loads include not only dead loads, wind, and ice as referenced in the paper, but many other dynamic loads such as craftsmen's ladders and platforms, "cable dancing" (because of aerodynamic instability), and shock loads. Abnormal loads can be almost anything that nature can muster. Experience with pole line design practices over the years indicates that factors of safety are small under heavy loading conditions and inadequate to cover extreme storm loading that can and does occur from time to time in many areas of the country.

Recent history in Southwestern Bell provides a dramatic illustration. On December 3, 1973, an unexpected ice storm hit, accompanied by 50-mph (80-km/h) north winds. The storm cut a 100-mile (160-km) wide swath from southwest to north central Kansas. In its wake it left more than 5,700 poles down and 27,500 miles (44 250 km) of wire affected. In a case such as this, the poles typically go down in a "domino" pattern. One pole fails, subjecting the adjacent poles to abnormal loads and shock; then they fail, and so on down the line. Thus even an occasional weakened pole could trigger an extensive collapse, particularly under storm loading. Potential safety hazards to the general public and to the utility workmen are obvious, particularly in the common situation where power and telephone companies are sharing the same pole.

The December storm was a multimillion dollar emergency repair job for Southwestern Bell, but more important were the consequences of service disruption (power as well as telephone) to the public at a time of emergency. About 34,000 phones were out of service, and 152 towns were isolated from the long distance network. About 45 percent of the poles in the storm area survived this disaster. It must be expected that virtually none would have remained if many of them had been intentionally weakened by a factor approaching 3 to 1.

The Bell System has had vigorous policies for the construction of below-ground plants since the 1950s. To the extent that economic resources permit, we are advocating to our Associated Operating Companies the continued implementation of this policy so as to phase out aerial plants wherever possible at the earliest date. Diversion of available funds to any large-scale modification of the existing aerial plant could only slow progress. We issued a letter to the Bell Companies early in 1973 to this effect. The following brief quote from this letter will summarize our position:

> Our recommendation is to vigorously proceed with our present policy of undergrounding:
>
> 1. Use below ground construction as a first choice in all new construction.
> 2. Replace existing aerial plant with out-of-sight plant whenever feasible in connection with plant relocation work, relief jobs, etc. It is important that we remove aerial plant wherever it is practical to do so.

3. In plant inspection work, and other quality survey activity, be sure that your forces identify pole lines and, in particular, individual poles that are in hazardous locations. The highest priority should be given to their relocation, or preferably to their removal. This same philosophy obviously applies to the placement of any new poles.

We feel that this program will achieve the objective but avoid wasteful expenditures and resultant excessive revenue requirements. Through its undergrounding program, the Bell System has been able to reduce its inventory of owned poles to 19 million in 1972. This number is now decreasing at a rate of ½ million per year, and may be expected to decrease even faster in the future.

H. A. Onishi, Commonwealth Edison Company, Maywood, Illinois

The authors propose to drill holes through the pole and to cut V grooves around the circumference to facilitate the breakaway concept. This concept appears to have two serious flaws:

1. The fiber content of the pole has been reduced to such an extent that the pole does not meet the strength requirements of the National Electric Code for the high-density loads common to the Commonwealth Edison Company. This situation is further compounded by the large number of poles that are shared jointly with the telephone company.
2. The proposed method of providing weakened sections of pole exposes heartwood that can only be superficially protected from decay by supplementary preservative treatment.

The paper states that a class 4-40 pole requires a minimum section modulus of 32.4 $in.^3$ (531 cm^3) for the most severe environmental loading areas. It also states that a section modulus "window" exists from 32 to 50 $in.^3$ (525 to 820 cm^3) where the functions of both breakaway and normal load-supporting capabilities are met. Not stated were the conductor sizes and span lengths used when the tests were made. The 32- to 50-$in.^3$ section modulus range would not meet load-supporting requirements of the Commonwealth Edison Company. The appendix shows that calculations for required section modulus of a class 4-40 pole with four commonly used Edison conductors is a minimum of 54.6 $in.^3$ (895 cm^3). Inasmuch as we frequently share the pole with the telephone company, the addition of a typical telephone cable changes the required section modulus to 67.7 $in.^3$ (1110 cm^3). These figures are with a minimum factor of safety of 2 per the 6th edition of the National Electric Code (ANSI C2.2). Higher voltage lines could require a grade B construction and a factor of safety of 4, further increasing the required section modulus.

For a fuller examination of the effect of reducing the strength of the pole, Table 4 gives the minimum section modulus for various classes of an uncut 40-ft (12.2-m) pole, both at the groundline and at the proposed weakened section 6 in. (152 mm) above the groundline. Also listed is the proposed weakened section modulus.

This table clearly illustrates the consequence of providing a weakened section in the pole. In effect the pole class is reduced to about the equivalent of a class 9 pole. As an economic consideration, we would be buying and installing a class 4 pole and only obtaining the benefits of a class 9 pole.

Commonwealth Edison Company has approximately 1,500,000 poles in plant. In 1973 we set 29,000 poles of which 44 percent were either (a) class 4 poles taller than 40 ft or (b) 30-ft and taller poles of class 2, 1, or H-1. These poles all have a greater section modulus than a 4-40 pole. It is obvious that the load-supporting requirements of these taller and/or larger poles would not be met if the section modulus were reduced to the range of 32.4 to 50 $in.^3$.

We question the adequacy of the test setup to simulate actual utility lines. A more typical test line would consist of at least five poles, all of which have been weakened by drilling of holes and cutting of V grooves. Then, when impact testing is conducted on the middle pole, the possibility of cascading failures to adjacent weakened poles can be observed.

Table 4. Minimum section moduli for various pole classes.

Class	Minimum Section Modulus (in.^{3})		
	At Groundline of Uncut Pole	6 In. Above Groundline of Uncut Pole	Range for Weakened Pole 6 In. Above Groundline
H-1	260.7	256.8	
1	218.4	215	
2	180.7	178	
3	147.7	145.5	
4	119.1	117.3	32.4 to 50
5	94.3	92.9	
6	73.3	72.2	
7	57.6	65.6	
9	35.5	34.9	

Slight angles in the pole line, vertical loading of poles due to equipment such as transformers, capacitors, or down guys, conductor galloping phenomena, and extreme weather conditions in excess of those used in calculating minimum pole strength to comply with regulatory agencies are examples of additional stresses placed on a wood utility pole. Past experience has indicated that factors of safety of current design standards are small and should not be further reduced.

The method of obtaining the weakened pole section exposes large amounts of heartwood to the action of the environment. Of the species of woods commonly used for utility poles, only cedar heartwood has natural resistance to decay. Sapwoods of all species have little or no decay resistance.

The heartwood of all poles is practically impenetrable to preservative treatment, even when subjected to the pressures in a treating cylinder at a pole company's preserving plant. Even packing the drilled holes with a heavy-bodied preservative that will remain in place would give only superficial surface protection to the heartwood. More permanent protection would be expected for any exposed sapwood.

Cutting a ½-in. (13-mm) deep groove around the pole is not too serious with a thick sapwood species such as southern pine, which normally has a penetration of preservative of approximately 3 in. (76 mm). However, with a thin sapwood species such as western red cedar, douglas fir, and western larch, all or almost all of the treated sapwood shell will be removed, necessitating supplemental treatment. The preservative would probably be held in place by a coated wrapper, which will be quite conspicuous at the upper weakened section. In the case of heartwood exposed by the V groove, the benefits of this supplemental treating will be minimal.

AUTHORS' CLOSURE

We express appreciation to Peacock and Onishi for their comments.

We are in complete agreement with AT&T's approach toward eliminating utility poles by burying the service lines; it is obvious that removal of poles from the roadside will eliminate a severe traffic hazard. However, in the meantime and as an acceptable alternate, it is suggested that poles located in proximity of a street or highway be (a) shielded by a guardrail or crash cushion or (b) modified to a structure that readily breaks away upon vehicle impact. Only those poles located in proximity of streets and highways represent a hazard to traffic and require treatment.

Onishi's concern with load capacity of a modified pole is recognized. It is anticipated that modified poles will exhibit a greater need for replacement after a severe storm than the overdesigned poles currently in inventory. However, given the high cost to society of every fatal vehicle accident, it would appear to be in the best interest of the utility companies as well as the country to accept the inconvenience associated with an occasional loss of service and the cost of replacing the broken poles.

A comparison is given in Table 5 between Commonwealth Edison's and Southwest Research Institute's calculations of pole strength requirement. The size of lines account for the largest part of the difference in section modulus required. It should be emphasized that the reduced section modulus has a factor of safety of 2.0. It may be appropriate to review the origin of this factor of safety to ensure that it is consistent with the safety of the public at large rather than some arbitrary overdesign factor of the pole.

Although the point was not emphasized in the paper, the breakaway mechanism (at the low zone) is actually a shearing phenomenon and is associated with shear area

Table 5. Comparison of section modulus requirements.

Typical Case	Wires					Moment at Weakened Section (ft-lb)			
	No.	Diameter (in.)	Height Above Weakened Section (ft)	Pole Spacing (ft)	Wind Load (psf)	Wind on Ice-Covered (½-in.) Wires	Wind on Pole	Total	Section Modulus Required ($in.^3$)
Commonwealth Edison	3	0.711	33.1	200	4	11,340			
	1	1.72	29.5	200	4	5,345	1,540	18,225	54.6
Southwest Research Institute	4	0.447	32.5	175	4	10,973	1,545	12,518	37.6

rather than section modulus. It is suspected that the design window is different for each pole class and not nearly so restrictive as indicated by Onishi.

Onishi and Peacock's concern with cascading failure of a series of weakened poles can be addressed with some practical engineering. For the case where only one of a line of poles is a hazard to traffic, then only that one pole need be modified and the two adjacent poles may be reinforced by guy wires and/or struts. Where several adjacent poles are considered hazards to traffic, it may be appropriate to provide struts to absorb wind loads in addition to modifying the poles.

It is recognized that modifying timber utility poles by cutting grooves and drilling holes will most probably shorten their expected useful life. However, because more than 80 percent of utility poles are creosote-treated southern pine, the reduction in useful life can be maintained within acceptable limits with proper field treating techniques.

Peacock discussed extensive pole damage in a 1973 Kansas storm. AT&T reported on the storm and restoration effort in a pamphlet entitled "Operation Icedown." Several comments are offered:

1. Kansas is located in a region requiring maximum pole design requirements (i.e., combination of ice and high winds),
2. Storm was probably atypical (maybe a 25-year storm),
3. Some of the poles that fractured seemed to have been in poor structural condition prior to the storm,
4. Poles appeared to be heavily overloaded with lines (18 or more), and
5. At least one pole appeared to be pushed over in the soil rather than broken.

Based on the information contained in the pamphlet, the writers feel the Kansas experience is not a valid example of typical pole performance in service; the large number of down poles is probably an indicator of a combination of an unusual storm and poles in substandard design conditions. It would seem that AT&T would consider strengthening an occasional pole to prevent or at least contain the "domino" pattern if this is a significant problem.

Although it was not reported in the paper, the Tennessee Valley Authority supplied the writers with service statistics on their poles. Approximately 1.5 percent of the poles in the TVA system need replacement yearly because of fire, lightening, insects, and rot. No replacements are necessary for pole breakage due to a combination of wind and ice. One could conclude that the timber poles are conservatively designed.

The research program on which the paper was based had a very modest budget, and the program scope was limited. The objective was to examine feasibility in an average case and not to prove application of the breakaway concept in general. The writers welcome the interest shown in the program by Peacock and Onishi and solicit their continued support in further developing the practicality and effectiveness of the breakaway concept.

U-POST INVESTIGATION

R. Strizki, J. Powers, M. Jagannath, and E. Reilly,
New Jersey Department of Transportation

The New Jersey Department of Transportation conducted 26 full-scale crash tests on 13 steel and 13 aluminum U-posts. The sign installations contained from one to four posts for both the steel and aluminum tests. The tests were conducted on 4-lbf/ft (58-N/m) steel sections and 4- and 8-lbf/ft (58- and 117-N/m) equivalent aluminum sections with both 2,000- and 4,500-lbm (907- and 1941-kg) vehicles; impact speeds ranged from 20 to 45 mph (32 to 72 km/h), and impact angles ranged from 0 (head-on) to 20 deg in accordance with Federal Highway Administration test conditions. Results of the dynamic testing indicate that simultaneously impacting more than one 4-lbf/ft steel U-post or more than three aluminum U-posts produces conditions that do not satisfy present FHWA criteria. Results also indicate that the use of aluminum bolts for the signpost connection yields less severe speed changes than stainless steel bolts when only a partial number of posts are impacted by the vehicle.

•MANY small and intermediate-sized highway signs in use today are supported by relatively small section steel channels, commonly referred to as U-posts. Because of lower post loads from smaller signs, larger, more substantial supports are not necessary. Research has produced various methods of providing a breakaway feature to ensure the safety of larger supports and has shown that breakaway installations effectively reduce injuries in vehicle crash situations.

However, there have been no concentrated efforts to determine safe limitations for U-post installations. This generally less expensive installation may become a hazard if too many posts are required to support a single sign.

U-posts were presumed to yield at the groundline upon impact, allowing the vehicle to pass over the posts. We call this action "bendaway," as opposed to breakaway in which the post detaches from its base and allows the vehicle to pass underneath.

Steel channel U-posts are provided in sections weighing from 2 to 4 lbf/ft (29 to 58 N/m). In addition, they can be bolted back to back to form sections weighing up to 8 lbf/ft (117 N/m). Aluminum channel U-posts have recently become available in sections whose cross-sectional strengths are equivalent to either 4-, 6-, or 8-lbf/ft (58-, 88-, or 117-N/m) steel sections.

The Federal Highway Administration advises the use of vehicle momentum change as the basic criterion for determining the relative safety of sign installations. According to this criterion, a support system producing a momentum change in excess of 1,100 lb·s (500 kg·s) during impact ceases to be a safe roadside installation. Research currently under way with the University of Cincinnati and unavailable for consideration in this study is investigating the possibility of using a set of criteria combining the time duration of vehicle occupant impact with the windshield and the speed change of the vehicle.

FHWA further advises that dynamic tests be run under varied conditions to ensure that the most critical situations are tested. The three conditions are (a) a 2,000-lbm (907-kg) vehicle traveling between 20 and 25 mph (32 and 40 km/h) and impacting the test sign at a 0-deg angle of incidence (measured from the perpendicular to the sign face), (b) a 2,000-lbm vehicle traveling between 35 and 45 mph (56 and 72 km/h) and

impacting at a 20-deg angle of incidence, and (c) a 4,500-lbm (1941-kg) vehicle traveling between 40 and 45 mph (64 and 72 km/h) and impacting at a 10-deg angle of incidence.

STUDY PROCEDURES

Posts Tested

The 4-lbf/ft (58-N/m) steel U-post section is the most commonly used when more than one post is required to support a sign. The 4-lbf/ft section is used almost exclusively for multipost installations of intermediate sign sizes on New Jersey highways. For this reason, all the steel posts tested were 4-lbf/ft sections. With one exception, all the aluminum posts tested were equivalent in strength to the 4-lbf/ft steel posts. This exception was an aluminum X section designed to be equivalent in strength to an 8-lbf/ft steel piggyback section (Figs. 1 and 2). The equivalent steel strength in an aluminum post is achieved by its increased cross-sectional depth producing a section modulus nearly double that of the steel post, which compensates for the higher allowable stress of the steel post.

Initial testing was designed to determine the maximum number of 4-lbf/ft steel U-posts that can be simultaneously impacted below the momentum criterion limits specified by FHWA. Three sign installations were erected: two-, three-, and four-posted signs. The posts were spaced at 1 ft (0.3 m) to facilitate simultaneous impact of all the posts and to test the most severe condition. It is also the minimum spacing used in field installations.

Crash Vehicle Tow System

A suitable test site was selected, and a system for towing and guiding crash vehicles was developed. The system used was basically the same as the method used by the University of Cincinnati in full-scale field testing.

The crash vehicle was mounted with a bar bolted through the center of the front bumper extending out 8 in. (200 mm) or more (Fig. 3). An eye was welded to the protruding end of this bar. A ½-ton (453-kg) pickup truck was used as the towing vehicle. This truck was fitted with a boom mounted on the rear bumper by means of a pintle type of hitch. The free end of the boom was suspended by a wire rope from the center of the stiffened tailgate. The boom was an 8-in. (200-mm) deep aluminum I-beam. A steel pin was mounted on the outboard end of the boom and bolted so as to allow a 60-deg rotation toward the rear. This system allowed the crash vehicle to be offset to the right of the towing vehicle approximately 12 ft (3.6 m) on centers. With this system, no steering or speed control equipment was necessary on board the crash vehicle.

The pin on the boom was slipped through the eye of the bumper-mounted bolt and restrained from rotation by a wire rope attached to a release pin mounted on the chassis under the passenger seat of the towing vehicle. This release pin extended vertically through the floor into the cab of the tow vehicle. Pulling this pin and accelerating the tow vehicle allowed the pin on the boom to disengage from the eye bolt on the crash vehicle. This released the crash vehicle from the control of the tow vehicle.

Initially, a pair of wire ropes was used to connect the boom pin to the crash vehicle, and later chains were used. Neither functioned as well as the eye bolt.

Recording Equipment

Each crash vehicle was prepared with test equipment and brought to proper test weight.

The test equipment included (a) accelerometers mounted directly behind the front seat for measuring longitudinal and lateral g forces, (b) a recorder to provide a permanent trace of the accelerometer data, (c) an electrically operated screw jack for brake application, (d) a 12-Vdc battery, and (e) a receiver with servo-operated switches for remote control of all equipment. A radio transmitter, operated from near the test sign installation, was used to activate the on-board test equipment.

The tests were monitored by two television cameras and two 16-mm movie cameras. The television cameras were located to show a pan view and a fixed side view of each

test. In later tests, the fixed view was head-on from behind the sign. This was made possible by a truck with a roof-mounted remote camera using a telescopic lens. One 16-mm camera provided a pan view of each test, whereas the other was fixed at 90 deg to provide a data source for impact information. The latter camera recorded data at 60 frames/s. Tape switches were located 6 ft (1.8 m) apart, 7 ft (2.1 m) in front of the test sign with one on the signpost itself, to monitor the crash vehicle speed.

Test Site

The test site was a section of southbound Interstate 95 adjacent to a section under construction. Entering traffic was rerouted to a nearby interchange on the test dates. Tests were conducted in the northbound direction, and an on-ramp was used as an escape route for the towing vehicle.

The macadam roadway course was removed from a small area in each of the three roadway lanes offset from each other at 50-ft (15-m) intervals (Fig. 4). Then the subbase, and shale if encountered, was removed to a depth of 3 to 4 ft (0.9 to 1.2 m) and filled with a shoulder material to within a foot of the surface. The top foot was filled with a cold patch material and smoothed so that vehicles would not hit any bumps. The posts for each sign installation were driven 3 to 4 ft into this base by using a pneumatic jackhammer or sledgehammer.

RESULTS

Table 1 gives the results of the 26 tests conducted. From the 16-mm film, a frame-by-frame plot of a fixed point on each crash vehicle was drawn for vehicle speed. These plots were used to determine all data except peak g readings, which were taken from the accelerometer trace. (See Figs. 9, 10, and 11 in the Appendix for typical plots with accelerometer traces superimposed.) In a few tests, either the 16-mm camera or the accelerometer failed to supply accurate data; subsequently, data from the operating source are reported. In most cases, test conditions were duplicated to verify the data.

Figure 5 shows the momentum change as computed for each test, post type, and number of posts impacted. The method used to compute momentum change was

$$M = V \times \text{mass}$$

where

M = change of momentum in lb·s,
V = change in speed for the duration of impact in fps (m/s), and
mass = weight of the crash vehicle in lbm (kg) divided by 32.2 ft/s^2 (9.8 m/s^2).

Figure 6 shows the peak g recorded for the various tests and post types. Figure 7 shows the relationship of impact duration to the materials and number of posts impacted.

DISCUSSION OF RESULTS

Order of Testing

The plan for the order of testing was to impact steel installations of two-, three-, four-, and then five-posted signs. However, the crash vehicle overturned while impacting the four-post installation; hence, the test on a five-post sign was not attempted. Further, it was necessary to use five different 2,000-lbm crash vehicles to complete the first seven steel post tests.

The steel posts, which frequently sheared at the bumper line, did not yield, and tended to cause considerable damage to the underside of the crash vehicle, prompted the change to aluminum posts for the next six tests (tests 8 through 13).

Subsequent to the six aluminum tests, a steel of higher plasticity was sought from the New Jersey DOT maintenance yard and from a steel supplier. Tests 14 through 19 were conducted on these posts to complete our testing of steel U-posts.

Figure 1. Typical shape of (a) aluminum equivalent of 4-lbf/ft steel post and (b) 4-lbf/ft steel post.

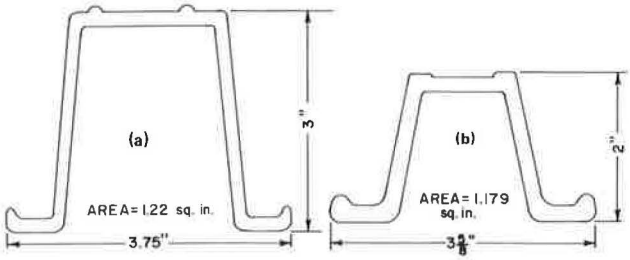

Figure 2. Typical design of aluminum equivalent of 8-lbf/ft piggyback steel post.

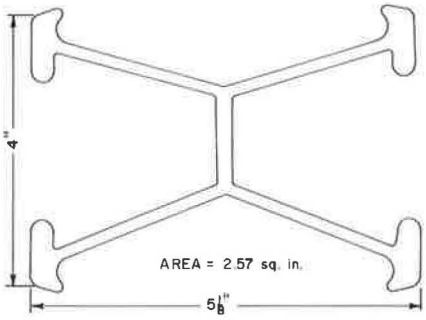

Figure 3. Crash vehicle tow system.

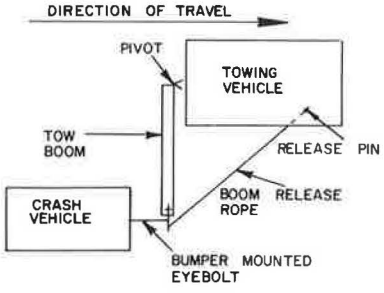

Figure 4. Test site.

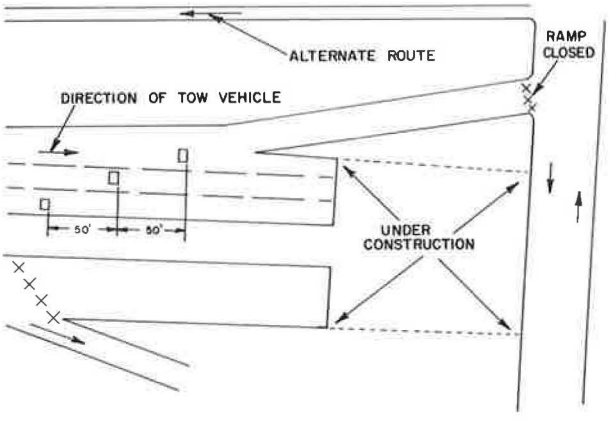

Figure 5. Momentum change for each test.

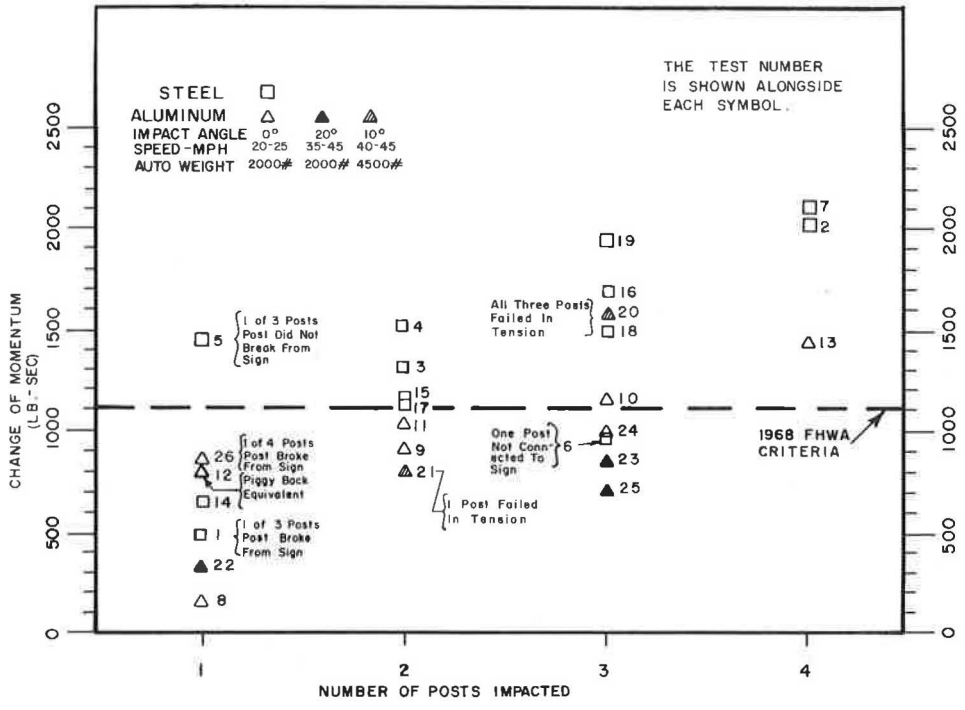

Table 1. Summary of test results.

Post	Test No.	No. of Posts Impacted	ΔV[a] (mph)	ΔM[a] (lb·s)	Peak g[b]	Impact Duration (s)
Steel	1	1 of 3[c]	5.3	485	5.9	0.069
	5	1 of 3[d]	16.0	1,450	7	0.284
	14	1 of 1	6.9	640	5.0	0.101
	3	2 of 2	14.6	1,320	7.4	0.210
	4	2 of 2	16.6	1,500	9	0.184
	15	2 of 2	12.6	1,160	8.6	0.154
	17	2 of 2	11.6	1,120	6.6	0.228
	6	3 of 3[e]	10.5	970	6	0.142
	19	3 of 3[f]	20.1	1,940	9	0.192
	16	3 of 3	18.4	1,700	7.8	0.210
	18	3 of 3	15.5	1,500	8.7	0.198
	2	4 of 4[g]	21.8	2,030	23	0.123
	7	4 of 4	22.8	2,100	10	0.196
Aluminum	22	1 of 3[c,h,i]	3.5	310	3.4	0.144
	26	1 of 4[c]	9.6	850	6.0	0.588
	8	1 of 1[h]	1.9	170	2.5	0.150
	12	1 of 1[j]	8.8	800	7.7	0.088
	9	2 of 2[h]	10.0	910	4.6	0.301
	11	2 of 2	11.5	1,050	4.6	0.317
	21	2 of 3[k]	3.9	800	3.9	0.170
	10	3 of 3[h]	12.6	1,140	7.3	0.231
	24	3 of 3	10.6	950	7.8	0.218
	23	3 of 3[i]	9.9	880	6.7	0.255
	25	3 of 3[i]	7.8	700	5.9	0.335
	20	3 of 3[k]	7.6	1,560	5.2	0.179
	13	4 of 4	15.9	1,440	6.9	0.277

Notes: Except where noted, tests were conducted with 2,000-lbm vehicle impacting at 0 deg and 20 to 25 mph (32 to 40 km/h). 1 mph = 1.609 km/h; 1 lb·s = 0.45 kg·s.

[a]Data during impact only.
[b]Accelerometer was used to record peak g; film data were used when accelerometer was not working.
[c]Post broke away from sign panel during impact.
[d]Post did not break away from sign.
[e]Left post was not attached to sign panel and was yielded at bumper height prior to impact.
[f]Power to accelerometer was lost during impact.
[g]Vehicle overturned during impact.
[h]No film to corroborate accelerometer data.
[i]2,000-lbm (907-kg) vehicle impacting at 20 deg and 35 to 45 mph (57 to 72 km/h).
[j]Post equivalent to 8-lbf/ft (117-N/m) steel piggyback.
[k]4,500-lbm (1941-kg) vehicle impacting at 10 deg and 40 to 45 mph (64 to 72 km/h).

Figure 6. Peak g for each test.

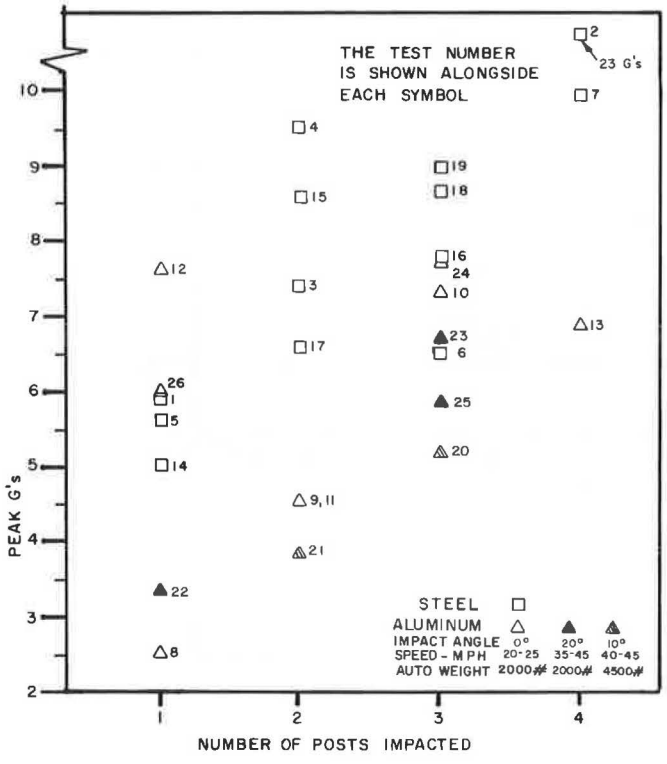

Tests 8 through 13 were conducted on aluminum posts, and vehicle damage was so minimal that only one 2,000-lbm vehicle was used for all the tests. Even after impacting four posts (test 13), the vehicle was considered usable for further tests with one minor repair—freeing the hood latch from the grille work.

The preliminary results of these 19 tests (13 with steel and 6 with aluminum) indicated that the aluminum posts gave consistently better results than the steel samples tested. Therefore, the last seven tests (tests 20 through 26) were conducted with aluminum posts. Five of these seven tests were designed to give information on increased speeds and angles of impact. The other two tests were designed to duplicate previous post-impact conditions. In addition, the post spacing was increased to that that would be found in actual installations for some of these latter tests.

Peak g Force

The symbol g refers to the constant acceleration due to gravity (32.2 ft/s^2 or 9.8 m/s^2). For a vehicle that decelerates at 128.8 ft/s^2 (39.26 m/s^2), there would be a negative force exerted on the vehicle of 4 g.

There are three factors to consider with deceleration forces: the actual peak g reading, the time duration of the g reading, and the onset rate.

Research conducted by J. P. Stapp over a period of 4 years and later work by others resulted in a composite graph indicating that the human body can tolerate 40 g in deceleration for up to 40 msec without injury. Additional work by New York State concluded that a 10-g deceleration lasting longer than 50 msec may produce injury to a human body.

The onset rate was also investigated by Stapp, who suggested a 1,000-g/s value as a tolerable rate. FHWA suggests 500 g/s as a more conservative value.

In this study, the only other measure of deceleration (besides the accelerometer tracing) is the speed change and calculated deceleration from frame to frame on the 16-mm film. From a review of the study films, it is safe to assume that maximum deceleration took place over a period of 17.5 msec (time between 16-mm frames). The more conservative onset rate of 500 g/s would permit a peak g force of approximately 8.7.

A review of Table 1 indicates that only four tests resulted in g forces exceeding 8.7, and three of these were less than 10 peak g. These latter g readings are far below the allowable peaks suggested by Stapp.

Momentum Change

The change in momentum is directly a function of the weight of the vehicle and the change in speed of the vehicle during impact. It is obvious that the speed parameter is more than minimally affected by certain factors. Those factors most readily defined are the post material and the number of posts impacted.

Less obvious but important conditions that also have a substantial effect on the speed change are the angle of impact, the bolt types used for the signpost connection, and the embedment of the posts (2).

Of the posts tested, there appear to be two distinct regions for the ranges of momentum change. Although this is not obvious from Figure 5, Figure 8 shows this feature in a plot of momentum change and duration of impact. The variation of momentum change in Figure 8 (for each material type) is mainly a function of the number of posts simultaneously impacted, whereas the variation in impact duration is mainly a function of the conditions of impact (e.g., number of posts of an installation impacted or angle of impact).

Most of the data samples shown in Figure 8 are for the 2,000-lbm (907-kg) vehicle. The 4,500-lbm (1941-kg) vehicle was only used to satisfy FHWA test conditions, inasmuch as towing this vehicle at 45 mph was hazardous. Hence, only the comparison of tests 20 and 21 can be made for the heavier vehicle. Although test 20 yielded a very high momentum change, the low peak g and speed change put this test in the acceptable region (less than 8.5 g) of the other impacts of three aluminum posts.

Figure 7. Impact duration for each test.

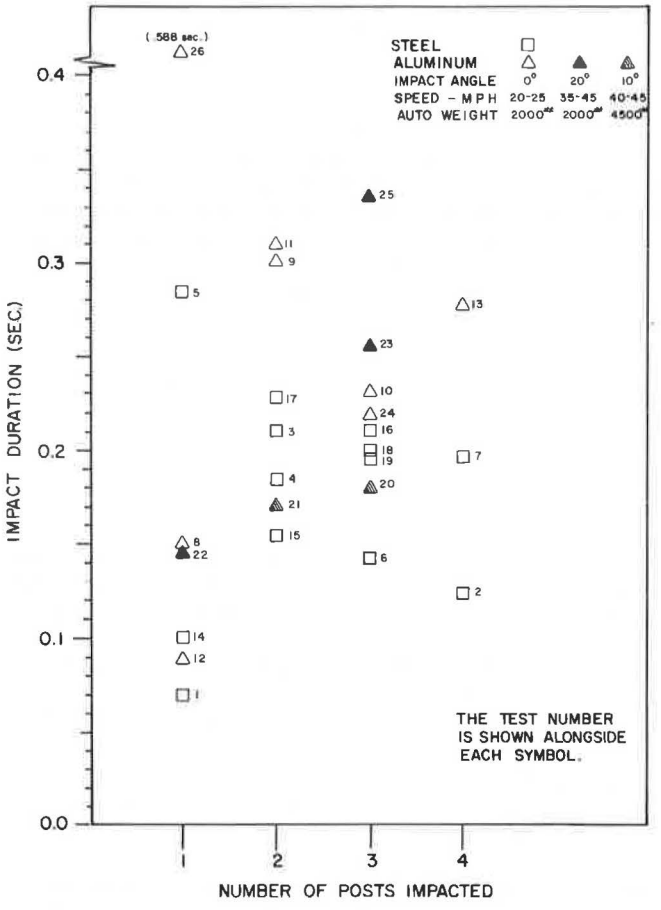

Figure 8. Relationship between change of momentum and duration of impact.

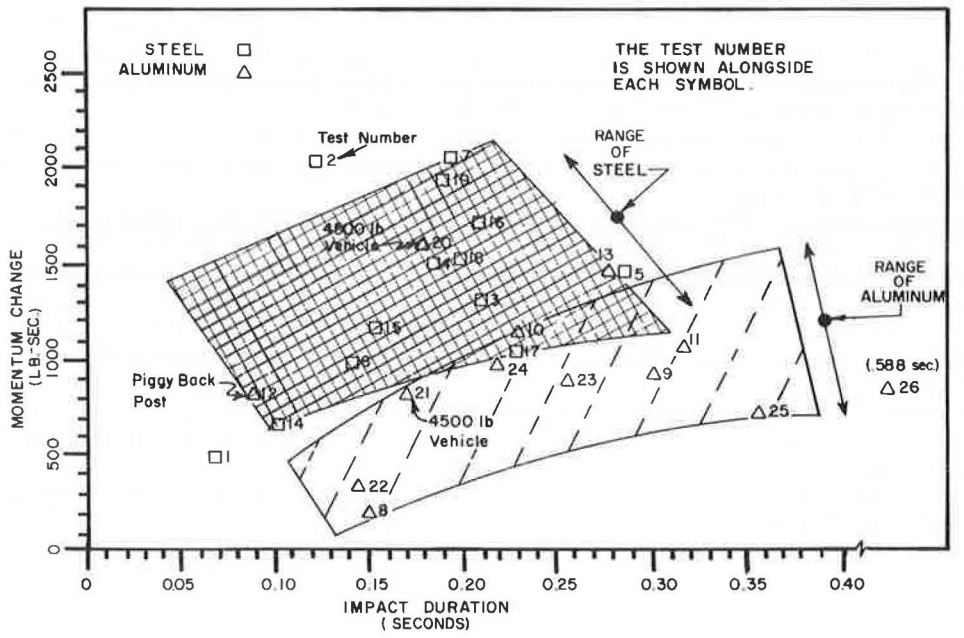

Aluminum Versus Steel Bolts

The comparison of aluminum and steel bolts is empirically possible when the crash vehicle impacts a partial number of posts of a test installation. If the impacted post (or posts) does not separate from the sign (i.e., the bolts do not fail), the sign acts as a structural member tying all the posts together. The effective resistance to the impacting vehicle is then greater than the number of posts impacted when a partial number of posts is impacted. There were five tests where fewer than all the posts of a multipost installation were impacted (tests 1, 5, 21, 22, and 26).

Two steel bolts per post, with washers at the sign face, were used to attach the posts to the sign panel in three tests: tests 1, 5, and 26. Only one post was impacted in each of these three tests. In all, only two of the six bolts involved broke immediately upon impact, both on the same post. The post was the one impacted in test 1, a steel post test. The post yielded at the base and allowed the car to pass easily. As a result, the momentum change was very low.

In test 5, impact conditions were identical. However, the bolts did not break. Consequently, the post did not yield at all, severe damage was done to the vehicle, and the resulting momentum change was excessively high for a one-post impact. The effect of the bolts remaining intact was to offer, to some extent, the resistance of the other two posts to the impacting vehicle.

In test 26, aluminum posts were used to support a 4- × 8-ft (1.2- × 2.4-m) sign, and the posts were spaced at 2 ft (0.6 m) rather than at 1 ft as in tests 1 and 5. Steel bolts with washers at the sign face were again employed. The bottom bolt did not break immediately, and, consequently, the post failed in tension near the base. The top bolt never broke, and the post, which hooked on the front end of the test vehicle, failed again in tension where the base of the sign panel was bolted. The momentum change was again high for a one-post impact. Again, the resistance of more than one post was felt by the impacting vehicle.

From the description of tests 1, 5, and 26, the advantage of the post bolts breaking upon impact can be clearly seen, regardless of post material, when fewer than all the posts of an installation are impacted.

To emphasize this point, tests 21 and 22 were also impacts of less than all the posts of a multipost installation. However, aluminum bolts were used. Both tests were run under higher speed conditions than in tests 1, 5, and 26. Test 21 was with a 4,500-lbm vehicle, and test 22 was with a 2,000-lbm vehicle. In each test, both bolts on each post impacted broke immediately, and the sign remained attached, as in tests 1, 5, and 26, to the remaining posts. The momentum change for test 21 was the lowest recorded for a two-post test, and only one test produced a lower momentum change for a one-post impact than test 22.

Although limited test results are available on steel and aluminum bolts, the benefits of the aluminum bolts appear to outweigh those of the steel on partial-post impacts. The main benefit is the ability of the post to disconnect from the sign (with the use of aluminum bolts), thus not giving the resistance of all posts to the impacting vehicle.

The only disadvantage to using aluminum bolts is that on some vehicle impacts the sign may be disconnected from the posts and hit the windshield of the vehicle.

Chemical and Physical Properties of Materials

The New Jersey DOT specification for the U-post stipulates that rail steel be supplied for all construction jobs. Chemical properties are not defined in the specification, except to indicate a high carbon content, nor are heat-treating procedures. Only the minimum physical limits for tensile and yield strengths are stated—80,000 and 60,000 psi (551 and 413 MPa) respectively.

With this background, testing commenced without the benefit of chemical and physical analyses. The posts used in the first seven tests were thought to be rail steel, but a subsequent chemical analysis of one post showed it to be in the billet range. Consequently, more extensive sampling was made of the steel posts used in the six subsequent steel post tests.

Extensive sampling of the initially tested steel posts (tests 1 through 7) is not available. Essentially, there appear to be two groups of steels, on the basis of the sampled ultimate strengths. The chemical analyses would indicate that there are four groups of steels: tests 1 through 7, tests 14, 15, and 16, tests 17 and 18, and test 19.

If we were to combine those steels with similar physical and chemical properties, there would be four possible groups. A more accurate interpretation of the chemical tests may indicate that every post used in the steel tests would have unique chemical properties.

An examination of Table 1 for the two-post impacts for steel shows two tests to be borderline with the FHWA momentum criteria. The four impact tests conducted on the two-post steel installations indicate no similarity in either the physical or chemical properties of the posts used. Hence, it would be difficult to write a specification on steel posts to guarantee a steel that will meet FHWA criteria.

In effect, the intermixing of the properties does not allow us to group the steels into two areas, as we had thought: low plastic and high plastic. If the steels have to be dynamically tested before grouping them in the plastic range, a specification stipulating this procedure could result in a very costly product. Besides, the two-post installation of an expected higher plastic steel does not meet FHWA criteria (test 17).

Prior to conducting the last series of six steel post tests, the extremely high momentum changes of the first seven steel post tests, even though only two steel posts were impacted, led us to seek materials of higher plasticity for testing. For this reason, six tests were conducted on aluminum posts, whose ultimate strengths were approximately one-third that of the steel.

SUMMARY AND CONCLUSIONS

Small channel-shaped sign supports, designed to bend at the base on impact, are commonly used in New Jersey and other states. Previous research into the safety of these posts has been mostly limited to verifying this "bendaway" action on impact with single-post installations.

Steel channels, which are most widely used, vary in size from 2- to 4-lbf/ft sections and are used for supporting highway delineators and highway signs up to about 60 ft^2 (5.6 m^2) in area.

An aluminum version of these posts, in limited sizes, has recently become available.

Results of dynamic testing indicate that simultaneously impacting more than one 4-lbf/ft steel U-post or more than three aluminum U-posts produces conditions that do not satisfy present FHWA criteria (1968 tentative criteria). The testing has also indicated that the use of aluminum bolts for the signpost connection yields less severe speed changes than stainless steel bolts when only a partial number of posts are impacted by the vehicle.

In all, 26 full-scale crash tests were conducted. Thirteen of these tests involved steel U-post supports, and 13 involved aluminum U-posts. The sign installations contained from one to four posts for both the steel and aluminum tests.

The tests were conducted on the 4-lbf/ft steel sections and the 4- and 8-lbf/ft equivalent aluminum sections with both 2,000- and 4,500-lbm vehicles; impact speeds ranged from 20 to 45 mph, and impact angles ranged from 0 (head-on) to 20 deg in accordance with FHWA test conditions.

REFERENCES

1. Application of Highway Safety Measures—Breakaway Luminaire Supports. Federal Highway Administration, Circular Memo., June 5, 1968.
2. Cook, J. P., and Bodocsi, A. Criteria for Yielding Highway Sign Supports. Univ. of Cincinnati, May 1970.
3. Edwards, T. C., Hirsch, T. J., and Olson, P. M. Design Criteria for Breakaway Sign Supports. Highway Research Record 222, 1968.
4. Tamanini, F. J. Designing Fail-Safe Structures for Highway Safety. Public Roads, Vol. 36, No. 6, Feb. 1971.
5. Design of Sign Supports and Structures. Highway Research Record 346, 1971.

6. Development of Design Criteria for Safer Luminaire Supports. NCHRP Rept. 77, 1969.
7. Development of Safer Roadside Structures and Protective Systems. Highway Research Record 259, 1969.
8. Shoemaker, N. E. Full-Scale Dynamic Testing of New Jersey Breakaway Sign Structure. Cornell Aeronautical Laboratory, Inc., Rept. VJ-2955-V-1, Sept. 1969.
9. Guardrails, Barriers and Sign Supports. Highway Research Record 174, 1967.
10. Rib-Bak Four Sign Post. Pollak Steel Company, 1965.

APPENDIX

Figure 9. Vehicle compartment data for test 1.

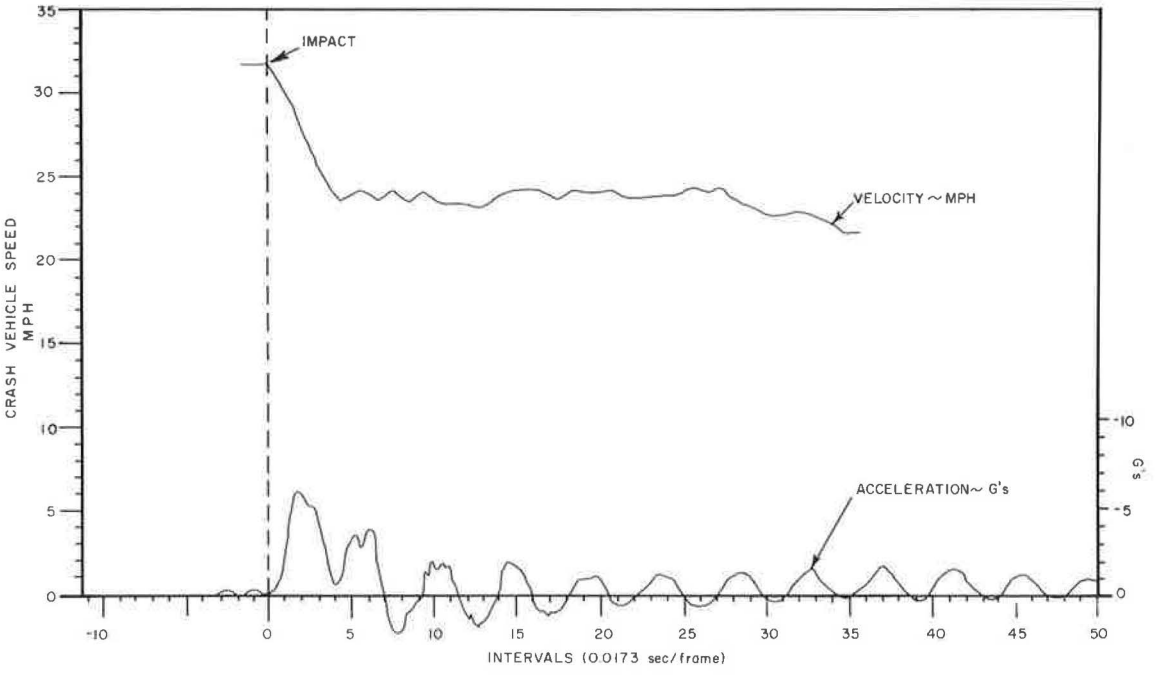

Figure 10. Vehicle compartment data for test 2.

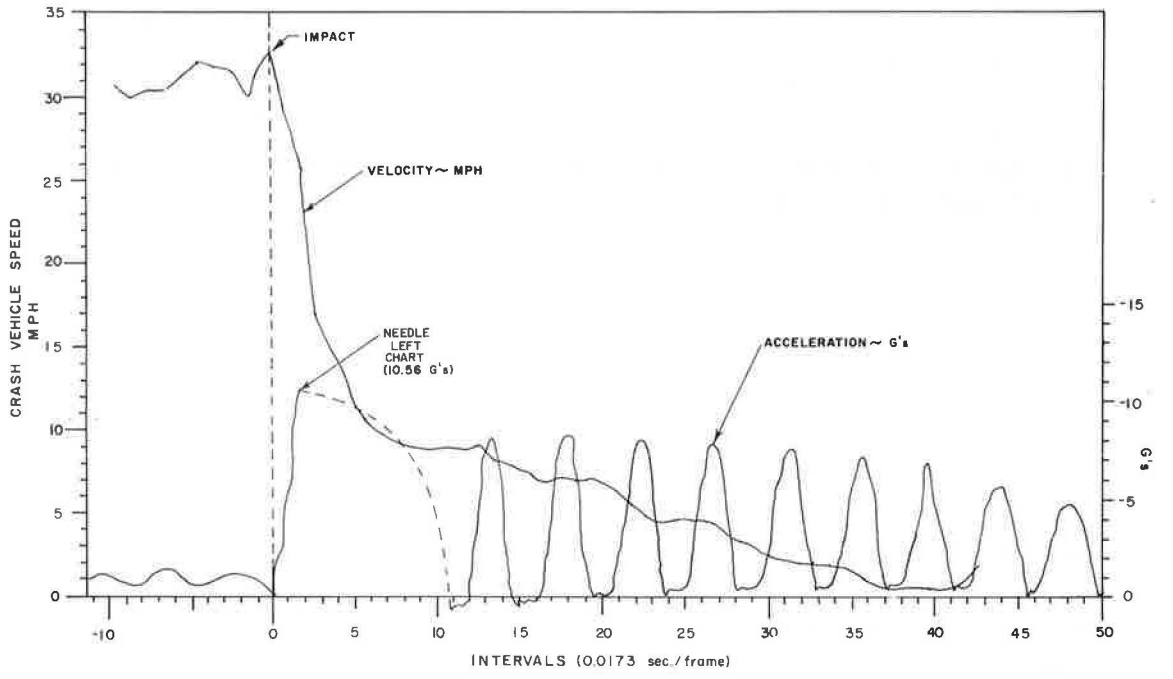

Figure 11. Vehicle compartment data for test 3.

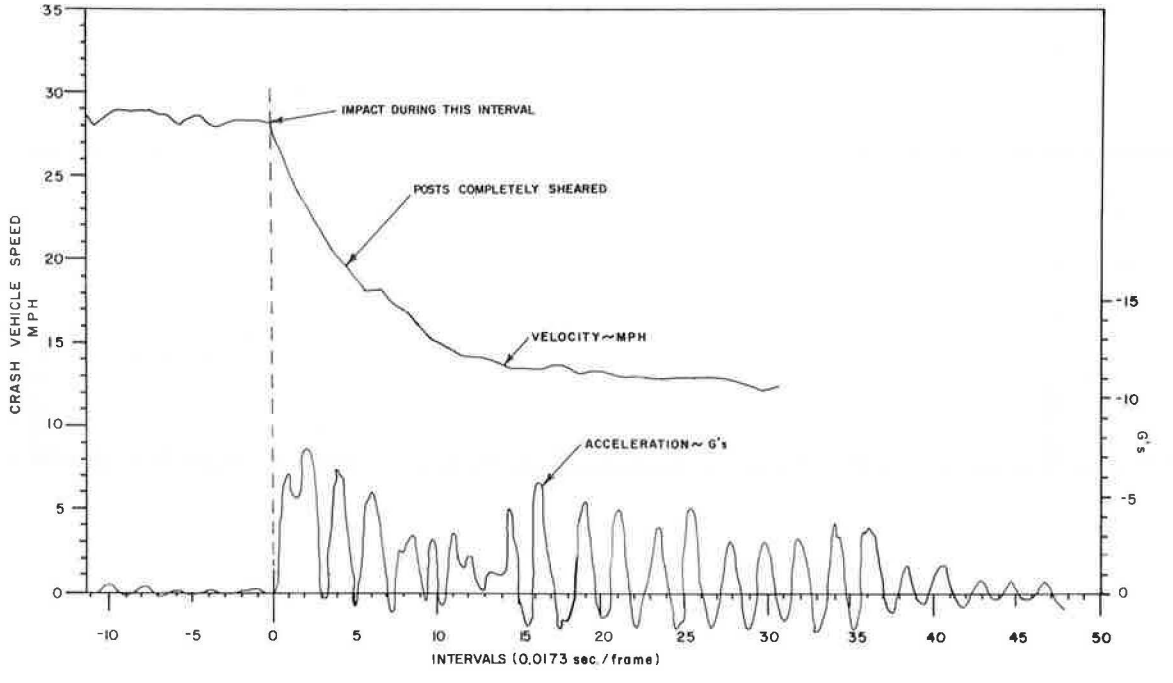

WIND-EXCITED VIBRATIONS OF TRI-CHORD OVERHEAD SIGN SUPPORT STRUCTURES

Vijay Kumar, Sargent and Lundy Engineers, Chicago; and
Chi Chao Tung, Jehangir F. Mirza, and J. C. Smith, Department of Civil Engineering, North Carolina State University at Raleigh

ABRIDGMENT

The dynamic response of two tri-chord truss overhead sign support structures under the action of wind loadings is examined analytically. Two structures, an 82-ft (24.9-m) steel frame and a 150-ft (45.6-m) aluminum frame, are used for this purpose. The wind loadings considered are the harmonic vortex-shedding excitations under moderate conditions and the random gusty drag force under extreme design conditions. The effectiveness of stockbridge dampers in reducing vortex excitation vibration of the aluminum frame is also investigated. The response of the two structures to random drag force is used to verify the adequacy of the gust factor recommended by the AASHO Specifications governing the design of sign support structures. For dynamic analysis, the structures are idealized as space frames with rigid joints. The masses are lumped at certain joints. The response of the frames to the two types of wind forces was determined by using the classical modal superposition method. Results of the study indicate that the stockbridge damper is effective in reducing vortex-excited vibration of the aluminum frame. The gust factor specified by the AASHO Specifications, however, appears to be insufficient.

•THE RESPONSE of two highway overhead sign support structures, one made of steel and one made of aluminum, of the tri-chord type to wind loadings is considered in this study. The wind loadings are considered to consist of a sinusoidal vortex-shedding force, transverse to the direction of wind velocity, and a drag force, in the direction of wind velocity. Under extreme design wind conditions, the drag force is accompanied by randomly fluctuating gusts that may induce vibratory motion in the structures. The gustiness of drag force and its dynamic effects are recognized by the AASHO Specifications (1) as gust factor in the computation of design wind loading. An attempt is made to verify, analytically, the adequacy of the value of the gust factor. Vortex-shedding forces have been observed to cause sustained vibrations of structures when the frequency of vortex shedding is close to that of one of the modes of vibration of the structure. This phenomenon occurs commonly at normal wind speeds that predominate during most of the life of the structures. To prevent large-amplitude vortex-shedding vibrations, AASHO Specifications (1) require the installation of damping devices (stockbridge damper) on all aluminum overhead sign support structures. In this study, the degree of effectiveness of stockbridge dampers in reducing vibrations of tri-chord overhead sign support structures is investigated analytically.

STRUCTURAL CHARACTERISTICS

A portion of the typical tri-chord overhead sign support structure is shown in Figure 1. Structure A is steel, and structure B is aluminum; their dimensions are shown in the figure. For dynamic response computations, the normal mode superposition method is employed. The structures are idealized as lumped-mass systems. For each structure, there are 18 lumped masses. The frequencies and mode shapes of these structures are computed by using the ICES STRUDL program. The first five natural frequencies are given in Table 1.

RESPONSE TO VORTEX SHEDDING

The vortex-shedding force exerted on the cylindrical members of the structures is considered (8) to be given by

$$F_1(t) = \tfrac{1}{2}\rho V^2 A \bar{C}_L \sin \Omega t \qquad (1)$$

where

ρ = density of air,
V = wind speed,
A_p = projected area of member,
$\bar{C}_L$ = root mean square value of random force coefficient C_L,
t = time,
Ω = SV/D = the vortex-shedding frequency,
D = diameter of the cylindrical member, and
S = the stouhal member.

In the present study, the maximum displacement amplitudes D_m of the two structures are computed both with and without signs mounted. Values of $\bar{C}_L = 1.0$, $S = 1.12$ (5), and structural damping coefficient $\lambda = 0.1$ percent of critical damping for all modes are used. For structure A, $D_m = 0.16$ in. (4.06 mm) with signs mounted and 1.1 in. (27.8 mm) without signs at 7-mph (3.13-m/s) and 6-mph (2.69-m/s) wind speeds respectively. For structure B, $D_m = 3.2$ in. (81.2 mm) with signs, and 5.9 in. (150.0 mm) without signs at wind speeds of 6 mph (2.69 m/s) and 11 mph (4.92 m/s) respectively. That signs shield off vortex-shedding forces and reduce structural response is clearly noted.

The effects of 31-lbm (14.1-kg) stockbridge damper on the response of the aluminum structure are also examined analytically. When no signs are mounted, D_m reduces from 5.9 in. (150.0 mm) with no damper attached to about 0.5 in. (12.7 mm) when damper is used. When signs are mounted, D_m diminishes from 3.2 in. (81.2 mm) without damper to 0.3 in. (7.6 mm) with damper, indicating that the stockbridge damper is in fact an effective means of preventing excessive vibrations due to vortex-shedding excitations.

RESPONSE TO RANDOM DRAG FORCE

The random drag force exerted on members of the structure is considered (3) to be given by

$$F_2(t) = \tfrac{1}{2}\rho C_D V(t) \mid V(t) \mid + C_M \rho \frac{A_o}{D} A(t) \qquad (2)$$

where

C_D = coefficient of drag,
C_M = coefficient of virtual mass,
A_o = reference area for virtual mass,
$A(t)$ = wind acceleration,
$V(t) = \bar{V} + v(t)$ = wind velocity,
$\bar{V}$ = mean wind speed, and
$v(t)$ = randomly fluctuating part.

In this study, the mean and standard deviation of the maximum displacement response of the two structures with and without the signs mounted are computed by using random vibrational analysis techniques. The values of $C_D = 1.73$ for cylinders, $C_D = 1.15$ for signs, and $C_M = 1.0$ are used (2). A value of 5 percent of critical damping, typical of the damping in these structures oscillating in high wind, is assumed for all modes. The spectrum for horizontal wind gusts is taken to be that proposed by Davenport (4). For an 80-mph (35.8-m/s) mean wind speed, the mean of maximum displacement $\bar{q}$, treated as the maximum static displacement under mean wind load, and the standard deviation σ_q of maximum displacement are computed and given in Table 2. The sufficiency of the gust factor recommended by the AASHO Specifications was examined (6) by using a peak

Figure 1. Dimensions of sign structures.

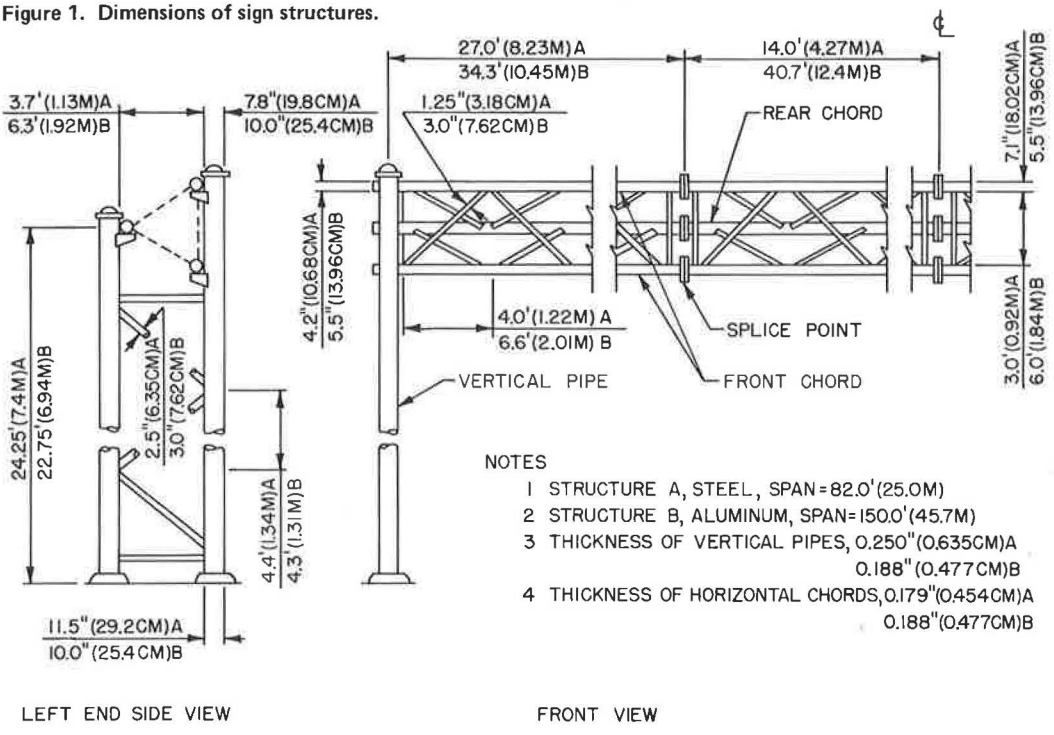

Table 1. Natural frequencies (in H_z).

	Structure A		Structure B	
Mode	Without Signs	With Signs	Without Signs	With Signs
1	2.254	1.913	2.638	2.094
2	3.479	2.909	3.229	2.496
3	3.833	3.072	3.432	2.574
4	7.749	5.681	9.787	5.966
5	11.857	7.806	10.501	7.837

Table 2. Maximum displacement (in inches) of structures to 80-mph wind.

	Structure A		Structure B	
Displacement	Without Signs	With Signs	Without Signs	With Signs
$\bar{q}$	0.59	1.94	5.04	6.78
σ_p	0.35	1.05	2.43	3.05
q_p	1.63	5.09	12.33	15.92
q_s	1.67	5.50	14.40	19.25
q_p/q_s	0.976	0.925	0.858	0.828

Note: 1 in. = 25.4 mm; 1 mph = 4.47 m/s.

displacement $q_p = \bar{q} + 3.0\sigma_q$. The quantity q_p so determined is compared with the quantity q_s (Table 2), the maximum displacement under statically applied wind drag force using a gust factor of 1.3 applied over the fastest mile wind speed (7) as specified by the AASHO Specifications. The ratio q_p/q_s, given in Table 2, ranges from 0.828 to 0.976, suggesting that the specified gust factor of 1.3 can be considered adequate for the type of structures examined.

ACKNOWLEDGMENTS

This study was made as a part of the North Carolina State Highway Research Program project. The investigation was conducted at the Department of Civil Engineering, North Carolina State University. The financial support and technical assistance provided by the North Carolina State Highway Commission and the Federal Highway Administration, U.S. Department of Transportation, are gratefully acknowledged.

REFERENCES

1. Specifications for the Design and Construction of Structural Supports for Highway Signs. AASHO, 1968.
2. Final Report of the Task Committee on Wind Forces. Trans. ASCE, Vol. 126, Paper 3269, 1961, pp. 1124-1198.
3. Davenport, A. G. The Application of Statistical Concepts to the Wind Loading of Structures. Proc., Institution of Civil Engineers, Vol. 19, 1961, pp. 449-472.
4. Davenport, A. G. The Spectrum of Horizontal Gustiness Near the Ground in High Wind. Quarterly Journal of Royal Meteorological Society, Vol. 87, No. 372, 1961, pp. 194-211.
5. Fung, Y. C. An Introduction to the Theory of Aeroelasticity. John Wiley and Sons, 1955.
6. Simiu, E. Gust Factors and Alongwind Pressure Correlations. Jour. Structural Div., Proc. ASCE, Vol. 99, No. ST4, 1973.
7. Vellozi, J., and Cohen, E. Gust Response Factors. Jour. Structural Div., Proc. ASCE, Vol. 94, No. ST6, 1968, pp. 1295-1313.
8. Weaver, W. Wind Induced Vibrations in Antenna Members. Jour. Engineering Mechanics Div., Proc. ASCE, Vol. 87, No. EM1, 1961, pp. 141-165.